POLITECNICO
MILANO 1863

SCUOLA DI INGEGNERIA INDUSTRIALE
E DELL'INFORMAZIONE

EXECUTIVE SUMMARY OF THE THESIS

A Novel Neuro-Motor Assessment to Quantify Dystonia and Spasticity in Children with Movement Disorders: Protocol Definition and Validation

TESI MAGISTRALE IN BIOMEDICAL ENGINEERING – INGEGNERIA BIOMEDICA

AUTHOR: MARCO TRONCONI

ADVISOR: PROFESSOR SIMONA FERRANTE

CO-ADVISOR: FRANCESCA LUNARDINI, PhD

ACADEMIC YEAR: 2020-21

1. Introduction

Dyskinetic movement disorders in childhood are due to dysgenesis or injury to motor pathways involving the central nervous system [1]; we can have different disability patterns with the involvement of upper limbs, lower limbs, or the totality of the body. Cerebral Palsy (CP) is the most common physical disability in childhood and affects 2-2.5 children per 1000 live births [2]; the most common hypertonia signs are spasticity and dystonia, which can be present singularly or in a mixed appearance. In the latter case, distinguish the different hypertonic movement disorders is challenging also for the trained eye, since the effects of the predominant one can cover the other one. Spasticity is defined as a velocity-dependent resistance of a muscle to stretch [1]. Dystonia is defined as a movement disorder in which involuntary sustained or intermittent muscle contractions cause twisting and repetitive movements, abnormal postures, or both [1]. Apart from CP, we can also have forms of spasticity and dystonia linked to gene mutations, namely respectively hereditary spastic paraplegias (HSPs) and Primary Dystonia. Making an early and reliable diagnosis is extremely important to select the most appropriate treatment, without the risk to leave some signs untreated: unfortunately, this is often the case when dealing with mixed hypertonia.

1.1. Evaluation of motor impairments

In order to deliver the best treatment, it is essential to make a reliable diagnosis from the evaluation of the motor impairments; nowadays, the assessment is mainly based on qualitative clinical scales. To evaluate spasticity, the most used clinical scale is the Modified Ashworth Scale (MAS), while the Barry-Albright Dystonia Scale (BAD) is widely used to assess dystonia. Finally, the Hypertonia Assessment Tool (HAT) is a clinical evaluation method of hypertonia in general to differentiate between hypertonia signs (spasticity, dystonia,

and rigidity). Coarse granularity and subjectivity are the main limits of clinical scales, that is why, starting from the end of the twentieth century, researchers started to develop quantitative assessments, integrating signals of different nature.

1.2. State of the Art

Regarding the need to quantify spasticity, early works used isometric machines to passively stretch the lower limbs while measuring the force applied to the supporting arm: the slope of the angle-torque relationship was an indicator of the subject's stiffness [3]. Similar protocols were developed to assess stretch reflex through the Tonic Stretch Reflex Threshold (*TSRT*) [4]. Methods that try to quantify dystonia are more recent and thus less developed. They basically aim at measuring overflow movements and musclar coordination when performing functional tasks [5], [6]. Unfortunately, all the conducted studies were limited in time and with a quite small statistical sample, but preliminary promising results were presented. Nowadays, only few studies aimed to differentiate spasticity and dystonia [7], [8], defining protocols with both passive stretching and functional tasks provided to children with different forms of CP.

1.3. Aim of the Thesis

The thesis was developed within the framework of the "DYSPA System", a Starting Grant project funded by Ministero della Salute and conducted at Movement Analysis Laboratory of Fondazione I.R.C.C.S. Istituto Neurologico Carlo Besta in Milan. The aim of the project is to devise a multi-signal system to extract spasticity-specific and dystonia-specific indicators for a quantitative neuro-motor evaluation. The specific aim of my thesis coincides with the first part of the project, dealing with the definition of meaningful protocols - both for upper and lower limbs - for the computation and extraction of the indicators. Such indicators should be able to provide the clinicians with quantitative parameters useful to support the diagnosis process and the treatment selection, combining data coming from kinematics, kinetics, and EMG signals. An important part of the work also consisted in the definition of the placement protocols for the passive markers of the motion capture system and the EMG probes.

2. Materials and Methods

2.1. Apparatus

The main equipment inside the laboratory is the motion capture system, an optoelectronic SMART-D system by BTS S.p.A. The setup is composed of 8 infrared cameras (sample frequency 70 Hz) connected to a workstation; the overall system is furthermore synchronized with 8 wireless surface EMG probes (sample frequency 1000 Hz) and 4 force plates. The software for the setting of the technical parameters of the equipment, the acquisitions, the tracking of the trials, the management of the subjects and the data analysis is embedded in the SMART package (v.1.10.469.0). Furthermore, MATLAB software (R2021a) was used for data analysis as well.

2.2. Placement Protocols

Placement protocols regard both the positioning of the passive spherical markers on the skin in specific landmarks and the positioning of the bipolar electrodes of the EMG probes on the muscles. Regarding the upper limb marker protocol, we developed a single-limb ad hoc model, mainly following the International Society of Biomechanics (ISB) recommendations [9], using a quite limited number of markers and detecting landmarks easily accessible and not covered during the execution of the tasks. The marker set is composed of 9 markers respectively placed on: right and left acromion, sternum, medial and lateral epicondyle, ulnar and radial styloid, 2° metacarpophalangeal joint and the tip of the index finger (Figure S1).

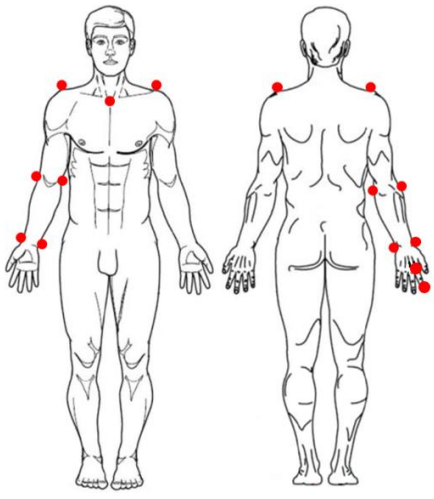

Figure S1: Front view and back view of right upper limb marker set.

For the validation of the upper limb protocol created for this study, we evaluated the 3D angles computed by the model, in order to verify the angle conventions. To do so, 2 control subjects performed several trials in which they executed, for each joint, separate movements for each rotation axis covering the entire Range of Motion (ROM). The related analysis focused on the sign of the angles and to the expected ROMs with reference to the executed movement.
Regarding the lower limb marker protocol, we decided to use the well-known and validated Davis marker set, composed of 22 markers [10].

For the EMG probes positioning, we followed the SENIAM (Surface ElectroMyoGraphy for the Non-Invasive Assessment of Muscles) guidelines, both for the upper limb and the lower limb [11]. Concerning the upper limb, the selected muscles are 8: Flexor Carpi Ulnaris (FCU), Extensor Carpi Radialis (ECR), Biceps (BIC), Triceps (TRIC), Anterior Deltoid (AD), Lateral Deltoid (LD), Posterior Deltoid (PD) and Supraspinatus (SS). Regarding the lower limb, we selected 4 muscles for both sides: Rectus Femoris (RF), Semitendinosus (ST), Tibilias Anterior (TA) and Soleus (SOL).

2.3. Acquisition Protocols

Protocols were developed to acquire data from the upper or lower limb, according to the subject, assessing the dominant side.

Upper Limb

The protocols to assess the functionality of the upper limb enclose 4 different tasks: reaching, finger tapping, writing and passive stretches. The *Reaching Task* is a common exercise in which the subject is asked to reach a target with his/her index finger. This movement is simple to understand and to perform by the children, but at the same time gives us a lot of information about the coordination, the followed motor scheme, and possible alterations. Two trials are acquired for 5 repetitions each. The *Finger Tapping Task* is a neuro-motor exercise in which the subjects are asked to tap their fingers, joining thumb and index of the same hand for a fixed amount of time. Again, the exercise is simple, so well performable by children, but can be compromised by dystonia and so worth to study. Two trials are recorded for 10 seconds on the ipsilateral arm (i.e., the arm with the probes and markers on it) and two additional trials, always for 10 seconds, on the contralateral arm. The *Figure-8 Writing Task* is a smooth movement, easy to execute and characterized by well-defined frequency aspects related to specific muscular patterns. The subject is asked to draw the figure-8 a certain number of times, following the boundaries of a template as precise as possible. Two trials are recorded for 10 repetitions of the figure. The last task is a series of passive extensions of the arm: an operator gently extends the arm of the subject from full flexion to full extension, using a metronome to synchronize the movements. We selected 3 different velocities (fast, medium, and slow), performing 8 repetitions for each velocity. Two trials are acquired for each velocity, with 5-10 seconds of rest between each stretching.

Lower Limb

We performed gait analysis (GA) to identify and quantify lower limb motor disorders. GA has a considerable potential for CP children, giving the possibility to evaluate the effectiveness of a treatment or modify surgical recommendations [12], [13]. Besides GA, passive flexions of the leg are performed to assess the presence of any possible form of spasticity. In this case, the Davis marker set is simplified using only 8 markers and 2 EMG probes. We selected again 3 different velocities and we performed 8 repetitions for each velocity. Two trials are acquired for each velocity, with 5-10 seconds of rest between each stretching.

2.4. Data Analysis

For the pre-processing of kinematics, the first step was to interpolate and filter all the acquired markers' trajectories, using a low pass Butterworth with the cut-off frequency set at 10Hz. As for the EMG data, we extracted the envelopes of the signals, applying a band pass filter (30-450 Hz), taking the absolute value, and finally low-passing the signal using a Butterworth at 3 Hz. Subsequently, each EMG signal was normalized to its corresponding Maximal Voluntary Contraction (MVC) so that we could make comparisons between sessions and subjects. We have extracted several dystonia and spasticity indicators, depending on the task, based on the available literature and the confrontation with the child neurologists of the Institute. Indicators related to the upper limb are summarized in Table S1.

REACHING	TAPPING	WRITING FIGURE-8	PASSIVE EXTENSION
- *SD, ROM and SD/ROM* for each angle (shoulder, elbow, wrist) - *SD* for each wrist velocity component - *3D Peak Velocity* - *Wrist Path Ratio* - *Accuracy* - *Jerk* - Cocontraction: *BIC-TRIC, ECR-FCU AD-PD*	- *Index of Dystonia* - *Modified Index of Dystonia* - *ROM* of the trunk	- *Spatial Repeatability* - SD, ROM and *SD/ROM* of the trunk - *CRPV* - *Jerk* - *TCI* for each muscle	- *TSRT* - *COFLEX and COEXT* - *EMG-change* - *ROM* of the elbow

Table S1: List of the indicators extracted from each upper limb task.

From the *Reaching Task*, we extracted features regarding the repeatability of the gesture, both in terms of trajectory and velocity: *Standard Deviation* (*SD*), *Range of Motion* (*ROM*), and the ratio between them (*SD/ROM*). It was also calculated the *Peak Velocity*. Other very important indicators are the *Wrist Path Ratio* [7], the ratio of the path length executed by the wrist over the length of the straight line connecting the start and the end positions (expected near 1 for controls), and the *Accuracy* of the gesture, the minimum distance between the target and the finger. From the derivative of the acceleration, we computed the *Jerk* to assess the movement smoothness (we calculated 8 different jerk-based measures), and, finally, from the EMG signals, we measured the *Co-Contraction Ratios* of 3 different muscle pairs. As for *the Finger Tapping Task*, the most important computed index was the *Index of Dystonia*, namely the sum of joint excursion of shoulder (flexion-extension, rotation, and abdo-abduction), elbow (flexion-extension and rotation) and wrist (flexion-extension) joints during the active movement of the other arm [7]. We also calculated a modified version, adding to the sum also the abdo-adduction of the wrist. Finally, the features extracted from the writing of the figure-8 regard both the variability of the trajectory, and the analysis of the muscular activation. In particular, we computed the *Continuous Relative Phase* (*CRP*), a coordination index between two adjacent segments [14], in our case adapted to arm-forearm and forearm-wrist, and its variability (*CRPV*). Moreover, it was extracted the *Task Correlation Index* (*TCI*), an indicator of the muscle activity correlated to the task [15].

Passing to the passive arm stretching, we selected a series of indicators mainly related to the analysis of the EMG signals, in order to highlight possible forms of spasticity. The *TSRT* was evaluated using two different activation thresholds set on the Teager-Kaiser (TK) transformed signal [16] or directly on the envelope, based on the subject signals' baselines. Moreover, we computed the *Co-Contraction Ratio* between flexor and extensor, and the *EMG-change*, namely the absolute change of the average EMG signal during stretching at fast and low velocities [17].

As for the lower limb (Table S2), from the GA, we extracted the classical parameters (spatiotemporal parameters, kinematics, kinetics, and EMG data). In addition, we calculated the *Step Profile*, namely the ratio between *Step Length* and *Step Width*, and we highlighted the maximum Ground Reaction Force in the medio-lateral plane (*MaxGRF_ML*); these values in literature are suggested to be altered in CP [18]. Whereas, for the passive leg flexions, the data analysis was exactly the same of the passive arm extensions.

GAIT ANALYSIS	PASSIVE FLEXION
- *Gait Cycle, Stance, Swing* and *Double Support* - *Stride Length, Step Length* and *Step Width* - *Step Profile* - *Walking Velocity* - Angles assessment - Moments and powers assessment *(MaxGRF_ML)* - EMG activity	- *TSRT* - *COFLEX and COEXT* - *EMG-change* - *ROM* of the knee

Table S2: List of the indicators extracted from GA and passive leg flexions.

3. Results

3.1. Participants

For this first part of the project, to test the feasibility of the protocols, we recruited 3 pathological children (1 for the upper limb and 2 for the lower limb) and 4 controls (2 for the upper limb and 2 for the lower limb). In addition, an adult pathological subject was tested to verify if the devised upper limb protocol could be suitable also for the adult pathological population. A summary is presented in Table S3.

SUBJECT	GROUP	SEX	AGE (YEARS)	EVALUATED LIMB
S001	Primary Dystonia	M	14	R ARM
S002	Unknown Diagnosis	M	45	R ARM
S003	Primary Dystonia	F	12	GAIT + R LEG
S004	Left Hemiparesis due to CP	M	15	GAIT + L LEG
C001	Control	F	7	R ARM
C002	Control	M	14	L ARM
C003	Control	F	12	GAIT + L LEG
C004	Control	F	15	GAIT + R LEG

Table S3: Participants.

3.2. Upper limb Placement Protocol Validation

The goodness of the validation trials can be seen in the ROMs of the angles during the movements. For example, the resulting ROMs from shoulder flexion-extension was about 180° for all the subjects (Figure S2), as we expected. Also the ROMs obtained from elbow and wrist flexion-extension, were validated with values around 120°. Some ROM values were more subject-related, like the trunk flexion, but in line with the two subjects' performed movements. Based on the validation trials, we could assess the angles' conventions: flexion is positive, and so extension is negative; internal rotation is positive, and so external rotation is negative; abduction/radial deviation is positive, and so adduction/ulnar deviation is negative.

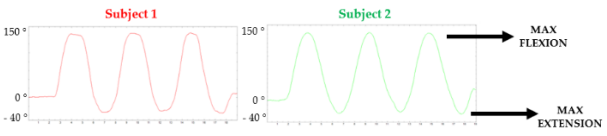

Figure S2: Resulting angles from shoulder flexion-extension validation trials.

3.3. Acquisition Protocol Validation

We evaluated the indicators extracted from the subjects; since the statistical sample was too small, we could not perform statistical tests in order to underline significant differences between groups. However, we can still draw some considerations on the data obtained.

Upper limb: Dystonia vs Control

We compared a 14-year-old subject with dystonia (*S001*) with an age matched healthy subject (*C002*). From the analysis of the *Reaching Tasks*, we could notice different motor strategies to approach the target. The *Wrist Path Ratio* resulted closer to 1 for the control (1.06 vs 1.52), *Accuracy* was the same for both subjects (17 mm), whereas the SDs of velocity of medial wrist marker was higher for dystonia in all the directions. As for the *Finger Tapping Task*, the *Index of Dystonia* resulted greater for the pathological subject in both tasks (ipsilateral 129.63° vs 42.12°; contralateral 39.14° vs 12.59°). Finally, considering the *Figure-8 Writing Task*, we observed that the *CRPV* was higher for the patient, both for arm-forearm (47.17° vs 18.77°) and forearm-hand (50.9° vs 19.25°) pairs.

Upper limb: Dystonia pre-DBS and post-DBS

The second set of results is relative to a subject with dystonia (*S001*), assessed before and 3 months after surgery. As for the *Reaching Task*, we noticed that the non-conventional motor strategy did not change, however the ROMs of the gestures were wider. Passing to the *Tapping Tasks*, it seemed that the *Index of Dystonia* was reduced on the contralateral arm (39.14° vs 58.79°), but increased on the ipsilateral (129.63° vs 108.48°). The writing trials were not performed before surgery, so comparison was not possible to perform.

Upper limb: Adult pathological subject

As for this subject (*S002*), the diagnosis was unknown, but the patient showed a visible tremor on the right arm. We performed *Reaching* and *Finger Tapping Tasks*. The sign of tremor was clearly visible in the angles' tracks during reaching, which altered in a significant way the quality of the execution of the task: the *Wrist Path Ratio* was higher (1.37) with respect to the previous control subjects and the *Accuracy* was worse (61 mm). Furthermore, as expected, the contralateral *Index of Dystonia* (98.82°), was the highest among all the evaluated subjects, and also the ipsilateral index (85.25°) was higher compared to the controls.

Lower limb: Dystonia vs Control

As for the GA, we could observe an alteration of the gait pattern for the pathological patients (*S003* and *S004*). The patient with dystonia (*S003*) had a more severe impairment on the right side: this was visible from the altered ratio, referred to the right

limb, between *Stance* and *Swing* phase (52.83% - 47.17%). Moreover, the *Step Profile* was quite different from right to left (8 – 6.5). Also for the subject with left hemiparesis (*S004*), the *Step Profile* is significantly different from the controls, due to an increased *Step Width*, and, in addition, the *Walking Velocity* was very low. The abnormalities were visible also on the kinematics graphs: as for *S003*, the gait pattern was characterized by a right foot greatly dorsiflexed and externally rotated. As for *S004*, the left knee was hyperextended during stance and had a reduced flexion; the left ankle was mainly in plantarflexion, with a very limited ROM (Figure S3). The *MaxGRF_ML* resulted, on average, to be higher for the pathological subjects. The alterations can be observed also analyzing the EMG signals, characterized by altered timings and activation bursts.

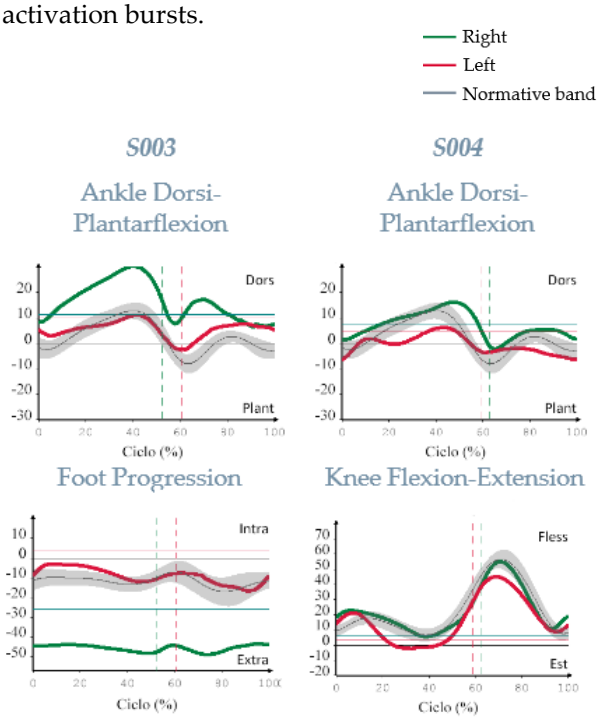

Figure S3: Selected kinematics graphs from pathological subjects *S003* (right impairment) and *S004* (left impairment).

4. Discussion

The validation trials confirmed the solidity of the upper limb marker set, showing meaningful results for all the selected joints in all the tested directions. Moreover, the limited number of the markers was devised in the direction of fostering freedom of movement, which is particularly important for paediatric patients and children in general.

From the trials performed on the subjects, we can identify the most promising indicators. Regarding the *Reaching Task*, the *Wrist Path Ratio* had better values for the 14-year-old control subject (*C002*) with respect to both patients (child *S001* and adult *S002*). This was also true considering the 2nd control subject, a 7-year-old child (*C001*). The fact that the indicator showed the same trend independently from the subjects' age suggests that it is a robust indicator of dystonia. As for the *Finger Tapping Task*, considering the *Index of Dystonia* calculated on the contralateral arm, our results reflect the outcomes found in literature. The parameter resulted higher in both pathological cases (child *S001* and adult *S002*) with respect to both control subjects. Again, this supports the robustness of this index. Also our modified version showed the same results. Passing to the *Figure-8 Writing Task*, another important achievement of the devised protocol can be seen in the use of the *CRP*, for the first time successfully applied to the upper limb. Our data underlined a reduced coordination of the pathological subject *S001*, compared to the age matched control *C002*.

From GA, the indicators of the pathological subjects reflected their impairments, especially on the right side of the body for *S003* and on the left for *S004*. Moreover, *Step Profile* showed a greater variability in pathological cases, assuming values significantly different from controls, and on average *MaxGRF_ML* was higher, in line with literature. In this case, it is important to underline that, in order to describe the whole situation, a single parameter is not enough, but we need to integrate all the information coming from the analysis. The same applies to the analysis of the upper limb protocols, for which valuable conclusion can be drawn not from a single parameter, but from the overall evaluation.

Our data showed great between-trial variability for the youngest control subject. First of all, this is due to the fact that motor performance, and so its variability, is really different between childhood and adolescence [19]. This is why it is more reliable a comparison between age matched subjects. Secondly, the between-trial variability could be due to the initial discomfort caused by the equipment mounted on her. This observation led us to the conclusion that future acquisitions should include some acquaintance trials to put the child at ease.

As for spasticity trials, the main limit was the fact that we managed to recruit and test only one paediatric subject with spasticity, but he did not show any catches during the acquisitions, probably because of the active support during stretching. Future work should focus more on this direction [20].

5. Conclusions

In conclusion, we successfully developed protocols – for upper and lower limb – easy to be performed both by children and grown-up patients, in order to extract meaningful parameters to assess the presence of spasticity and dystonia. The developed upper limb marker set is composed of a limited number of markers located in easily accessible body landmarks and allowing a fast preparation. Moreover, the tasks executed are easy and fast to be performed, two fundamental points when dealing with children.

6. Bibliography

[1] T. D. Sanger, M. R. Delgado, D. Gaebler-Spira, M. Hallett, and J. W. Mink, "Classification and Definition of Disorders Causing Hypertonia in Childhood," 2003. [Online]. Available: www.aappublications.org/news

[2] D. S. Reddihough and K. J. Collins, "The epidemiology and causes of cerebral palsy," *Australian Journal of Physiotherapy*, vol. 49, no. 1. Australian Physiotherapy Association, pp. 7–12, Jan. 01, 2003. doi: 10.1016/S0004-9514(14)60183-5.

[3] J. R. Engsberg, K. S. Olree, S. A. Ross, and T. S. Park, "Quantitative clinical measure of spasticity in children with cerebral palsy," *Archives of Physical Medicine and Rehabilitation*, vol. 77, no. 6, pp. 594–599, Jun. 1996, doi: 10.1016/S0003-9993(96)90301-9.

[4] A. Jobin and M. F. Levin, "Regulation of stretch reflex threshold in elbow flexors in children with cerebral palsy: a new measure of spasticity," *Developmental Medicine & Child Neurology*, vol. 42, no. 8, pp. 531–540, Feb. 2007, doi: 10.1111/j.1469-8749.2000.tb00709.x.

[5] A. Kawamura, S. Klejman, and D. Fehlings, "Reliability and validity of the kinematic dystonia measure for children with upper extremity dystonia," *Journal of Child Neurology*, vol. 27, no. 7, pp. 907–913, 2012, doi: 10.1177/0883073812443086.

[6] R. Pons *et al.*, "Upper Limb Function, Kinematic Analysis, and Dystonia Assessment in Children with Spastic Diplegic Cerebral Palsy and Periventricular Leukomalacia," *Journal of Child Neurology*, vol. 32, no. 11, pp. 936–941, 2017, doi: 10.1177/0883073817722451.

[7] L. M. Gordon, J. L. Keller, E. E. Stashinko, A. H. Hoon, and A. J. Bastian, "Can Spasticity and Dystonia Be Independently Measured in Cerebral Palsy?," *Pediatric Neurology*, vol. 35, no. 6, pp. 375–381, 2006, doi: 10.1016/j.pediatrneurol.2006.06.015.

[8] M. K. Lebiedowska, D. Gaebler-Spira, R. S. Burns, and J. R. Fisk, "Biomechanic characteristics of patients with spastic and dystonic hypertonia in cerebral palsy," *Archives of Physical Medicine and Rehabilitation*, vol. 85, no. 6, pp. 875–880, Jun. 2004, doi: 10.1016/j.apmr.2003.06.032.

[9] G. Wu *et al.*, "ISB recommendation on definitions of joint coordinate systems of various joints for the reporting of human joint motion - Part II: Shoulder, elbow, wrist and hand," *Journal of Biomechanics*, vol. 38, no. 5, pp. 981–992, May 2005, doi: 10.1016/j.jbiomech.2004.05.042.

[10] R. B. Davis, S. Õunpuu, D. Tyburski, and J. R. Gage, "A gait analysis data collection and reduction technique," *Human Movement Science*, vol. 10, no. 5, pp. 575–587, Oct. 1991, doi: 10.1016/0167-9457(91)90046-Z.

[11] H. J. Hermens *et al.*, "European Recommendations for Surface ElectroMyoGraphy Results of the SENIAM project".

[12] J. R. Gage, "Gait Analysis in Cerebral Palsy (Clinics in Developmental Medicine (Mac Keith Press))," p. 206, 1991, Accessed: Oct. 04, 2021. [Online]. Available: https://books.google.com/books/about/Gait_Analysis_in_Cerebral_Palsy.html?hl=it&id=bof4MQEACAAJ

[13] D. PA, D. RB, O. S, R. S, and S. R, "Alterations in surgical decision making in patients with cerebral palsy based on three-dimensional gait analysis," *Journal of pediatric orthopedics*, vol. 17, no. 5, pp. 608–614, Sep. 1997, doi: 10.1097/00004694-199709000-00007.

[14] H. J, van E. RE, H. BC, and L. L, "A dynamical systems approach to lower extremity running injuries," *Clinical biomechanics (Bristol, Avon)*, vol. 14, no. 5, pp. 297–308, 1999, doi: 10.1016/S0268-0033(98)90092-4.

[15] F. Lunardini, S. Maggioni, C. Casellato, M. Bertucco, A. L. G. Pedrocchi, and T. D. Sanger, "Increased task-uncorrelated muscle activity in childhood dystonia," *Journal of NeuroEngineering and Rehabilitation*, vol. 12, no. 1, Jun. 2015, doi: 10.1186/s12984-015-0045-1.

[16] S. Solnik, P. Rider, K. Steinweg, P. Devita, and T. Hortobágyi, "Teager-Kaiser energy operator

signal conditioning improves EMG onset detection," *European Journal of Applied Physiology*, vol. 110, no. 3, pp. 489–498, Oct. 2010, doi: 10.1007/S00421-010-1521-8.

[17] L. Bar-On *et al.*, "A clinical measurement to quantify spasticity in children with cerebral palsy by integration of multidimensional signals," *Gait and Posture*, vol. 38, no. 1, pp. 141–147, 2013, doi: 10.1016/j.gaitpost.2012.11.003.

[18] J. R. Davids, T. Foti, J. Dabelstein, D. W. Blackhurst, and A. Bagley, "Objective assessment of dyskinesia in children with cerebral palsy," *Gait and Posture*, vol. 6, no. 3, p. 269, 1997, doi: 10.1016/S0966-6362(97)90067-9.

[19] C. Branta, J. Haubenstricker, and V. Seefeldt, "Age changes in motor skills during childhood and adolescence.," *Exercise and Sport Sciences Reviews*, vol. 12, no. 1, pp. 467–520, Jan. 1984, doi: 10.1249/00003677-198401000-00015.

[20] A. M. Sherwood, W. B. Mckay, and M. R. Dimitrijevic, "Motor control after spinal cord injury: Assessment using surface EMG," *Muscle Nerve.*, vol. 19(8), pp. 966–79, 1996, doi: 10.1002/(SICI)1097-4598(199608)19:8.

POLITECNICO
MILANO 1863

SCUOLA DI INGEGNERIA INDUSTRIALE
E DELL'INFORMAZIONE

A Novel Neuro-Motor Assessment to Quantify Dystonia and Spasticity in Children with Movement Disorders: Protocol Definition and Validation

TESI DI LAUREA MAGISTRALE IN
BIOMEDICAL ENGINEERING - INGEGNERIA
BIOMEDICA

Author: **Marco Tronconi**

Student ID:	10750401
Advisor:	Professor Simona Ferrante
Co-advisor:	Francesca Lunardini, PhD
Academic Year:	2020-21

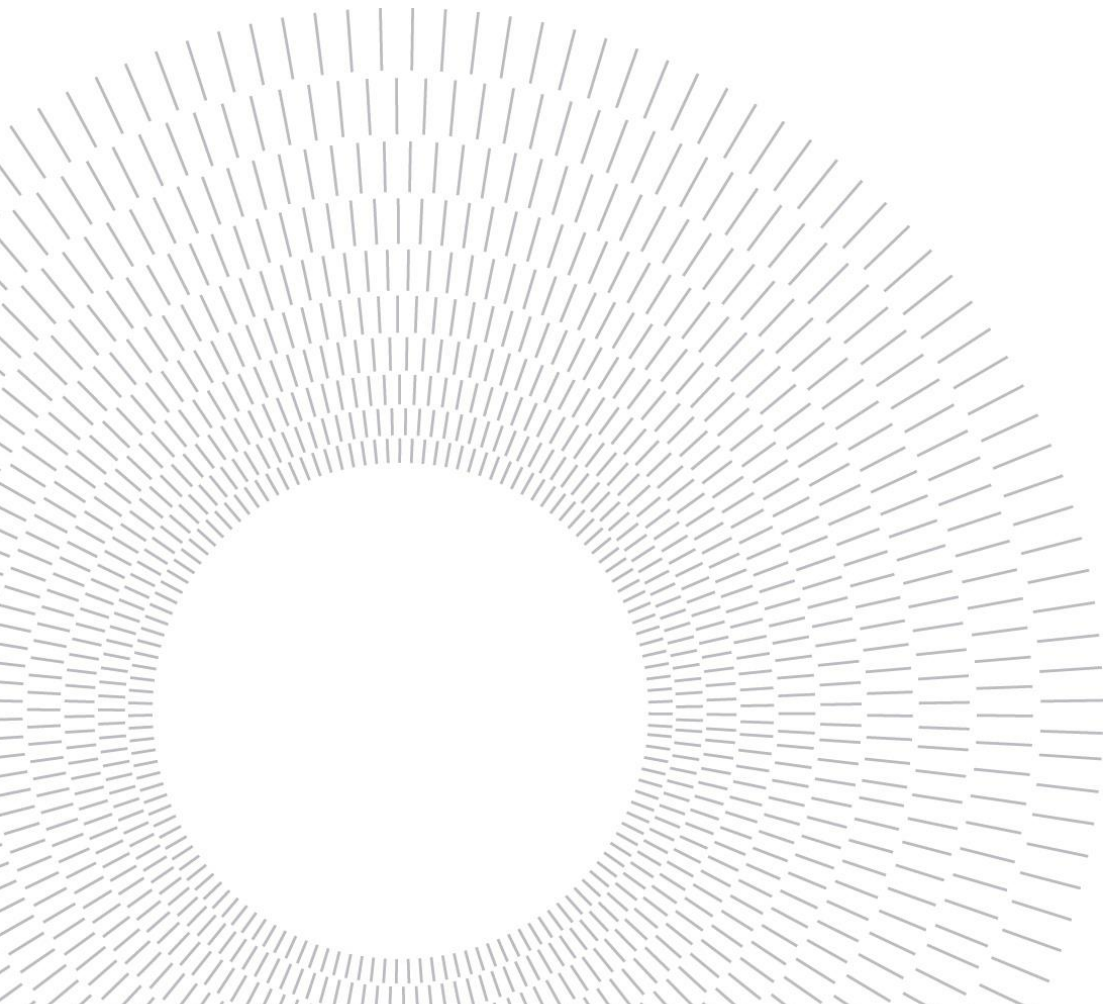

Abstract

Selecting and evaluating appropriate treatments for children with hypertonic movement disorders is nontrivial, especially when more than one motor impairment coexist. This is the case, for instance, of mixed hypertonia with components of spasticity and dystonia, which is likely to be found in the vast majority of children with Cerebral Palsy (CP). In this context, the "DYSPA System" aims at achieving quantitative assessment of children with hypertonic movement disorders, encompassing kinematic, kinetic and electromyographic (EMG) measures, in order to quantify the neuro-motor performance during functional tasks and assess the presence of motor impairments through specific dystonia and spasticity indices. My thesis work corresponds to the first part of this project and deals with the definition and the validation of the protocols - for both upper and lower limbs - and of the related quantitative indices computed.

We developed an ad hoc monolateral 9-marker set for the upper limb. The upper limb protocols embed 3 functional tasks (reaching, finger tapping, and figure-8 writing), whereas the gait analysis was performed for the lower limb. Moreover, instrumented passive stretching of both limbs was performed to evaluate any presence of spasticity. From the different trials we extracted a series of indicators assessing, among others, variability, coordination, and EMG activity. We tested the feasibility of the protocols and the goodness of the indicators on 3 paediatric patients and 4 control subjects. Also a pathological adult was evaluated.

We successfully developed a solid upper limb marker set with a limited number of markers. Results regarding the extracted indicators were in line with the literature. The most reliable parameters resulted the *Wrist Path Ratio* for reaching, the *Index of Dystonia* for finger tapping, and the *Continuous Relative Phase* for figure-8 writing. As for gait analysis, the reports showed differences between controls and patients, in terms of spatio-temporal parameters, kinematics, kinetics, and muscle activation. Among the devised indicators, the *Step Profile* and the maximum Ground Reaction Force in the medio-lateral plane (*MaxGRF_ML*) presented altered values for the pathological subjects, as reported in literature.

The preliminary results coming from the validation trials are encouraging and consistent with the literature. These early results were useful to devise refinements and modifications to the protocols - especially for the instrumented passive stretching - in order to optimize the future acquisition campaign.

Keywords: movement disorders, dystonia, spasticity, clinical movement analysis, quantitative neuro-motor evaluation.

Abstract in lingua italiana

Selezionare e valutare trattamenti appropriati per bambini con disturbi del movimento ipertonico non è banale, specialmente quando coesistono più di una disabilità motoria. È il caso, ad esempio, dell'ipertonia mista con componenti di spasticità e distonia, che è verosimile riscontrare nella stragrande maggioranza dei bambini con Paralisi Cerebrale (PC). In questo contesto, il "Sistema DYSPA" mira a ottenere una valutazione quantitativa dei bambini con disturbi del movimento ipertonico, comprendendo misure cinematiche, cinetiche ed elettromiografiche (EMG), al fine di quantificare le prestazioni neuro-motorie durante compiti funzionali e valutare la presenza di disabilità motorie attraverso specifici indici di distonia e spasticità. Il mio lavoro di tesi corrisponde alla prima parte di questo progetto e riguarda la definizione e la validazione dei protocolli - sia per arti superiori che inferiori - e dei relativi indici quantitativi calcolati.

Per l'arto superiore, abbiamo sviluppato un protocollo di posizionamento monolaterale composto da 9 marcatori. I protocolli dell'arto superiore includono 3 compiti funzionali (raggiungimento, tocco delle dita, e scrittura della cifra 8), mentre l'analisi del cammino è stata eseguita per l'arto inferiore. Inoltre, è previsto uno stretching passivo di arto superiore ed inferiore per valutare l'eventuale presenza di spasticità tramite cinematica e EMG. Dalle diverse prove abbiamo estratto una serie di indicatori che valutano, tra gli altri, la variabilità, il coordinamento e l'attività EMG. Abbiamo testato la fattibilità dei protocolli e la

bontà degli indicatori su 3 pazienti pediatrici e 4 soggetti di controllo. È stato valutato anche un adulto patologico.

Abbiamo sviluppato con successo un protocollo tecnico per il posizionamento di marcatori per arto superiore con un numero limitato di marker. I risultati emersi dal calcolo degli indicatori proposti sono in linea con la letteratura; i parametri più affidabili sono risultati il *Wrist Path Ratio* per il raggiungimento, l'*Index of Dystonia* per il tocco delle dita e *Continuous Relative Phase* per la scrittura dell'8. Per quanto riguarda l'analisi del cammino, i report hanno mostrato differenze tra controlli e pazienti, in termini di parametri spaziotemporali, cinematica, cinetica e attivazione muscolare. Tra gli indici proposti, lo *Step Profile* e la massima forza di reazione con il terreno nel piano medio-laterale (*MaxGRF_ML*) sono risultati alterati nei pazienti, come riportato in letteratura.

I risultati preliminari delle prove di validazione sono incoraggianti ed in linea con la letteratura. I risultati ottenuti ci hanno permesso di trarre spunto per alcune modifiche - soprattutto per l'estrazione di indici di spasticità durante lo stretching passivo - al fine di ottimizzare i protocolli in vista della campagna di acquisizione.

Parole chiave: disturbi del movimento, distonia, spasticità, analisi clinica del movimento, valutazione neuro-motoria quantitativa.

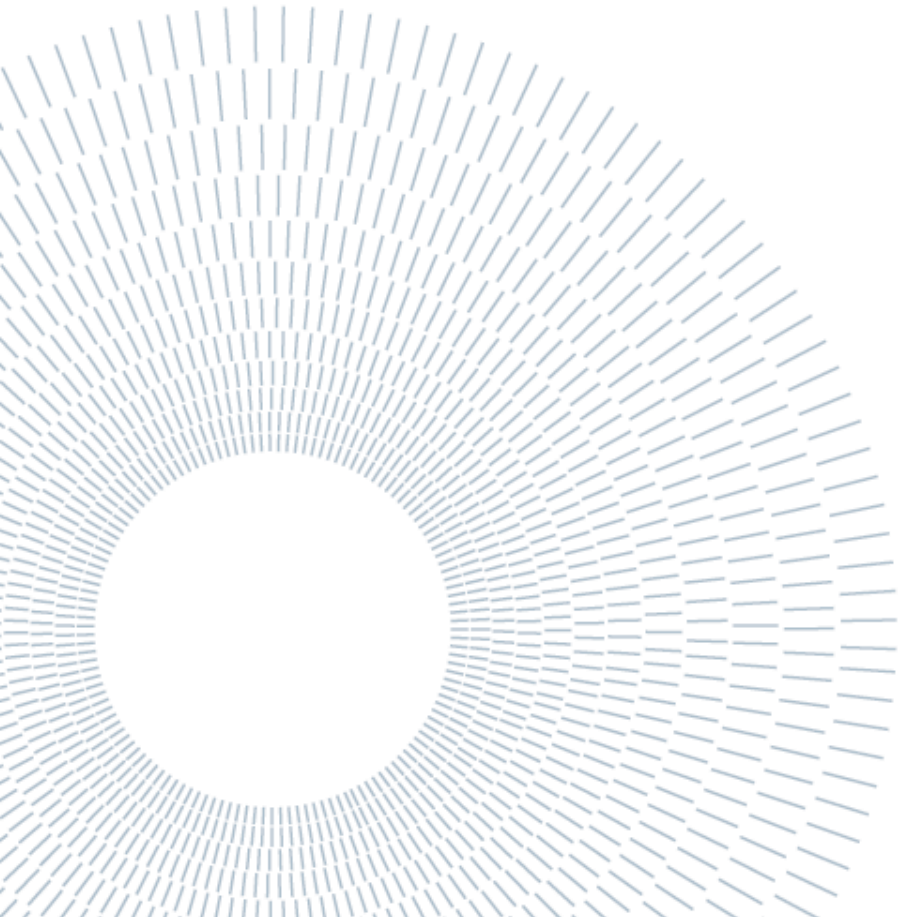

Contents

1. Introduction

1.1 Dyskinetic movement disorders in children

Dyskinetic movement disorders in childhood are due to dysgenesis or injury to motor pathways involving the central nervous system [1]. In particular, when the lesion or defect occurs before 2 years of age we talk about cerebral palsy (CP) [2]. Cerebral palsy is the most common physical disability in childhood and affects 2-2.5 children per 1000 live births [3]. Prematurity is the leading cause of CP, affecting for approximately 75% of all cases [3], [4]. From the anatomic involvement, we can discern three different CP patterns: hemiplegia, when the impaired parts are ipsilateral upper and lower extremities, diplegia, when there is a greater reflection in lower limbs, and quadriplegia, the worst case, with the involvement of the totality of the body [5]. Signs and symptoms are different from case to case. However, in most children with CP, we can observe two different hypertonia signs: spasticity and dystonia, which can be present singularly or in a mixed appearance.

Spasticity is defined as a velocity-dependent resistance of a muscle to stretch [1], mainly caused by the hyperexcitability of spinal motoneurons (other causes are, for

instance, the reduction of inhibition on muscular fibers), resulting in different manifestations, among which the most common are involuntary contractions, joint stiffness, and presence of clonuses. From an estimation, we can say that about 75% of patients with CP have spasticity [6], [7].

Conversely, dystonia is defined as a movement disorder in which involuntary sustained or intermittent muscle contractions cause twisting and repetitive movements, abnormal postures, or both [1]. Dystonic postures can be triggered by voluntary movements and postures, or by specific tasks [8].

Unfortunately, subjects with cerebral palsy have a permanent impairment that is not possible to heal with the time, so the goal of treatments is to increase functionalities, improve capabilities and sustain health in terms of locomotion, cognitive development, social interaction, and independence [7]. Treatments are various and are subject-dependent, but we can point out four different approaches with the possibility to compose them: i) physical therapy; ii) medications (Botulinum toxin and Baclofen); iii) surgical treatments (e.g., dorsal rhizotomy); iv) orthoses to prevent inappropriate movements [7]. It is also important to underline that an early and reliable diagnosis might result in better outcomes [9].

Spasticity and other neurologic disorders can also be linked to gene mutations, and they are named hereditary spastic paraplegias (HSPs) [10]. HSPs are heterogenous, depending on the locus and the possible coexisting abnormalities, however the predominant symptom is spastic weakness in lower limbs [10]. The prevalence of HSP is very variable, by the way it was predicted by Polo *et al.* ranging from about 1 to 9 per 100,000 people [11], with the onset that can be observed even in pediatric age [12], [13].

In case of cerebral palsy, clinicians talk about secondary dystonia because it arises from other diseases (i.e., the cause of CP), but this is not the only possibility, in fact can exist also forms of pure dystonia possibly related to genetic disorders (the real etiology is still unknown), namely primary dystonia [8]. However, dyskinetic cerebral palsy is nowadays the most common cause of dystonia in children [8].
Primary dystonia can occur both in children and adults: in the first case, usually, the disorder is more likely to develop in arms or legs and then spread it to other body parts, while in the second case it starts from the neck or in the face and hardly spread it widely. Moreover, in children, it is more likely to manage to discover the cause of the disease (studies suggested that could be a relationship with lesions at the level of basal ganglia [14]), while in adults it is mostly idiopathic. Besides, also calculate the true prevalence is a complex process, that is why it is considered unknown, however a study from Steeves *et al.* suggested that the overall prevalence of primary dystonia is 16.43 per 100,000 people [15].

1.2 Evaluation of motor impairments

In order to deliver the best treatment, it is essential to make a reliable diagnosis from the evaluation of the motor impairments. Nowadays, the assessment is mainly based on qualitative clinical scales [16]–[18], suitable both for upper and lower limbs and easy to perform, but whose coarse granularity and subjectivity do not allow to make an accurate evaluation. Children with cerebral palsy are clinically classified as “spastic” - if spasticity is the main sign - or “extrapyramidal” - if dystonia is the main sign - and treated accordingly, without taking into consideration that often subjects present mixed motor disorders, difficult to detect, whose identification could lead to a better managing [19]. In fact, only with the involvement of a quantitative reliable assessment of motor disorders we can improve both the

treatment and the monitoring of the patients, giving to the clinicians an objective measurement of the situation, following the principle of evidence-based medicine [20].

To evaluate spasticity, the most used clinical scale is the Modified Ashworth Scale (MAS) developed by Bohannon in 1987 [16], as the name suggests, from the revisitation of the original evaluation method of 1964 [21]. Both the evaluation and the scoring procedure are simple, basically composed of an ordinal scale providing six different levels of spasticity. The assessment is performed by a clinician or a physiotherapist with the patient placed in supine position; the starting position depends on the fact that the testing muscle primary flexes or extends a joint, so the assessor will move the joint in the maximal flexed or extended position respectively, and then he will extend or flex it for one second. The scoring procedure goes from 0 (no increase in muscle tone) to 4 (rigid flexion or extension), in between there are different shades of spasticity from slightly to considerable increase of muscle tone. The difference between the original version of the scale and the modified one resides exactly in the scores, with the addition of one level, namely 1+, between 1 and 2. Critical issues of this method are the moderate number of assessment levels, the subjectivity of the final score, and the fact that the evaluation is performed only at one velocity, managed by the assessor, rather than by a torque motor, and so resistance is not fully understandable.

Modified Ashworth Scale (MAS)	
Score	
0	No increase in muscle tone
1	Slight increase in muscle tone, manifested by a catch and release or by minimal resistance at the end range of motion when the part is moved
1+	Slight increase in muscle tone, manifested by a catch, followed by minimal resistance throughout the remainder (less than half) of the range
2	More marked increase in muscle tone throughout most of the range, but affected part is easily moved
3	Considerable increase in muscle tone, passive movement is difficult
4	Affected part is rigid

Table 1.1: *Modified Ashworth Scale (MAS).*

One of the first clinical scale that assessed dystonia was the Burke-Fahn-Mardsen Scale (BFM), created in 1985 [22]. BFM is a method to assess primary dystonia only, concerning nine body regions (eyes, mouth, speech and swallowing, neck, trunk, and limbs) and two different factors for each region: a provoking factor, which evaluates circumstances, and a severity factor [23]. The score for each region is the product of the provoking factor, the severity factor, and a weighting factor for a maximal score of 120 [23]. Furthermore, the scale is also composed by another component (disability scale) concerning how dystonia affects daily living activities (e.g., speech, handwriting); in this case, the maximum score is 30 [23].

Starting from BFM, the Barry-Albright Dystonia Scale (BAD) [17] is nowadays widely used, also in the assessment of secondary dystonia. The BAD evaluates eight different body regions: eyes, mouth, neck, trunk, and each upper and lower limb. The assessor asks the subject to make simple tasks and reports a score for each region from 0 (no dystonia) to 4 (severe dystonia, present more than 50% of the time and prevents function); in between there are other 3 different possible scores from slight to moderate. In the end, it is possible to make a summation of all the body

region scores and achieve a final score: of course, higher is the score, higher is the severity of dystonia, until a maximum score of 32 points. As for the MAS scale, the granularity of this method is not enough to make a precise evaluation. Moreover, the score is given in a possibly subjective way, enforced by the fact that a manual of the procedures to be followed it is not available; this results in a significant intra-operator variability, since each assessor decides to make the subject tasks more suitable according to his knowledge and experience, but without a standardized protocol.

Barry-Albright Dystonia Scale (BAD)	
Score	
0	No dystonia
1	Slight dystonia, present less than 10% of the time
2	Mild dystonia, present less than 50% of the time and does not interfere with function
3	Moderate dystonia, present more than 50% of the time and interferes with function
4	Severe dystonia, present more than 50% of the time and prevents function

Table 1.2: *Barry-Albright Dystonia Scale (BAD).*

The Hypertonia Assessment Tool (HAT) is a clinical evaluation method of hypertonia in general for children/youth between 4 and 19 years, composed of seven different items: two regarding spasticity, three regarding dystonia, and the remaining two concerning rigidity [24]. Each item is composed of a simple task to be performed; items 3 and 4 regard spasticity and they consist in a movement from full flexion to full extension (or vice versa, depending on the joint) to assess the resistance of the muscle and the possible presence of a spastic catch. Elements 1, 2, and 6 assess dystonia: the first item concerns rubbing the skin of the unaffected limb and waiting for any unvoluntary movement/posture of the designated limb. The second item consists in a list of five simple tasks among which the assessor has to

choose two, depending on the ability of the subject; each task has to be performed for ten seconds, and involuntary movement/postures of the designated limb are monitored. The sixth item is basically the mixture of item 3 and item 2, looking for an increased tone with a movement of another body part. The remaining items deal with rigidity. If at least one item of the subgroup is considered positive, it confirms the presence of the subtype.

The detailed description of the protocol is reported in table 1.3.

HAT ITEM	SCORING GUIDELINES (0=negative or 1=positive)	SCORE 0=negative 1=positive *(circle score)*	TYPE OF HYPERTONIA
1. Increased involuntary movements/postures of the designated limb with tactile stimulus of a distal body part	0= No involuntary movements or postures observed	0	DYSTONIA
	1= Involuntary movements or postures observed	1	
2. Increased involuntary movements/postures with purposeful movements of a distal body part	0= No involuntary movements or postures observed	0	DYSTONIA
	1= Involuntary movements or postures observed	1	
3. Velocity dependent resistance to stretch	0= No increased resistance noticed during fast stretch compared to slow stretch	0	SPASTICITY
	1= Increased resistance noticed during fast stretch compared to slow stretch	1	
4. Presence of a spastic catch	0= No spastic catch noted	0	SPASTICITY
	1= Spastic catch noted	1	
5. Equal resistance to passive stretch during bi-directional movement of a joint	0= Equal resistance not noted with bi-directional movement	0	RIGIDITY
	1= Equal resistance noted with bi-directional movement	1	
6. Increased tone with movement of a distal body part	0= No increased tone noted with purposeful movement	0	DYSTONIA
	1= Greater tone noted with purposeful movement	1	
7. Maintenance of limb position after passive movement	0= Limb returns (partially or fully) to original position	0	RIGIDITY
	1= Limb remains in final position of stretch	1	

Table 1.3: *Hypertonia Assessment Tool (HAT).*

MAS and BAD scales do not differentiate between hypertonia signs, while HAT aims to do that, but it does not give a clear and reliable representation of the clinical state, as all the clinical scales. However, the protocol is very detailed, showing a good reliability and validity for the assessment of spasticity and rigidity, while it is moderate for dystonia [18], [25].

In the end, the last clinical scale is not related to the assessment of functional tasks, but it represents a more general evaluation of the capabilities of a subject, useful to compare, for example, the efficacy of a treatment or possible degeneration of the disease. The Gross Motor Function Classification System (GMFCS) aims to do that [26]. It is a five-level evaluation system with different versions according to the age of the subject (five different versions - ranging from less than 2 years old to 18 years old - were developed), highlighting basic functions like sitting, or climbing stairs, fundamental to live in community. This approach can be useful to give a general idea of the conditions of a patient, but it lacks quantities to compare in a more objective way.

Only providing objective quantities it is possible to achieve a reliable diagnostic tool in order to select the most suitable treatment and to assess its effects in a long-term view [27]. This is why, pushed by this strong clinical need, starting from the end of the twentieth century, researchers started to develop quantitative assessments, implying the use of dynamometers, torque motors, optoelectronic and motion capture systems, and the analysis of the electromyography (EMG) signals.

1.3 State of the Art

1.3.1 Spasticity

Regarding the need to quantify spasticity, one of the first work was conducted by Ensgberg *et al*. in 1996 [28], who observed a population of 17 children with spastic diplegic cerebral palsy and 6 controls. Using an isometric machine (KinCom dynamometer), they passively stretched lower limbs at four different velocities (10, 30, 60 and 90°/sec) through the entire range of motion (ROM) of the patients,

aligning the knee axis to the axis of the machine and using stabilization straps to keep the desired position, measuring the force applied to the supporting arm. From these measurements, they computed and used the slope of the angle-torque relationship as an indicator of stiffness. As they expected, compromised subjects showed greater slopes compared to healthy subjects, with encouraging results for good reliability, despite a low correlation with the Ashworth scale for spasticity.
The importance of this pioneering work consists in the use of a single number parameter, the slope of the calculated line, which is easy to calculate and embeds the three major components that characterize spasticity: speed, resistance, and ROM.

The same stiffness parameter, with a similar approach, was achieved by Damiano *et al.* in 2002 [29], using in addition surface EMG (sEMG) electrodes placed over quadriceps and hamstrings muscles, respectively knee extensor and knee flexor, to verify if a stretch response occurred. In this way, it was possible to detect the onset angle of the stretch response at 30, 60 and 120 °/sec in 22 individuals with spastic CP (mean age 11.9 years) and 9 controls for comparison. They demonstrated, as they expected, that responses occur sooner in patient with more severe spasticity (previously assessed with the Ashworth scale). Moreover, a strong correlation with MAS scale was found for both the stiffness parameter and the onset angle (0.73 for stiffness at 120 °/s and -0.80 for onset angle at 30 °/s), while peak resistance torque was less significant (0.64 at maximum at 30 °/s).

Similar protocols were developed to assess stretch reflex [30]–[32]. The first step of all these research works consisted in the determination of the Dynamic Stretch Reflex Thresholds (DSRTs), namely the angles where there is an increasing in the EMG signal in correspondence of a given velocity; these points can be found using an isometric machine or just applying a manual flexion/extension. Starting from the

experimental points and applying a linear regression, it is then possible to compute the angle-velocity relationship. This operation allows to derive the Tonic or Static Stretch Reflex Threshold (TSRT or λ_+), the intersection at zero velocity, which cannot otherwise be directly measured. This parameter is fundamental according to the so called λ model, developed by Fieldman in 1986 [33], showing that if the TSRT is inside the physiological range of motion of the joint, it means that the subject is not able to completely relax his/her muscle. Furthermore, all the subjects were tested with the Ashworth clinical scale to find possible correlation.

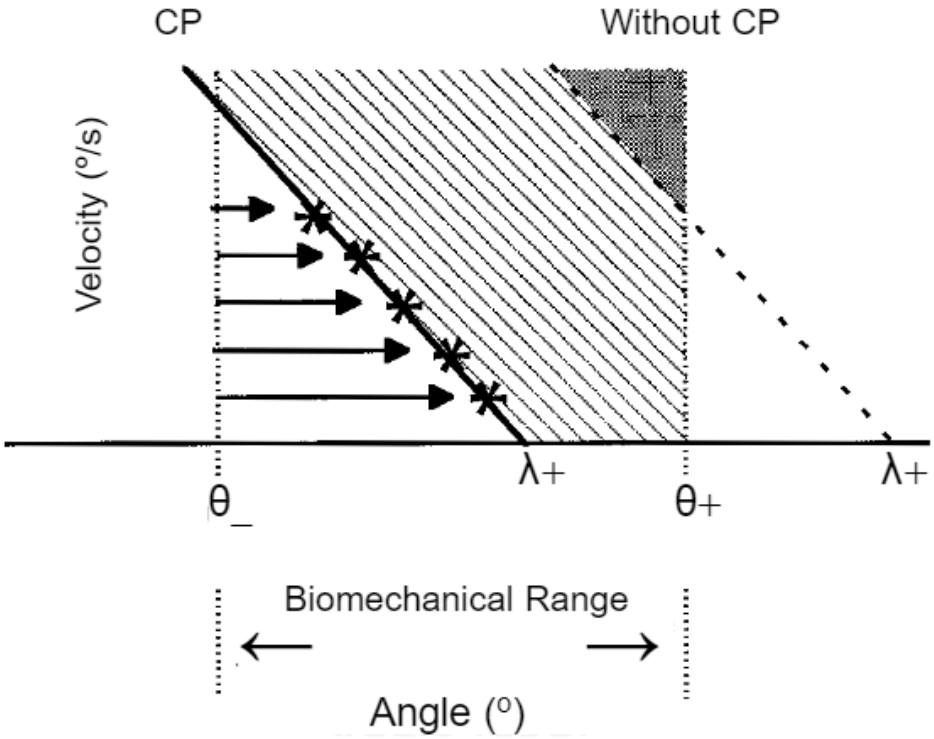

Figure 1.1: *Derived angle-velocity relationship showing the TSRT inside the biomechanical range (CP) or outside the range (without CP) from Jobin et al.* [30].

Jobin *et al.* studied a population of 14 children with spastic CP and 8 healthy subjects, using a torque motor at seven different velocities (8, 16, 32, 53, 80, 120 and

160 °/sec) and analysing the sEMG during arm stretched from full extension to determine the angle-velocity relationship [30]. In this case, the onset points of elbow flexors were defined as the first burst overcoming 2 standard deviations of the resting EMG signal, recorded at the beginning. From the line, it was possible to derive the Tonic Stretch Reflex Threshold and an indicator of velocity sensitivity computed as the reciprocal of the slope of the line, with changed sign. Despite the low correlation between the measurements and the clinical scale, they found a good test-retest reliability for λ_+ (0.73) – although not statistically significant - and a further proof that more severe spasticity results in lower TSRTs. The authors suggested that the large age range of the participants could have influenced the results or perhaps synergistic cocontractions. However, they propose to use this method to assess the efficacy of treatments aimed at decreasing spasticity.

In 2008, Calota *et al*. developed a simple and portable setup consisting in a single channel EMG, an electrogoniometer, and a PC for data analysis to evaluate stretch reflexes during a manual flexion of the elbow performed at different velocities [31]. From a sample of 20 subjects with chronic stroke-related spasticity, they extracted, as in the previous work, the TSRTs and used them as indicators of spasticity. Even in this work, the DSRTs were defined as the values corresponding to an EMG signal above 2 SDs with respect to the baseline. The results are also comparable, showing a good intra- and inter-evaluator reliability for moderate to high spasticity, without correlation with Ashworth scale. *The importance of the work consists in the simplicity of the equipment used and the easiness of the protocol, without lacking in solidity.*

With the aim to investigate if velocity dependence can be mediated not only by spasticity, but also by dystonia, Marinelli *et al*., in 2017, used an analogous method [32]. They studied a population of 30 subjects with Multiple Sclerosis (mean age 51.3

years) to differentiate between spasticity and dystonia on the base of the stretch reflex. Starting from a supine position, the subjects' knee was flexed, by an examiner, up to 90° at a selected speed to elicit SRs, while sEMG was recorded and angles were measured by an electrogoniometer. To help the examiner to elicit an accurate velocity, a metronome was used. A subject was classified as "dystonic" if tonic muscle activity was present during 1-min recording in rest position. The results show that SRs were present in both spasticity and dystonia: after repetitive stretches, in spastic subjects habituation (decreasing magnitude of SR) occurred, while in dystonic facilitation (increasing magnitude of SR) was observed. *This work is very important because, even if the aim was not to quantitatively differentiate spasticity and dystonia, it shows for the first time that velocity dependence can be caused by the two aforementioned hypertonia signs.*

More recent studies imply the use of Inertial Measurement Units (IMUs) [34], [35], which can be useful in localizing limbs in space and so, for instance, to measure kinematics parameters; in addition, they are generally easy to use and low-cost. Bar-On *et al*. in 2012 assessed 38 subjects (28 with spastic CP and 10 controls) manually stretching gastrocnemius and medial hamstrings at low and high speed over the entire ROM [34]. During this manoeuvre, sEMG signal was recorded and 2 IMUs were utilised to measure joint angles, angular velocities, and accelerations. Moreover, a force sensor load cell, anchored to the orthosis used as support, was used to compute torque. From these three synchronized signals, performance parameters were computed: ROM at low and high speed, maximum angular velocity (Vmax) at low and high speed, maximum voluntary isometric contraction, changes in RMS-EMG and torque at Vmax between low and high speed, and change in work, computed as the area underneath the torque-position relationship, again between low and high speed. Results show a moderate correlation with computed

parameters and clinical scales; in this case, also the Modified Tardieu Scale (MTS), a 5-level ordinal scale similar to the MAS, was performed [36]. Authors concluded that the extracted parameters are sensitive to measure spasticity, while scales are not enough precise to investigate it.

In 2018, Choi *et al*. as well quantified spasticity through IMUs, in a version without magnetometer not to interfere with other possible electromedical devices [35]. They assessed 28 spastic CP subjects and 5 controls, manually stretching the leg; the assessor was helped in reaching the Passive Stretch Velocity (PSV) by a visual biofeedback, high enough to evoke muscle reactions, and more reliable than just applying fast movements according to the experience of the assessor. The program allows to show simultaneously the target PSV, manually set, and the PSV measured by the gyroscope; the limit of this operation is the choice of the target, for which there is still uncertainty [37]. In this case, they choose the average PSV between the three maximum velocities collected by the clinician. Only IMUs were implied in the setup and the signals derived from them were used to develop a complex joint angle calculation method and a muscle reaction detection function. The assessment was compared with the Modified Tardieu Scale: the method showed good accuracy and test-retest and inter-rater reliabilities, while the results for MTS were poorer.

It is worth to mention that the studies in which it is not used a dynamometer for stretching, but instead just manual stretching is performed, are not less relevant [31], [32], [34], [35]. Rabita *et al.* even pointed out that SRs are more easily evoked with manual stretching because isokinetic devices cannot simulate transient acceleration [38].

1.3.2 Dystonia

Methods that try to quantify dystonia are more recent, compared to those devised for spasticity, and thus less developed. They basically aim at measuring overflow movements using an optoelectronic system. Unfortunately, until now, all the conducted studies were limited in time and with a quite small statistical sample (lower than 20 individuals); however, preliminary promising results were presented.

One of the first study was conducted by Jaspers *et al*. in 2011 on a population of 12 hemiplegic CP subjects with ages ranging from 6 to 15 years [39]. They developed an upper limb 3D motion analysis protocol composed of three reaching tasks (forward, upward, and sideways), two reach-to-grasp tasks, and three gross motor tasks (common daily activities) performed with the impaired arm at self-selected speed, in order to highlight movement peculiarities of CP subjects. All these exercises were recorded by an optoelectronic system; markers location was chosen according to [40], for a total of 17 markers placed on hand, forearm, arm, shoulder, and sternum. From the measurements, it was possible to extract joint angles and temporal parameters (duration and speed), following the recommendations of the International Society of Biomechanics (ISB) [41]. Despite the small statistic sample, results show good reliability within and between sessions.

Another work lead by Kawamura in 2012 asked participants to tap fingers of unaffected hand in time with an auditory cue, while possibly dystonic movements were recorded by a motion capture system [42]. In this case the population was composed by 11 children (4-18 years old) with upper extremity dystonia derived by stoke, traumatic brain injury, or cerebral palsy. Moreover, for those not able to tap

fingers, the protocol consisted in eye blinking. The extracted parameter (Index of Dystonia) was the sum of arm joint motion during active movement of the arm not involved in the task; this measure, firstly computed by Gordon *et al.* in 2006 [19], is regarded as a promising indicator for dystonia. Indeed, *Index of Dystonia* showed an excellent test-retest reliability for hand tapping (intraclass correlation coefficient 0.95) and for eye-blinking (0.74); moreover, *Index of Dystonia* correlated with BAD scale.

Secondary dystonia, derived from spastic diplegia CP or periventricular leukomalacia, was also recently assessed by Pons in 2017 on a sample of 7 children with ages ranging from 6 to 15 years old [43]. The protocol is an extension of the ELAPAP protocol [44], concerning the execution of nine tasks in a motion analysis lab: 5 functional tasks (hand to contralateral shoulder, hand to back head, hand to back pocket and drinking), 4 reach-to-grasp tasks, and 1 reach-and-point task at self-selected speed. After the assessments, 5 parameters were extracted: movement duration, average and maximum velocity, index of curvature, target accuracy and the previously cited Index of Dystonia [19]. As expected, compromised subjects showed a higher index of curvature, lower velocity, and poor target accuracy, reflecting the problems and the grade of compromission of the subjects. The results, furthermore, show a significant correlation between the Index of Dystonia and the Burke-Fahn-Marsden Dystonia Scale scores, considered the predecessor of the BAD scale.

Other studies deal with writing tasks, in particular with the execution of an 8-figure drawing [45], [46]. Casellato *et al*. studied a population of 15 children with different gene mutations (primary dystonia), asking the patients to draw two 8s on a paper; the execution was recorded by a motion capture system and EMG signal was

extracted from surface electrodes [45]. As indicators of dystonia, they used finger path curvature, finger velocity and its peak, symmetry between acceleration and deceleration, smoothness of the path and precision. During writing, children showed a compromised multisegment coordination, whereas healthy subjects showed a greater control and smoothness, with a good correlation with the BAD clinical scale.

A similar approach was used in 2015, where an iPad with an 8-figure to be followed by the subjects was introduced [46]. In this case, a Fourier analysis of the EMG signal was performed, and it was calculated accuracy and speed of the motion. The task correlation index, derived as the ratio between the sum of the spectral energy of the peaks in the task-relevant components and the full spectrum energy, showed a greater magnitude of task-uncorrelated components in the EMGs of dystonic subjects; the ratio between accuracy and speed resulted lower in dystonic subjects, meaning a lower quality product. Differently from the previous article, no correlation with the BAD scale was found.

From these works, we can conclude that also writing tasks, in addition with the more tested reaching and grasping tasks, can be useful in assessing and quantify dystonia.

1.3.3 Spasticity & Dystonia

The methods and procedures presented up to now aimed to quantify spasticity and dystonia separately, but, as previously mentioned, CP children often present mixed signs. For this reason, it is important to deliver a reliable and solid diagnosis, able to distinguish and quantify different dyskinetic symptoms, without the risk to leave untreated signs.

One of the first attempt to quantitively differentiate between spasticity and dystonia was done by Lebiedowksa in 2004 with a study on 17 CP children [27]. The protocol consisted in different parts: passively flexion and extension of the knee at three different velocities (0.2, 2 and 5 rad/s), using a handheld force transducer coupled with an electrogoniometer; measurement of the exertion of maximal voluntary flexion and extension with the knee at 90°, using a strain-gauge force transducer; measurement of patellar tendon reflex, using a reflex hammer and recording by a force transducer coupled with an electrogoniometer; gait analysis at self-selected speed, using an optoelectronic system. The observed parameters included resistance, maximum torque, patellar reflex, and classical indicators related to gait evaluation. Results showed that patients with dystonia had a greater co-contraction, increased resistance to external motion at slow velocities, impaired muscle strength, and slower walking. The most promising tool for the discrimination of the spastic or dystonic origin of hypertonia seems to be the analysis of EMG signal during stretch: prominent dystonic subjects showed muscular activation independent from the velocity of the motion and the amount of stretch.

Despite all the cited articles, which are important and contributed to develop the research in the dyskinetic field, it is worth to mention that the work of Gordon *et al*. in 2006 can be considered the most important study for our aim to differentiate spasticity and dystonia using reliable and quantitative measures [19]. Based on a sample of 13 children with spastic or extrapyramidal cerebral palsy and 8 controls, the procedure starts with a manual passive stretching of the elbow of the subjects at three velocities (25, 100 and 175 beats/minute) inspected by a rigidity analyser, composed of a force sensor and a gyroscope. Moreover, a reaching task (reach a target with the forefinger upon a "go" command) and a tapping task (tapping forefinger and thumb upon a "go" command) were recorded using a motion

capture system. From passive stretching, they derived the angle-velocity relationship using the slope as a stiffness parameter (similar approach used in [28], [29]), whereas overflow movements were summarized as the sum of arm joint motion during the active movement of the other arm performing the tapping task (the aforementioned *Index of Dystonia*); angles considered were shoulder flexion-extension, abduction-adduction and internal-external rotation, elbow flexion-extension and pronation-supination and wrist flexion-extension. Finally, from the study of the reaching task, it was possible to assess peak velocity, wrist path ratio, end point error and hold distance. For the recording, they used four to five markers placed on upper arm, forearm and hand, whose infrared emissions were captured by an optoelectronic system. Results are remarkably good: measures correlate with respective clinical scales, but not each other, meaning that parameters are clinically significant and independent.

1.4 Aim of the Thesis

The work deals with the definition of meaningful protocols for the extraction of dystonia-specific and spasticity-specific indicators within the context of the "DYSPA System", a research project aiming to quantify motor disorders in children aged 5 to 18, overcoming the limits linked to the traditional clinical scales. The main aim of my thesis work was to develop simple but effective protocols - both for upper limbs and lower limbs - according to the available literature and to an open discussion with child neurologists of the Besta Institute in Milan. The protocols consist in functional tasks (e.g., reaching, finger tapping and writing), passive stretching, and the more traditional gait analysis. We used the equipment available at the Motion Analysis Laboratory of the Institute, combining synchronized data coming from kinematics, kinetics and EMG signals of selected muscles; an

important part of my work consisted in the definition of the placement protocols for the EMG probes and for the passive markers of the motion capture system. Moreover, my thesis work focused on the extraction and computation of relevant indicators from the defined tasks and the related sensor placement. Such indicators should be able to provide the clinicians with quantitative parameters useful to support the diagnosis process and the treatment selection. Furthermore, they can be useful to compare pre and post treatment scenarios, evaluating possible improvements or worsening.

In the last part of my thesis, we tested the feasibility of the defined protocols, and we obtained some preliminary data on 3 pathological children and 4 healthy age-matched controls. In addition, an adult pathological subject was tested to verify if the protocol can be suitable also for grown-up pathological population.

2. Materials and Methods

The present work was carried out at the Movement Analysis Laboratory of Fondazione I.R.C.C.S. Istituto Neurologico Carlo Besta in Milan within the framework of the research project "The DYSPA System: a novel neuro-motor assessment to quantify dystonia and spasticity in children with acquired and genetic movement disorders", under the guidance and supervision of the Principal Investigator Francesca Lunardini.

2.1 Participants

The DYSPA Project intends to recruit patients with movement disorders followed at the Child Neuropsychiatry Unit of the I.R.C.C.S. Carlo Besta. Both inpatients and outpatients will be recruited, following these inclusion criteria:

- Diagnosis of genetic or acquired movement disorder with a clinical phenotype of pure dystonia, pure spasticity or mixed form of spasticity and dystonia
- Age: 5-18 years
- Ability to understand and perform the experimental procedure

And exclusion criteria:

- Severe weakness

A control group consisting of healthy children of comparable age will also be recruited.

In addition, preliminary testing on a subgroup of 5 healthy subjects and 5 patients will be performed to check the quality of the collected data and optimize the system (apparatus and protocols). My thesis work is conducted within this part of the project, with the aim of testing and validating the developed protocols.

2.2 Apparatus

The Istituto Neurologico Besta gave me the opportunity to use all the instrumentation located in the laboratory, including both hardware and software, in order to develop and extract meaningful parameters from the subjects.

2.2.1 Hardware

The main equipment inside the Movement Analysis Laboratory is the motion capture system, an optoelectronic SMART-D system by BTS S.p.A. [47]. The setup is composed of 8 infrared cameras connected to a workstation; the overall system is furthermore synchronized with 8 wireless surface EMG probes and 4 force plates.

a. Optoelectronic system

The working principle of an optoelectronic system is as simple as efficient, providing a very accurate estimation of kinematic parameters (trajectory, velocity, acceleration and jerk), in a non-invasive and totally painless modality. The cameras are composed of 2 different parts: an external circular crown provided with LEDs

emitting in the Near InfraRed (NIR) at 880 nm, and a coaxial central containing the circuitries for the detection of the luminous signal and the transduction into an electrical signal. In this way, covering the subjects' bodies with reflective passive markers, it is possible to exactly detect their position in space by enlightening from the LEDs and reading the rays that are scattered back to the cameras. It is important to underline that a reconstruction to 3D coordinates is only possible when a marker is seen at the same time by at least 2 cameras, otherwise the marker's position would be missed for those frames.

In this context, in order to allow the best possible view, the 8 cameras are permanently installed at the perimeter of the room at the top of the walls, and six of them are mounted on runners in order to slightly adjust their position according to the acquisition. Furthermore, 4 movable cameras are available in case of finer movements in order to reconstruct the trajectories with high grade of reliability.

In this system, the sample frequency is set at 70 Hz.

Figure 2.1: *SMART-D cameras by BTS S.p.A.* [47].

The markers used in this kind of setup are passive (just reflect the NIR light), since they are more practical than the active markers. Active markers directly generate the luminous signal, but are generally less used due to their uneasiness. Moreover, markers have different shapes and dimensions; for the most part they are spherical, but, for specific regions like the hells or the sternum, hemispherical ones are more suitable. They can be directly attached to the body skin or mounted on ad-hoc supports to minimize skin artifacts (e.g.: adjustable width band specifically provided for the thigh with a marker included).

Anytime we use an optoelectronic system, the first step is the calibration of the acquisition volume. To do that, the company provides a reference triad on which markers are mounted: 4 for the X-axis, 3 for the Y-axis, and finally 2 for the Z-axis. The first step is to acquire the triad laying on the floor, usually placed on a fixed point like the corner of a force plate, for nearly 1000 frames. The second step expects to spin the Y removable axis - the wand - all around the volume in which we would perform the acquisitions for about 6000 frames The calibration procedure is correctly performed if the image error calculated by the 3D reconstruction algorithm is below a certain threshold. Of course, higher is the acquisition time, higher will be the accuracy and so lower will be the error. If a camera is inadvertently moved, the calibration has to be redone; this is the reason why having the equipment fixed on the walls is an advantage.

Figure 2.2: *Calibration triad.*

The workstation is the processor of the system on which a Windows XP-operating system runs. All the peripherals are connected to the workstation. Apart from the traditional connectors for mouse, keyboard and monitor, there are a series of pair data-power connectors, one for each camera, and a section for analog connections to EMG probes. Finally, we can find 2 USB ports for data exchange and 2 LANs ports for ethernet communication.

Figure 2.3: *Back view of workstation SMART-D by BTS S.p.A.* [47].

b. EMG probes

The system is integrated with 8 bipolar EMG wireless probes (FREEEMG 1000 by BTS S.p.A. [47]). The absence of wires enhances the quality of the acquisition, reducing the time of each session and all the errors due to the encumbrance of a wired system; communication with the workstation exploits the LAN. Each probe is composed of a mother electrode (containing the A/D converter and the battery) and a satellite electrode (containing the signal conditioning unit), linked together with a flexible cable, allowing the positioning at variable distance as needed. Each probe presents a serial labelling number and a status LED, indicating the level of battery and the status of the connection. An ad-hoc charger is available to recharge the probes. A snap connector on each part of the probe allows the insertion of disposable electrodes, which are subsequently attached to the skin. Before

application, the skin is appropriately cleaned with alcohol to reduce the noise on the EMG signal; sensor placement follows appropriate positioning protocols ([48]). Probes communicate with a PocketPC and an acquisition unit, which together constitute the receiving unit. The handheld device, based on a Windows operating system, connects to the acquisition unit through a Compact Flash port, managing the data coming from the probes. All the probes are also equipped with a solid-state memory, used to secure data safety in case of signal loss; this memory is used only during acquisition, while if we want only to see the real-time situation, data are directly sent to the workstation

The sample frequency is 1000 Hz.

Figure 2.4: Receiving unit and *FREEEMG 1000 probe by BTS S.p.A.* [47].

c. Force platforms

The last devices inside the laboratory are 4 force platforms (P-6000 by BTS S.p.A. [47]), integrated and synchronized with the overall system. They measure the 3D ground reaction forces that the subject exchanges with the ground, standing or moving across them, and so they are in charge of extracting kinetic parameters.

They can be combined in order to create a sensory modular floor by placing the platforms one adjacent to the other, with a coverage on top of them. At the Besta laboratory, the 4 platforms are combined in a pattern represented in figure 2.4. The platforms are not clearly visible by the patient, so that his/her gait is not affected by disturbances.

Also, the position of the force platforms has to be calibrated, preferably before every acquisition session; calibration is conducted using the triad without the wand, so basically using only the X- and Z- axes, which are placed in the plate's corner.

For all the platforms, the acquisition frequency is set at 280 Hz and the full-scale of the vertical direction at 10000 N (platforms 1 and 3) and 20000 N (platforms 2 and 4).

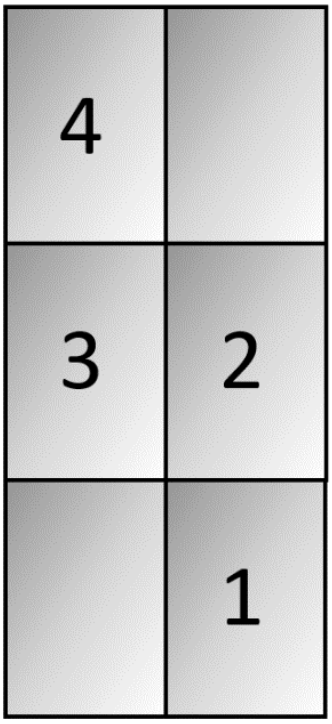

Figure 2.5: *Force plates arrangement in Besta laboratory.*

Figure 2.6: *Movement Analysis Laboratory of Fondazione I.R.C.C.S. Istituto Neurologico Carlo Besta in Milan.*

2.2.2 Software

The software for the setting of the technical parameters of the equipment, the acquisitions, the tracking of the trials, the management of the subjects and the data analysis is embedded in the SMART package (v.1.10.469.0), a powerful set of programs provided by BTS S.p.A.

The first software used in any acquisition is SMART Clinic. It is firstly needed to conduct the calibration procedure, both for kinematics and dynamics, and to setup all the technical parameters, for instance the sample frequency of cameras and force plates, and the full-scale of the platforms. All the parameters are stored so that when we open a new session, we do not need to insert again these data if not changed.

From the button in the top band “SMART Activation”, it is possible to activate only the devices that we need for that specific trial, preventing the storage of unnecessary data. This program is also essential for the management of the subjects and the trials associated to them. The first step is to select a patient or to create a new one; in the second case we have to fill the opening form with all the information required (name, surname, birth date and gender) and eventually the optional ones (name of clinician, address, town etc.). The subject will be associated to a unique ID code, and he/she will be displayed in the left panel of the screen and from now on it will be possible to create new sessions and new trials. We can have multiple sessions for each subject and multiple trials within each session, with the possibility to remove any of these in case of error. Every time a session is created, we have to give it a meaningful name to make easier the retrieval, select the pathology (in case of controls it will be “normal”) and the specific marker protocol that can be also “undefined”. Some marker protocols, like the Davis protocol, also need a set of anthropometric measures that will be inserted on an explicit opening table.

The right panel of the screen divides the trials into 3 different sections, depending on their level of processing: the first one contains the trials to be tracked (the very next step after acquisition), the second one contains the trials to be processed, while the last section presents the trials ready to be reported.

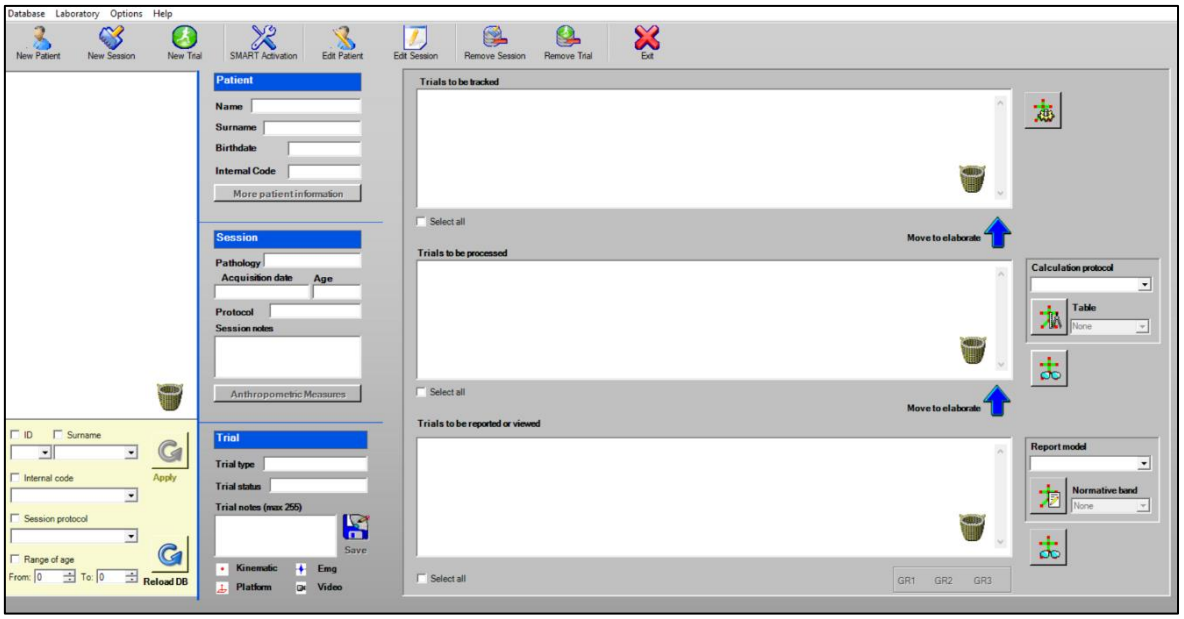

Figure 2.7: *SMART Clinic main panel.*

Whenever an acquisition is performed, the SMART Capture program opens, launched from SMART Clinic. From this software, we can monitor the environment looking from the different cameras and checking if all the markers are well visible. It is important to look for possible sources of errors that could generate false reflections, mostly mirrors and light coming from the windows. It is also possible to view in real-time the signals read by the EMG probes and the force platforms.
When the monitoring phase seems good, we can proceed to the acquisition phase, in which the cameras and all the other equipment record the task from a start to a stop command, always maneuvered from the SMART Capture. After having saved the data, the result will be a .tdf file, which can be read from the SMART Analyzer (the data analysis program) or other external software as MATLAB.

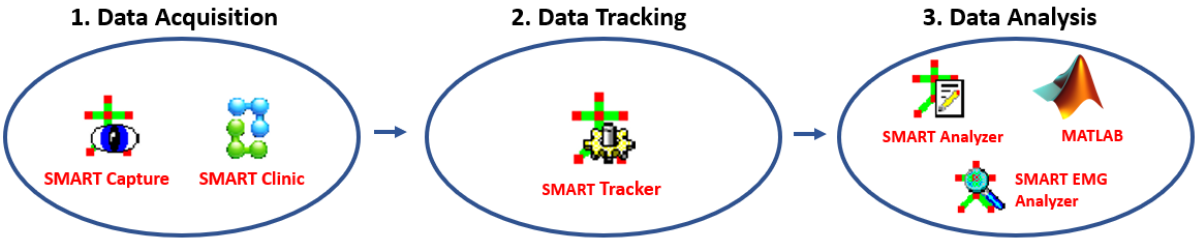

Figure 2.8: *Flow diagram with the software used in each protocol phase.*

Once the acquisition phase is done, it is good practice to immediately track the markers in order to detect any possible error; the software used is the SMART Tracker. From this program, we can firstly decide to open an existing model, like for example the preinstalled Davis Protocol, or to create a new one. A model is composed of points, corresponding to the markers, and links that will complete the prototype; to each marker is assigned a characterizing label name to detect it. Once the model is opened, we can load the acquisition and assign to each marker the corresponding label of the model. This procedure is crucial because we need to be very accurate in assigning labels, otherwise the 3D reconstruction will be wrong. Often markers are covered for some frames due to the movements performed and so we need to re-label them if the software misclassifies them.

In figure 2.7 we can look at a model in the left panel and the reconstructed acquisition on the right. The plots represent the position of a specific marker in the three axes, very useful during tracking so that we can check for any possible misclassifications.

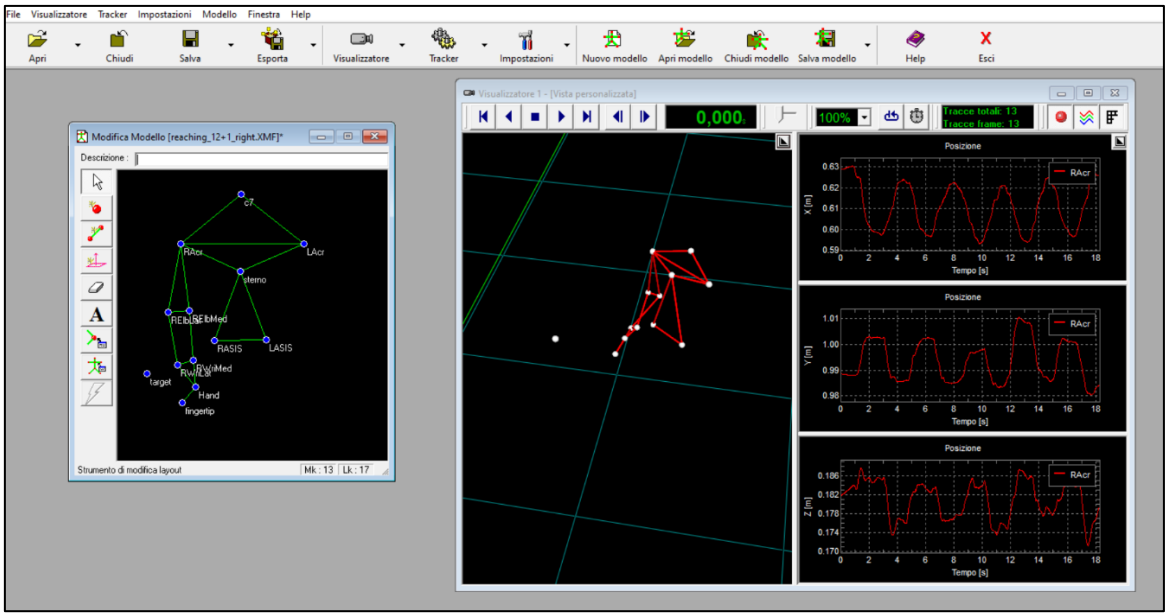

Figure 2.9: *SMART Tracker main panel.*

The SMART Analyzer, as said before, is the data analysis program, from which we can load single or multiple trials and make several computations. The key element is the protocol, where we can build the code using a sequence of different blocks, basically acting as black boxes, selecting the appropriate inputs and deriving the corresponding outputs. The blocks are several, organized on the specific output type they give; the most important types are vectors, scalars, 1D and 3D points, 1D and 3D velocities, 1D and 3D accelerations, 1D and 3D angular velocities, frequencies, times and EMG signals. The difference in 1D and 3D resides in how many coordinates we are analysing, just a single component (X, Y or Z) or the three-dimensional trajectory. Inside each "family output" we have different functions, the blocks, divided in mathematical operators (sum, difference, product etc.), MAX-MIN-MEAN operators and filtering operators (low pass, high pass and so on).

On a track, we can sign multiple time events corresponding usually to the start/stop of a specific movement while looking at the 3D viewer, so that we can be as precise as possible. Specific event operators allow dealing with these kind of data, for

example extracting the defined value of a track at that specific time event. Combining tracks and events, we can obtain cycles, from which it is possible to assess trends, averages and so on.

In figure 2.8, on the left panel there are folders divided by trial and type where we can find all the objects created in the protocol, helpful when dealing with very large protocols to find the data needed. The central part is the protocol itself; it is good practice to keep it tidy by using titles (text data) and by ordering the blocks in rows and columns according to the operation. The right part of the panel contains all the data we want to visualize, like for instance the 3D viewer of the acquisition, plots and numbers, with the possibility to superimpose data of the same type. Raw and computed data can then further be analysed by exporting the whole .tdf file, or the single .emt file relative to a particular data, in other environments like MATLAB.

From the SMART Analyzer it is also possible to create reports in which we can collect all the significant parameters calculated in the protocol, adding images and tables; this function is particularly useful to report gait trials.

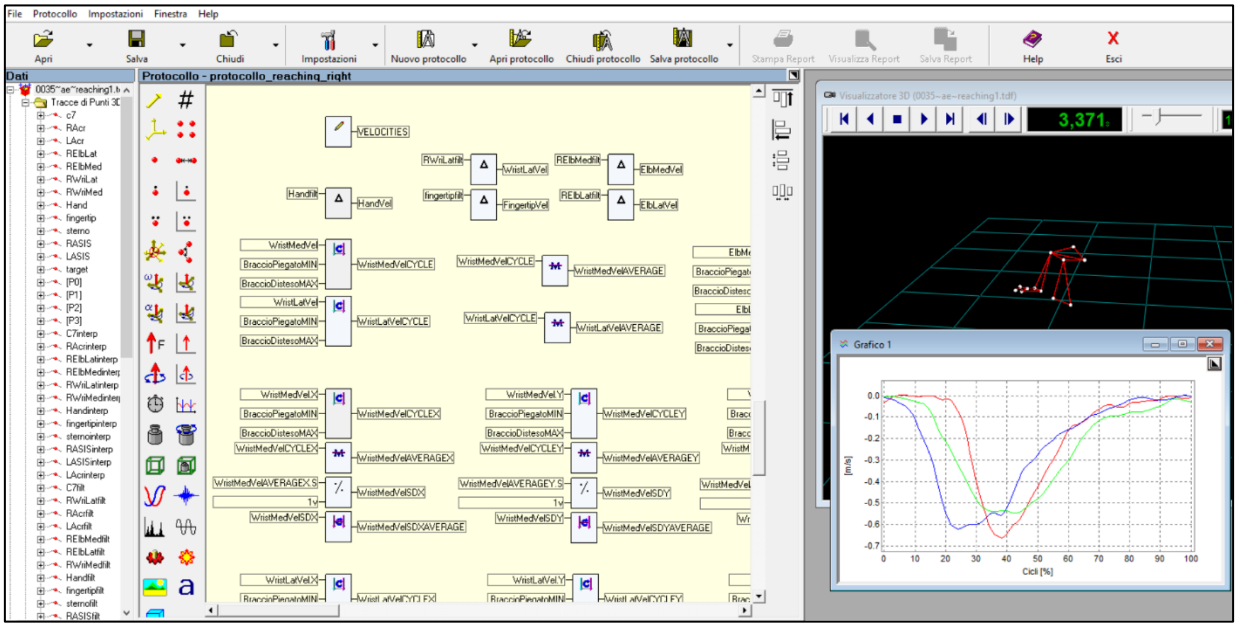

Figure 2.10: *SMART Analyzer main panel.*

There is also one more Analyzer software, the EMG Analyzer, dedicated to EMG signals management and analysis. From this program, it is possible to create new EMG protocols, selecting the probes and the relative muscles, and eventually running trials with the aim to record only the muscular activity, so without kinematics and kinetics. From the main panel, we can see at the same time all the signals coming from the probes, check if the probes are working in an appropriate way and their corresponding battery level. Additionally, it is possible to monitor the status of the connection through a simple indicator, green or red, depending on the situation.

2.3 Placement protocols

Placement protocols regard both the positioning of the passive spherical markers on the skin in specific landmarks and the positioning of the bipolar electrodes of the EMG probes on the muscles. In both cases, we have to follow as much as possible standardized protocols, in order to achieve robust and comparable results.

2.3.1 Markers placement

The positioning of the markers is a very crucial point because we want to replicate a model as near as possible to the anatomical reality, but without using a large number of markers. This is particularly true for children, especially pathological ones, for which wearing several markers could induce distress and interfere with the naturalness of the movement; therefore, the number of markers must be minimized, limited to easily accessible locations [49].

a. Upper Limb

Regarding the upper limb marker protocol, we developed an ad hoc model, mainly following the International Society of Biomechanics (ISB) recommendations [41]. The marker set is composed of 9 markers respectively placed on:

- Right acromion (RA)
- Left acromion (LA)
- Sternum (STE)
- Medial epicondyle (ME)
- Lateral epicondyle (LE)
- Ulnar styloid (US)
- Radial styloid (RS)
- 2° metacarpophalangeal joint (2MCP)
- Tip of the index finger (IND)

The markers on the acromion and the fingertip have chosen to be hemispherical, in order to better adhere to the skin, while the remaining ones are spherical.

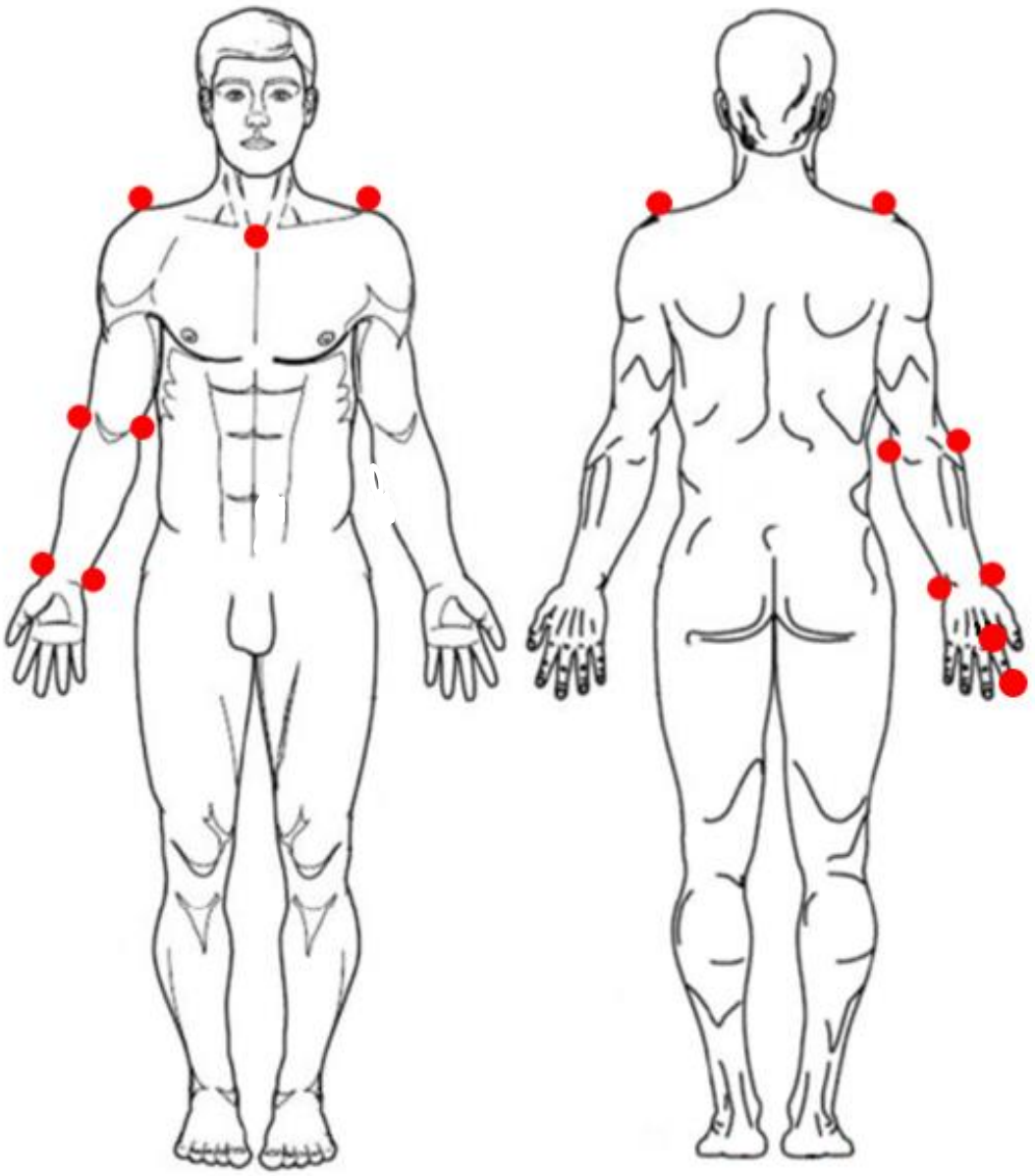

Figure 2.11: *Front view and back view of right upper limb marker set.*

The marker set is mounted on the right arm or on the left arm, depending on the subject. The quite limited number of markers allows a fast preparation of the patient, using landmarks easily accessible and hopefully not covered during the movements.

This model allows us to build 4 body segment coordinates systems: trunk, humerus, forearm and hand. Below, we report the details of the reference systems for a right-limb-mounted subject.

For the trunk coordinate system, we followed the biomechanical model presented by Hingtgen *et al.* [50], because the model presented in ISB guidelines expects the identification of the spinal process of the 8th thoracic vertebra (T8) and the suprasternal notch, which would be covered by the back of the chair/wheelchair, since the tasks of our protocol are intended to be performed while seated. The X-axis is the vector passing through the right and left acromion, the Y-axis is the cross product between X and a construction vector passing through the acromion mid-point (calculated) and the sternum, and finally the Z-axis is the cross product between X and Y. The reference system is centered in the mid acromion.

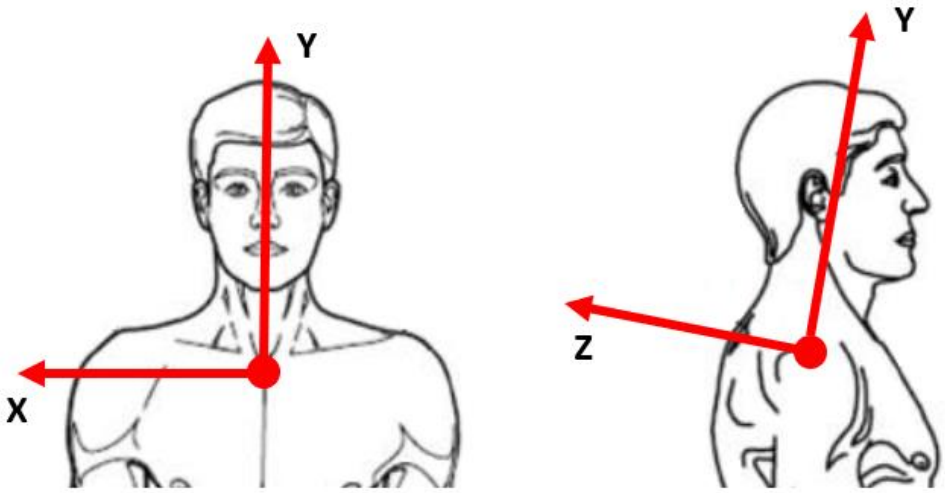

Figure 2.12: *Trunk reference system.*

The humerus reference system strictly follows the ISB guidelines, in particular we choose the 2nd option described, more suitable when the distance between the

medial and lateral epicondyles becomes shorter, as for children. In this context, it is firstly necessary to build a technical reference system, fixed in the acromion, using the acromion markers, the elbow markers, and the elbow mid-point to delineate the axes. Knowing from Rab *et al.* that the glenohumeral joint (GH) is approximately displaced to the 17% from the acromion distance in the vertical direction [51], we can pass from relative to absolute coordinates. In this way, the Y-axis of the anatomical reference system passes through the elbow mid-point and GH, the Z-axis is the cross product between two construction vectors, respectively passing through the lateral elbow and GH, and the lateral and medial elbow, while the X-axis is simply the cross product between Y and Z. The origin of the reference system is placed in GH.

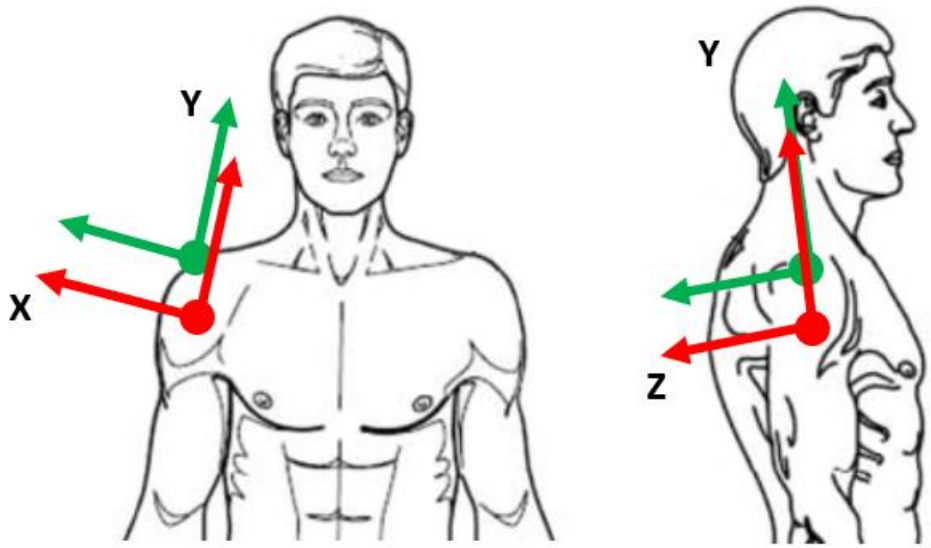

Figure 2.13: *Technical humerus reference system (green) and anatomical humerus reference system (red).*

The forearm reference system is centered in the medial wrist marker; the Y-axis passes through the medial wrist and the elbow mid-point, the Z-axis is obtained as the cross product between Y and the construction vector connecting the wrist

markers, and finally the X-axis is computed as the cross product between Y and Z, as described in the ISB recommendations, and similarly to the humerus reference system.

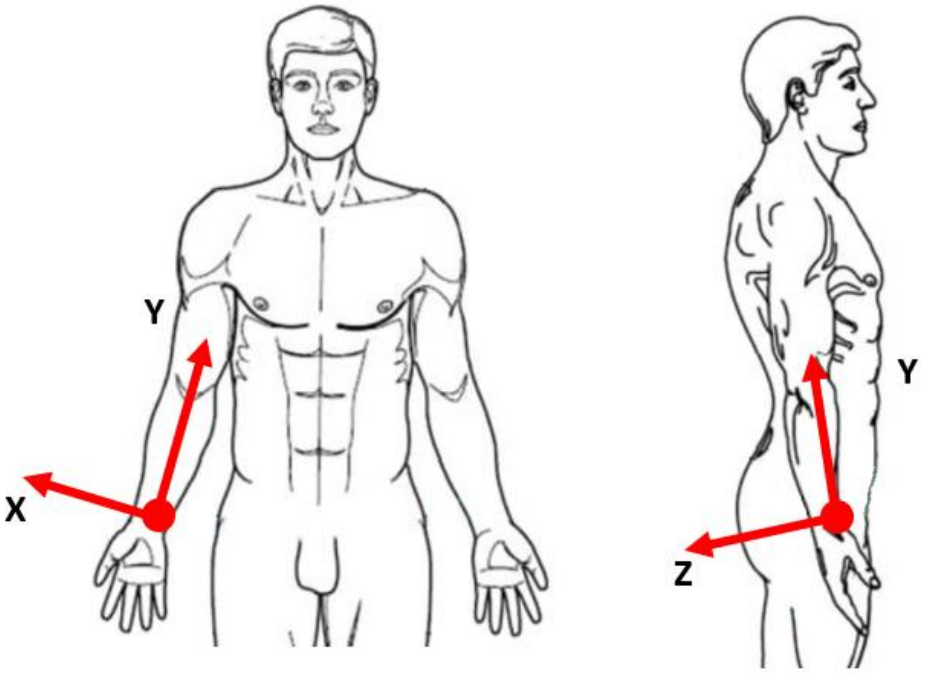

Figure 2.14: *Forearm reference system.*

The last body segment took under consideration is the hand, in this case developing a simplified version of ISB model, to allow a straightforward preparation and computation. The X-axis passes through the wrist markers, the result of the cross product between the latter and the vector connecting the medial wrist and the 2° MCP is the Z-axis, while the Y-axis is obtained as the cross product between Z and X. The origin is the marker placed on the 2° MCP.

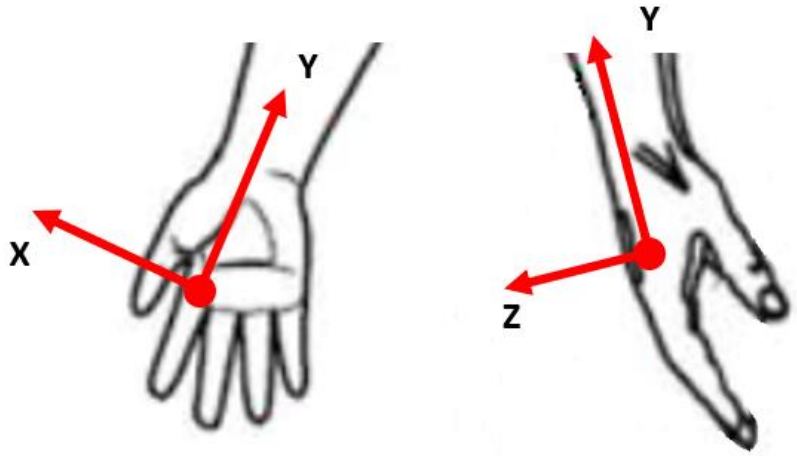

Figure 2.15: *Hand reference system.*

The Euler angles describe the position of a reference system, joined with a rigid body, through a series of rotations starting from a fixed reference. The resulted rotation will depend on the order on which the rotation angles are applied. In this way, considering two adjacent body segments, it is possible to derive the joint angles between them by applying one possible Euler convention: ISB recommendations suggest applying the XZY Euler convention. In this way, we can compute the upper limb joint angles: shoulder (trunk-humerus), elbow (humerus-forearm) and wrist (forearm-hand). Furthermore, considering the trunk reference system and the laboratory triad, we can assess the trunk inclination.

From these conventions, X is the mediolateral axis, Y is the vertical axis and Z is the anteroposterior axis; rotation around X is the movement of flexion-extension, rotation around Y is the internal-external rotation, and the rotation around Z is the movement of abdo-adduction.

b. Lower-Limb

Regarding the lower limb marker protocol, we decided to use the well-known Davis protocol [52], composed of 22 markers respectively placed on:

- Spinous process of the 7th cervical vertebra (C7)
- Sacrum (SAC)
- Right and left acromion (RA, LA)
- Right and left anterior superior iliac spine (RASIS, LASIS)
- Right and left great trochanter (RGT, LGT)
- Right and left mid femur (RMF, LMF)
- Right and left head of the fibula (RHF, LHF)
- Right and left lateral femoral epicondyle (RFE, LFE)
- Right and left mid tibia (RMT, LMT)
- Right and left malleolus (RMAL, LMAL)
- Right and left hell (RHELL, LHELL)
- Right and left V metatarsus (RVM, LVM)

In this setup, all the markers are spherical, except for the heel markers that are hemispherical; the markers placed on the femur and the tibia are mounted on a specific bandage support in order to minimize skin artifacts.

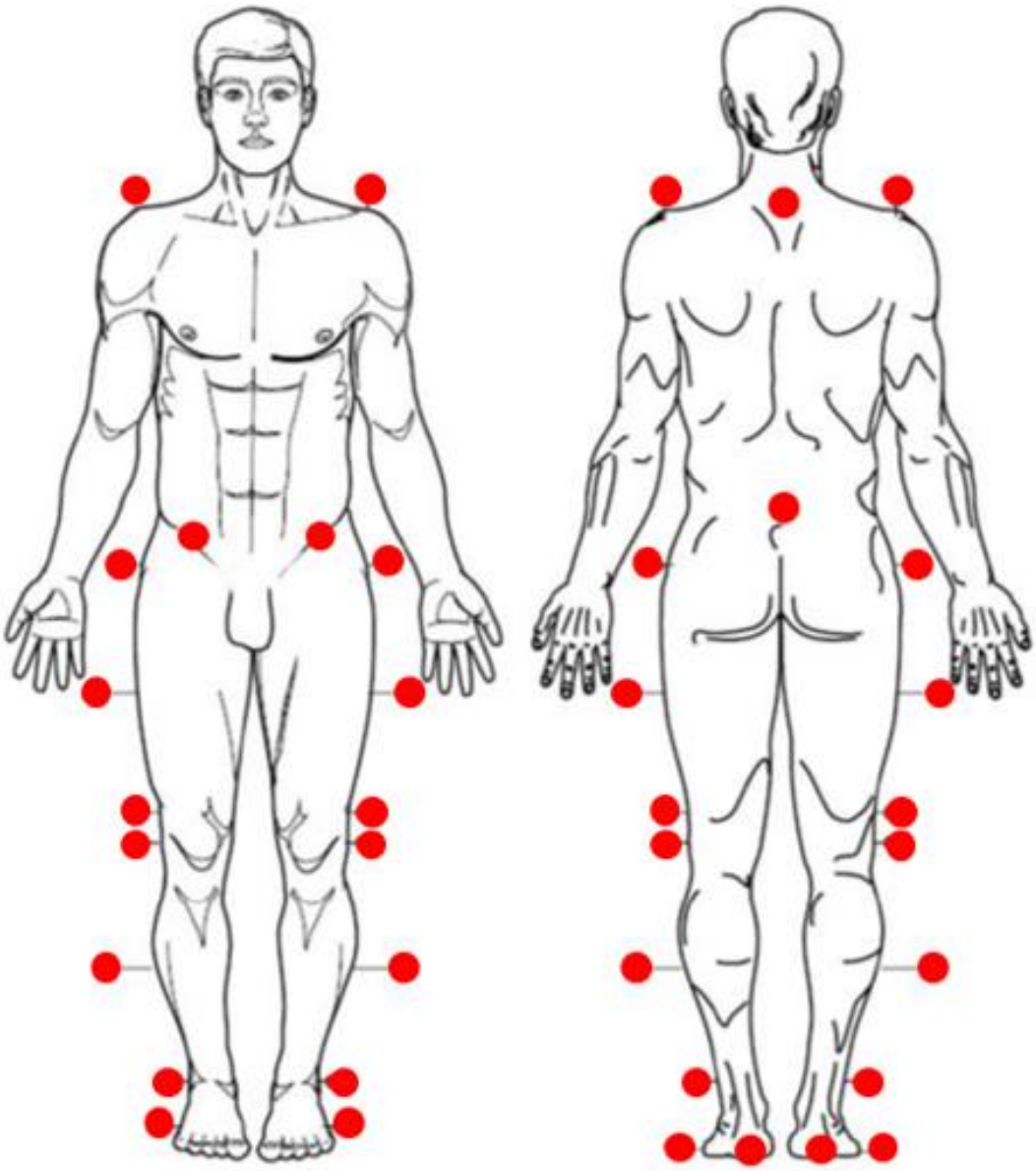

Figure 2.16: *Davis protocol marker set.*

For the Davis protocol, it is also mandatory to collect a set of anthropometric measures in order to detect the internal joint centres of rotation; in addition to height and weight, we need to measure the pelvis width and the diameters of knees and ankles, using a pelvimeter. Moreover, it is necessary to assess pelvis height and width, and the length of the legs.

The body segment reference systems for the lower limb are pelvis, thigh, calf and foot, and similarly to the upper limb case, we can derive pelvis, hip, knee and ankle angles. In the SMART Analyzer, the protocol is already embedded.

2.3.1.1 Upper Limb Protocol Validation

For the validation of the upper limb protocol created for this study, we evaluated the 3D angles computed by the model, in order to verify the angles conventions. To do so, we performed several trials in which control subjects executed, for each joint, separate movements for each rotation axis covering the entire ROM, paying attention to the sign of the angles and to the expected ROM with reference to the executed movement. The sequence of the movements for each joint is the following:

- Shoulder: 3 flexion-extensions (rotation around X), 3 internal-external rotations (rotation around Y), and 3 abdo-adductions (rotation around Z)
- Elbow: 3 flexion-extensions and 3 internal-external rotations
- Wrist: 3 flexion-extensions and 3 abdo-adductions
- Trunk: 3 flexion-extensions

Figure 2.17: *Subject performing validation trials.*

In order to achieve also the correct absolute values of the angles, we captured a standing trial in order to derive the offset angles of the upper limb and subtract these values from the tracks obtained from the validation trials.

2.3.2 EMG probes placement

For the EMG probes positioning, we followed the SENIAM (Surface ElectroMyoGraphy for the Non-Invasive Assessment of Muscles) guidelines [48], both for the upper limb and the lower limb. SENIAM is a European project aimed to standardize the use of sEMG, in order to enhance the exchange of data and their interpretation. The guidelines cover the preparation of the skin, the dimension, shape and material of the surface electrodes, the distance between them, and most important, their positioning over the muscles.
Not following a standardized protocol means to record data that could lead to a misinterpretation of the real scenario.

In order to reduce the voltage potential between the bipolar surface electrodes and the skin, due to the outermost layer of skin, the child's skin is properly scrubbed using alcohol before the positioning of the electrodes.

a. Upper Limb

Concerning the upper limb, the selected muscles are 8:

- Flexor Carpi Ulnaris (FCU)
- Extensor Carpi Radialis (ECR)
- Biceps (BIC)
- Triceps (TRIC)

- Anterior Deltoid (AD)
- Lateral Deltoid (LD)
- Posterior Deltoid (PD)
- Supraspinatus (SS)

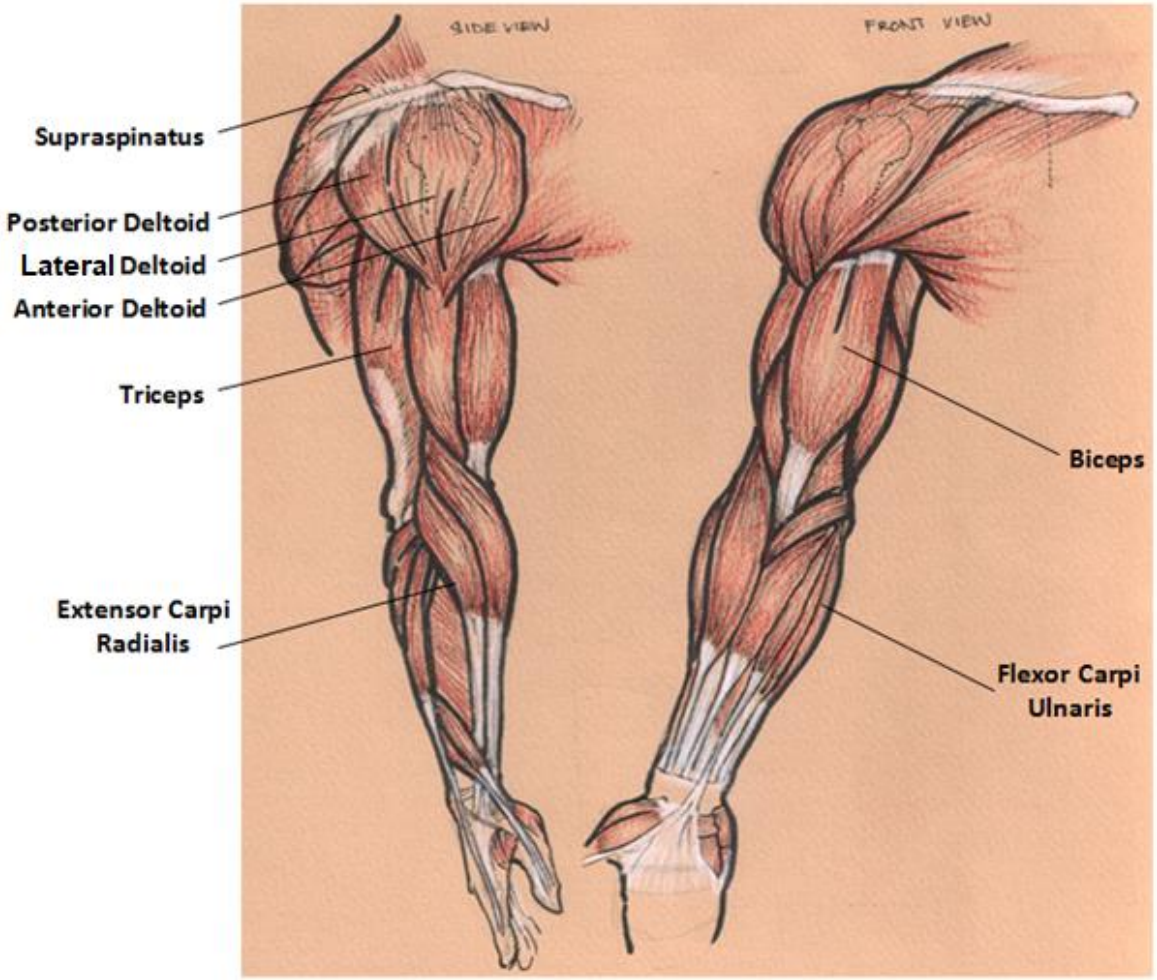

Figure 2.18: *Upper limb EMG protocol.*

The distance between each pair of electrodes is 20 mm, placed in the direction of the muscular fibres. Depending on the function of the muscle, the patient is asked to

exert an isometric force against the operator; in this way, it is possible to identify the exact location where to apply the electrodes.
In SENIAM guidelines, there is a page with a detailed table for each muscle. Below, I reported only the instruction relative to the biceps and the triceps.

The biceps is a flexor of the elbow joint, so we ask the patient to sit on a chair with his elbow flexed so that the forearm is in a horizontal downwards position. In this position, we ask the patient to try to flex his arm, while we block this movement pressing against the forearm in the direction of the extension. The electrodes have to be placed on the line between the medial acromion and the fossa cubit at one third from the fossa cubit.
Conversely, the triceps is an extensor of the elbow joint, so we ask the patient to sit on a chair with his shoulder at 90° in abduction with the arm 90° flexed and the palm pointing downwards. We request the patient to extend the elbow while we apply pressure to the forearm in the direction of the flexion. The electrodes need to be placed at 50% on the line between the posterior crista of the acromion and the olecranon at two finger widths medial to the line.

b. Lower Limb

Regarding the lower limb, we selected 4 muscles for both sides:

- Rectus Femoris (RF)
- Semitendinosus (ST)
- Tibilias Anterior (TA)
- Soleus (SO)

We make this choice in order to have one flexor and one extensor of the knee (ST and RF), and one dorsiflexor and one plantarflexor of the ankle (TA and SO).

Figure 2.19: *Lower limb EMG protocol.*

Also in this case, following the SENIAM guidelines, the bipolar electrodes are placed at a distance of 20 mm on specific landmarks.

For the Rectus Femoris, an extensor of the knee joint, we place the patient sitting on a table with the knees in slight flexion; in this position, we ask the patient to try to extend his knee without rotating the thigh while applying the pressure against the leg, above the ankle, in the direction of flexion. The electrodes will be positioned at 50% on the line from the anterior spina iliac superior to the superior part of the patella. On the contrary, the Semitendinosus is a flexor of the knee, and we have to place the electrodes in the direction of fibers, as always, on the line between the ischial tuberosity and the medial epicondyle of the tibia. The clinical test expects the

patient to lay down on the belly with the knee flexed less than 90°; in this position we ask the patient to flex the knee while applying pressure in the direction of knee extension.

Passing to the muscles concerning the ankle, to localize the landmarks on the Soleus we have to put a hand on the knee and push the knee downwards while asking the subject, sitting on a chair, to lift the heel from the floor. The electrodes need to be placed at two-thirds of the line between the medial condyle of the femur to the medial malleolus. For the assessment of the Tibilias Anterior, finally, the electrodes will be placed on the line between the tip of the fibula and the medial malleolus at one third. The clinical test is the opposite of the latter, applying pressure in the direction of the plantar flexion supporting the leg above the ankle.

2.4 Acquisitions Protocols

Protocols are developed to acquire data from the upper or lower limb, according to the subject, assessing the dominant side. Each protocol embeds a series of different tasks based on the available literature and discussed with expert child and adult neurologists, in order to extract meaningful indicators of spasticity and dystonia.

Each protocol has to be simple and as agile as possible, in order to be administered to children without any difficulties and minimizing the fatigue effects. Protocols have been tested on controls in order to select the best experimental design.

2.4.1 Upper Limb Protocols

The protocol to assess the functionality of the upper limb encloses 4 different tasks: reaching, finger tapping, writing and passive stretches.

The very first thing to do is to perform a Maximal Voluntary Contraction (MVC) acquisition of the muscles assessed in order to normalize the EMG signals for these values and so to make possible comparisons between sessions and between subjects. In these trials, we just ask the patient to exert the maximal force, blocking the corresponding movement, and measuring the EMG signals from the probes (similar to the procedure for the identification of the landmarks of the EMG electrodes).

a. Reaching Task

Reaching task is a common exercise in which the subject is asked to reach, or at least get closer to a target with his/her index finger [19], [39], [43]. This movement is simple to understand and to perform by the children, but at the same time gives us a lot of information about the coordination, the followed motor scheme and possible alterations.

In our setup the subject is comfortably seated on a chair with his/her arms relaxed. In front of him/her, we placed a structure on which we fixed a reflective marker as target. Upon a go command, the subject is asked to reach the target with his/her index finger at a self-selected speed in order to approach the target as good as he/she can, according to his/her possibilities.

Two trials are acquired for 5 repetitions each.

The marker set is the above mentioned in section 2.3.1, with the addition of the target, while the EMG protocol is described in section 2.3.2, mounted on one single arm, selected according to the subject.

b. Finger Tapping Task

The tapping task is less studied in literature, but it very common in clinical practice. It consists in asking the patient to join thumb and index of the same hand for a fixed

amount of time [19], [42]. Again, the exercise is simple, so well performable by children, but can be compromised by dystonia and so worth to study.

The subject is seated on a chair and, upon a go signal, he/she is asked to perform the task for 10 seconds, with his/her arm flexed at about 90° and abducted. The operator does not give any specifications about the number of movements he should have to fulfil, but just tell the patient to focus on the execution.

Two trials are recorded for 10 seconds on the contralateral arm (i.e., the arm without the probes and markers on it), as shown in literature [19]; moreover, we decided to perform two additional trials, always for 10 seconds, on the ipsilateral arm. This is done because it can happen that dystonia shows up during an active movement or during the motion of other body parts.

The marker and EMG protocols are the same of the reaching task, with the removal of the marker on the index to allow a better movability.

c. <u>Figure-8 Writing</u>

The writing of a figure-8 is a smooth movement, easy to execute and characterized by well-defined frequency aspects related to specific muscular patterns. Moreover, writing in general is crucial, especially for children, and it is often compromised in dystonia.

Briefly, the subject is sitting at a desk with an A4 paper sheet and a pen; the outline of a figure-8 is printed on the paper (18 cm (Y) x 9 cm (X), 2.5 cm width). The subject is asked to draw the figure-8 a certain number of times, following the boundaries as precise as possible, without stopping or removing the pen from the sheet; similar studies reported the same task [45], [46].

Two trials are recorded for 10 repetitions of the figure.

The marker set and the EMG protocol are the same of the tapping task, so without the fingertip marker.

d. Arm Passive Stretching

The last task is a passive extension of the arm; passive stretching is a well-studied task, particularly useful to detect possible forms of spasticity [30], [31].

In our setup, the patient is seated on a chair with the shoulder flexed at about 70° and slightly abducted, as described by Jobin *et al.* [30]. An operator gently extends the arm of the subject from full flexion to full extension, using a metronome to synchronize the movements.

We selected 3 different velocities, 60 BPM, 24 BPM and 12 BPM – namely fast, medium and slow – and we performed 8 repetitions for each velocity. Two trials are acquired for each velocity, with 5-10 seconds of rest between each stretching.

We selected a subset of the complete marker set used in the previous exercises. We are interested in the movement of flexion-extension of the elbow, so we can only leave the 2 markers on the acromion, 2 on the elbow (medial and lateral) and the lasts 2 on the wrist (medial and lateral), for a total of just 6 markers, removing the others. In addition, the EMG protocol is simplified just using 2 probes, one the triceps and one on the biceps.

2.4.2 Lower Limb Protocols

e. Gait Analysis

Walking is an essential activity for daily living and social participation; therefore, gait analysis (GA) is generally used to identify, quantify and understand the deficits of a specific patient and is fully integrated into the clinical decision-making of patients with complex gait disorders [53]. GA is a subset of the general quantitative

movement analysis, and it can be defined as the instrumented measurement of the movement patterns that make up walking and the associated interpretation of these [54]. It is a test easy to perform, but we need to pay attention to its correct execution, otherwise we could misinterpret the results. Gait analysis has a considerable potential in particular for CP children, in fact it gives the possibility to evaluate the effectiveness of a treatment as any other clinical tool [55] and modify surgical recommendations in about half of the cases [56].

Depending on the marker protocol selected, the first step is usually the collection of anthropometric measures useful to accurately define the internal centres of rotation of the joint; in our protocol, the marker set is the Davis, presented in section 2.3.1. In addition, an EMG protocol not too invasive, but effective, is necessary to investigate the muscular activity; in our case we selected 4 muscles for each leg, as described in section 2.3.2.

Once the patient is fully mounted, as for the upper limb, the first acquisition is an MVC trial of the analysed muscles. Then we can start to assess the first trial, the standing, in which the subject just stands in orthostatic position with one foot for platform. This task is necessary to make a postural analysis and collect the so-called offset angles, corresponding to the angles of pelvis, hip, knee and ankle in standing position. It is also important that the subject is aligned with the direction of axis along the longitudinal side of the room. After the single standing trial, we can proceed to acquire the walking trials, in which the subject is simply asked to walk along the room, at a self-selected speed, in a straight line corresponding to the axis of the laboratory. It is essential that during a gait analysis the subject touches only one platform for each foot, but without influence the pace, otherwise the trial will be discarded.

In order to have robust data, we decided to collect at least 3 walking trials per subject, a right compromise between reliability and the duration of the acquisitions. In our setup, gait analysis is even easier to perform thank to the integration with the SMART software.

f. Leg Passive Stretching

Besides gait analysis, another task is performed to assess the presence of any possible form of spasticity, a passive flexion of the leg, as described in previous works available in literature [32], [34]. In this case, we focus only on the flexion-extension of one leg, the more compromised, so the marker set is simplified using only 8 markers (2 on the ASIS, 1 on the great trochanter, 2 on the knees, 2 bands on thigh and calf, and the last marker on the malleolus). The EMG protocol is focused only on the flexor and the extensor of the knee, so we just use 2 probes, one on the RF and one on the ST of the tested limb.

After that, we can position the subject on the examination table in a supine position. Preventing the probe placed on the Semitendinosus to be in contact with the table, and so disturbing the EMG signal, we place a pillow under the hell. Starting from the maximum extension, the operator flexes the leg (hip and knee simultaneously) until maximum flexion, using a metronome for synchronization.

We selected 3 different velocities, 72 BPM, 48 BPM and 24 BPM – namely fast, medium and slow – and we performed 8 repetitions for each velocity. Two trials are acquired for each velocity, with 5-10 seconds of rest between each stretching.

2.5 Data Analysis

For the analysis of the data, the first step is to track the acquisition, acquired by the SMART Capture, using the SMART Tracker with ad-hoc models created following the marker sets explained in section 2.3.1. Once the tracking is successful, we can save the tracked data in a .tdf file and open it in the SMART Analyzer. For some protocols, we need to load different trials in order to perform all the expected computations. We developed different SMART protocols for each task (reaching, tapping, figure-8 writing, passive extension of the elbow, passive flexion of the knee and gait analysis), with right and left version for each task. In some cases, it was more practical to export the data, after some computations in SMART Analyzer or directly after the tracking, in MATLAB ®; for our project we used the version R2021a.

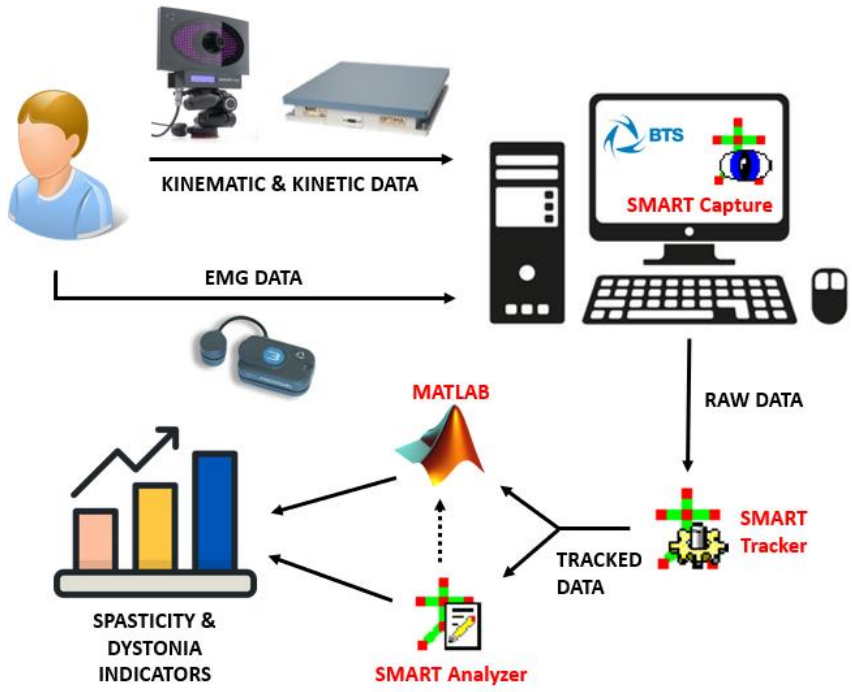

Figure 2.20: *Flow diagram from acquisition to indicators extraction.*

2.5.1 Pre-processing

The first step in order to analyse data is the pre-processing; in our case it is performed on the SMART Analyzer for kinematic data and on MATLAB for EMG data, even if it would be possible to do all the preliminary computations on the SMART Analyzer, but for practical reasons we used both.

During the acquisition phase, it is possible that some markers are accidentally covered for some of the frames, making it impossible to track them. In this case, the first thing to do is to interpolate the 3D data, using cubic spline curves. After that, to remove noise, all the trajectories are filtered using a low pass Butterworth with the cut-off frequency set at 10Hz.

For the EMG data, the pre-processing is done together with the calculation of the envelope of the signal, as described in the signal processing procedure by William Rose [57]. The first thing to do is to apply a band-pass filter (30-450 Hz) to remove low and high frequencies, then is essential to take the absolute value, the full wave rectification phase, and finally low-pass the signal using a Butterworth at 2 Hz, capturing the "envelope" of the signal. After this procedure, the signal will result easier to read. Subsequently, each signal is divided by its corresponding MVC so that we can make comparisons between sessions and subjects.

2.5.2 Indicators

We have extracted several dystonia and spasticity indicators, depending on the protocol, in order to have an overview as wide as possible of the subject's situations.

a. <u>Reaching Task</u>

For the reaching task, the first set of parameters regards the repeatability of the gesture; we expect that a pathological subject has a higher variability [19]. To compute it, first of all, we selected the time events corresponding to the beginning (flexed arm) and the end (extended arm) of the movement, looking at the 3D viewer of the acquisition on the SMART Analyzer. After that, we used these time events to create cycles in order to verify the repeatability of the gesture on the upper limb angles. The 8 selected angles were:

- Flexion-extension of trunk, shoulder, elbow and wrist
- Internal-external rotation of shoulder and elbow
- Abdo-adduction of shoulder and wrist

For each angle track, we take into account only the 3 central movements, when the gesture can be considered stable; we normalized the duration in percentage (0-100%) and, for each cycle, we selected the maximum and the minimum angles to compute the Range-Of-Motion (*ROM*) of each cycle and then the average *ROM* over the three cycles. Moreover, we calculated the average curve, corresponding to the trend of the angle, which can be completely altered in pathological cases, and from it we derived the standard deviation (*SD*) between cycles for each point and so the average *SD* [58]. Finally, we divided the latter result by the average *ROM* (*SD*/*ROM*), because it could happen that the amplitude of the movement influences the variability.

We just considered the absolute values of the angles as presented, without any computation, because we are interested in the *ROM* and the repeatability of the gesture, so the real values of the angles are not significant in this case.

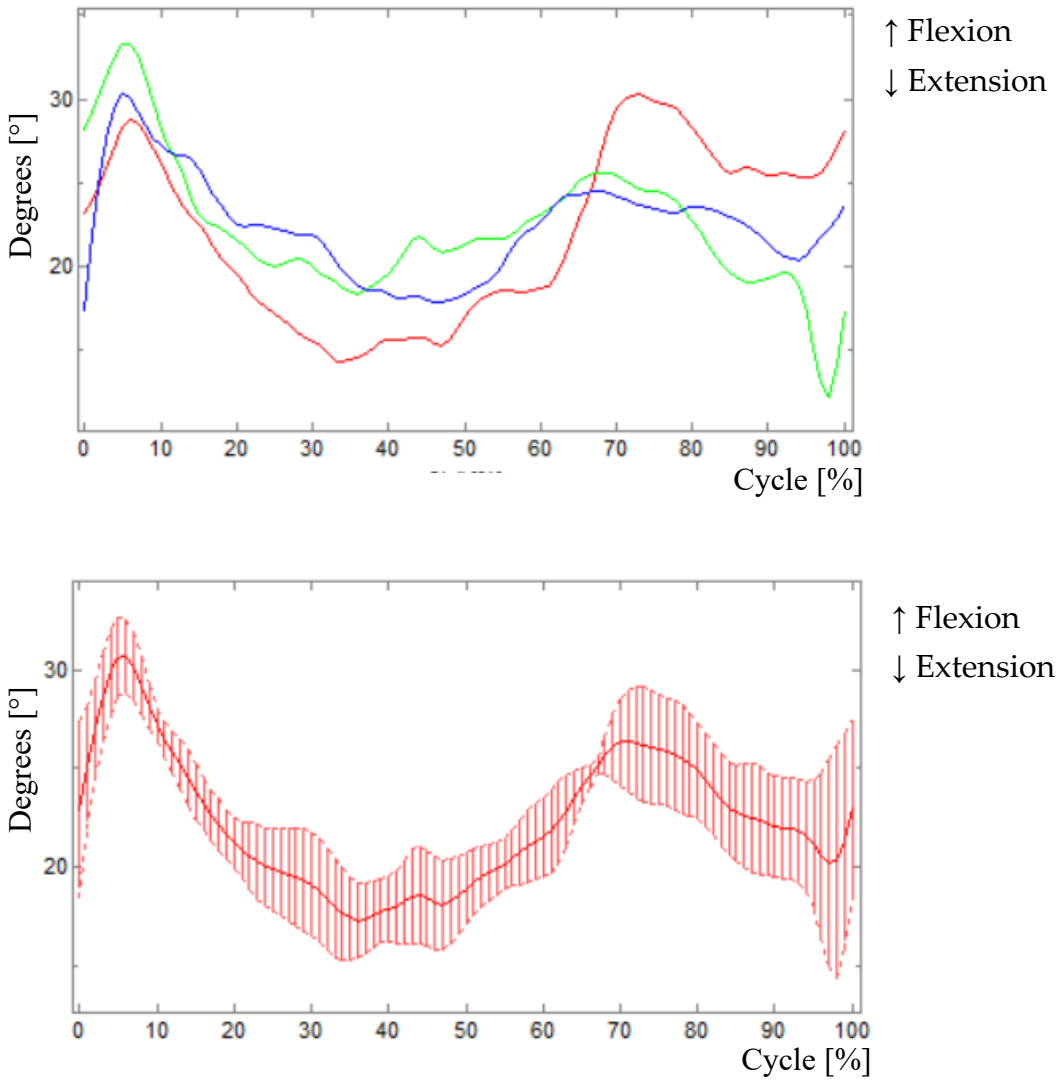

Figure 2.21: *Example of wrist flexion-extension angle in a pathological subject during reaching task; 3 central movements (top) and the average curve (bottom).*

A similar approach was followed to assess the repeatability of the velocity pattern, using the marker on the medial wrist as indicator. The velocity was derived computing the derivate of the trajectory. As described above, the normalized cycle of each movement and the average curve over the 3 central movements were computed. Moreover, it was also computed the *3D Peak Velocity* for each cycle and

then the global maximum, as illustrated in other works [19], [43], [45]. It is expected that in dystonic subjects the peak velocity is significantly lower than in controls.

Another relevant feature that can be extracted from the reaching task is the *Wrist Path Ratio*, that is the ratio of the path length executed by the wrist, over the length of the straight line connecting the start and the end positions [19], [43], [45]. The *Wrist Path Ratio* is expected to assume values close to 1 for controls, and greater values for pathological subjects, as reported in literature. In our setup, we used the marker on the medial wrist as indicator at the time events selected at the beginning, but also we calculated the same parameter using as reference the positions of the finger at the beginning of the movement, for each cycle, and the position of the target. The final parameter is the average of the ratios over the 3 selected movements.

The *Accuracy* of the task is another parameter already studied in other researches ([19], [43], [45]), calculated as the minimum distance between the fingertip and the target at the end of each movement. The indicator is again averaged over the three repetitions. The accuracy is expected to be lower for patients.

The last parameter computed for the reaching task is the *Jerk*, namely the time derivative of the acceleration [59], used as an indicator of smoothness and coordination of the movement [45]; lower is the value, smoother is the movement. However, this value is sensitive to the movement amplitude and the duration, that is why, sometimes, it is better to express it as a dimensionless jerk, in order not to have counter-intuitively results [60]. The formula of dimensionless jerk is:

$$J = \left(\int_{t_1}^{t_2} \dddot{x}(t)^2 dt \right) D^3 / v^2$$

where D is the duration of the movement and v is the velocity (mean or peak).

In our protocol, we calculated 8 different jerk-based measures, presented in [60]; these values are the *Normalized Jerk by Peak Velocity* and by *Mean Velocity*, the

Integrated Squared Jerk, the *Mean Squared Jerk*, the *Root Mean Squared Jerk*, the *Mean Squared Jerk Normalized by Peak Velocity*, the *Integrated Absolute Jerk* and, finally, the *Mean Absolute Jerk Normalized by Peak Velocity*.

Measure	Formula	Dimensions	Study
Integrated squared jerk	$\int_{t_1}^{t_2} \dddot{x}(t)^2\,dt$	$\frac{L^2}{T^5}$	Platz, Denzler, Kaden, & Mauritz (1994)
Mean squared jerk	$\frac{1}{t_2-t_1}\int_{t_1}^{t_2} \dddot{x}(t)^2\,dt$	$\frac{L^2}{T^6}$	Wininger, Kim, & Craelius (2009)
Cumulative squared jerk	$\sum_{k=1}^{n} \dddot{x}(t_k)^2$	$\frac{L^2}{T^6}$	Smith, Brandt, & Shadmehr (2000)
Root mean squared jerk	$\sqrt{\frac{1}{t_2-t_1}\int_{t_1}^{t_2} \dddot{x}(t)^2\,dt}$	$\frac{L}{T^3}$	Young & Marteniuk (1997)
Mean squared jerk normalized by peak speed	$\frac{1}{v_{peak}(t_2-t_1)}\int_{t_1}^{t_2} \dddot{x}(t)^2\,dt$	$\frac{L}{T^5}$	Hester et al. (2006)
Integrated absolute jerk	$\int_{t_1}^{t_2} \lvert\dddot{x}(t)\rvert\,dt$	$\frac{L}{T^2}$	Goldvasser, McGibbon, & Krebs (2001)
Mean absolute jerk normalized by peak speed	$\frac{1}{v_{peak}(t_2-t_1)}\int_{t_1}^{t_2} \lvert\dddot{x}(t)\rvert\,dt$	$\frac{1}{T^2}$	Rohrer et al. (2002)

Figure 2.22: *List of jerk-based measures from Hogan et al.* [60].

The last parameters exploit the EMG signals recorded during the gesture, calculating the *Co-contraction Ratios*, expressed as percentage, as showed by Lebiedowska *et al.* [27]. In particular, we computed the ratio of the activity of the biceps over the triceps (*BIC/TRIC*) during the first part of the movement - from rest position to fully extended arm - and the inverse ratio (*TRIC/BIC*) considering the last part of the movement, from fully extension to rest position again. The result is averaged considering all the movements of each task. Similarly, we computed the co-contraction considering the pairs *AD-PD* and *ECR-FCU*.

b. Finger Tapping Task

For the tapping task, the number of extracted indicators is lower. In particular, we have calculated the so-called "Index of Dystonia", already presented in section 1.3.2. The *Index of Dystonia* is the sum of joint excursion (ROM) of shoulder (flexion, rotation and abduction), elbow (flexion and rotation) and wrist (flexion) joints during the active movement of the other arm [19]. It has been shown that dystonic children present higher values compared to healthy subject, also in task different from the tapping [42], [43]. We calculated the *Index of Dystonia* as reported in literature and also adding to the sum the abdo-adduction of the wrist (*Modified Index of Dystonia*). Moreover, we asked the patient to perform the tapping with the not-mounted-arm, the contralateral trial, and the mounted-arm, the ipsilateral trial, also reflecting the possible variability in the gesture of the active arm.

Finally, also the *Trunk Inclination* was studied as illustrated above for the reaching task.

c. Figure-8 Writing

The features extracted from the writing of the figure-8 regard both the variability of the trajectory and the analysis of the muscular activation [46].

The *Spatial Repeatability* of the gesture was assessed, similarly as above, considering the time instants in which the movement begins and dividing the trajectory of the hand marker in 8 different cycles (the number of total movements without the first and the last ones). After that, it was possible to derive the average curve and to calculate the mean standard deviations along the X- and Z- axes, and the average between them. Moreover, the *Time Variability* was considered a significant parameter because we decided not to use a metronome for the time regularization

of the movement in order not to interfere with the natural gesture. Furthermore, jerk-based measurements were extracted, as in the reaching task.

Regarding the study of the coordination of the upper limb, and in particular between two adjacent segments, the *Continuous Relative Phase* (*CRP*), developed by Hamill *et al.* in 1999 [61] was computed. This measure was previously used in works applied to cycling [62]; here, we apply it to study the upper-limb coordination during the figure-8 writing task. The *CRP* is defined as the difference between the normalized phase angles (i.e., the four-quadrant inverse tangent of the ratio between the normalized angular velocity and the normalized angle at the same time instant) of proximal and distal body segments. To calculate it, first of all, it is necessary to divide the trajectories of shoulder, elbow and wrist joint angles and angular velocities of the 8 central movements, equalizing the durations. After that, we can proceed to the normalization using the following formulas:

$$\omega_{i,\ norm} = \left(\frac{\omega_i}{max\ \{|\omega|\}} \right)$$

$$\theta_{i,\ norm} = \left(\frac{2\ [\theta_i - \ min(\theta)]}{max(\theta) - min(\theta)} \right) - 1$$

where i denotes each data point of the cycle; the maximum velocity is taken considering all the cycles, while the maximum and minimum angles are confined to each cycle.

The phase of each data point for each joint is:

$$\Phi_i = atan\left(\frac{\omega_{i,\ norm}}{\theta_{i,\ norm}} \right)$$

Now it is possible to calculate the CRP, according to the equation:

$$CRP_i \ = \ \Phi_i^{proximal} \ - \ \Phi_i^{distal}$$

In our work, we considered the pairs arm-forearm and forearm-hand.

A *CRP* of 0° means that the segments are in phase, while 180° means perfectly anti-phase; positive or negative values indicate the prevalence, respectively, of the proximal or the distal joint phase. The variation of the *CRP*, the *CRPV*, is calculated as the standard deviation of each point on the *CRP* curve and quantified considering its average.

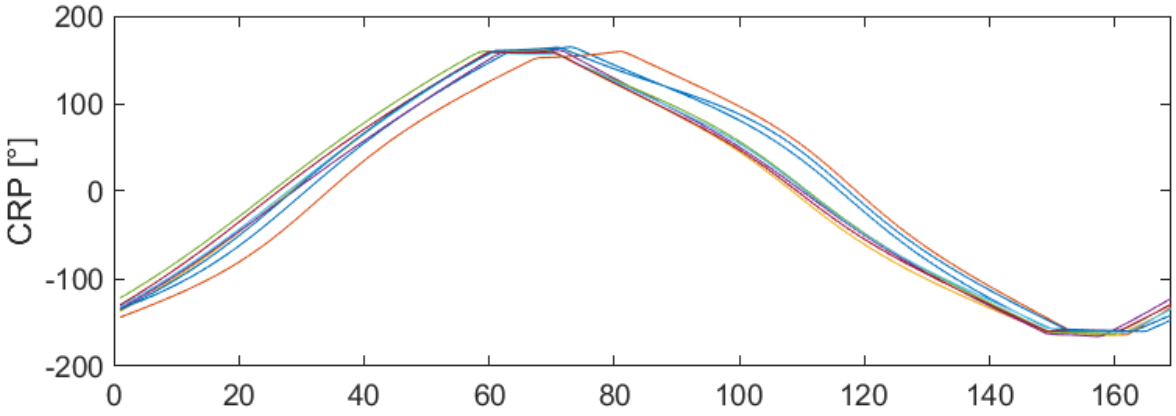

Figure 2.23: *Example of a CRP curve arm-forearm of a control subject.*

Finally, also the *Trunk Inclination* was assessed deriving the SD and the SD/ROM indicators, as reported above.

Figure-8 task is important not only for the repeatability of the gesture, but also for the study of the muscular activity involved during the movement; in this context, we calculated the "*Task-correlation Index*" (*TCI*), firstly proposed by Lunardini *et al.* in 2015 [46]. The first thing to do is dividing each EMG signal envelope into the 10 single figure-8 movements, based on the kinematics, then equalize the durations and re-assemble the sequence. The indicator exploits the computation of the Power Spectral Density (PSD) based on the Fourier Transform coefficient of the signals and the fact that frequency components relative to the horizontal movement (f_x) and the vertical movement (f_y) are expected to be in a ratio of 2:1.

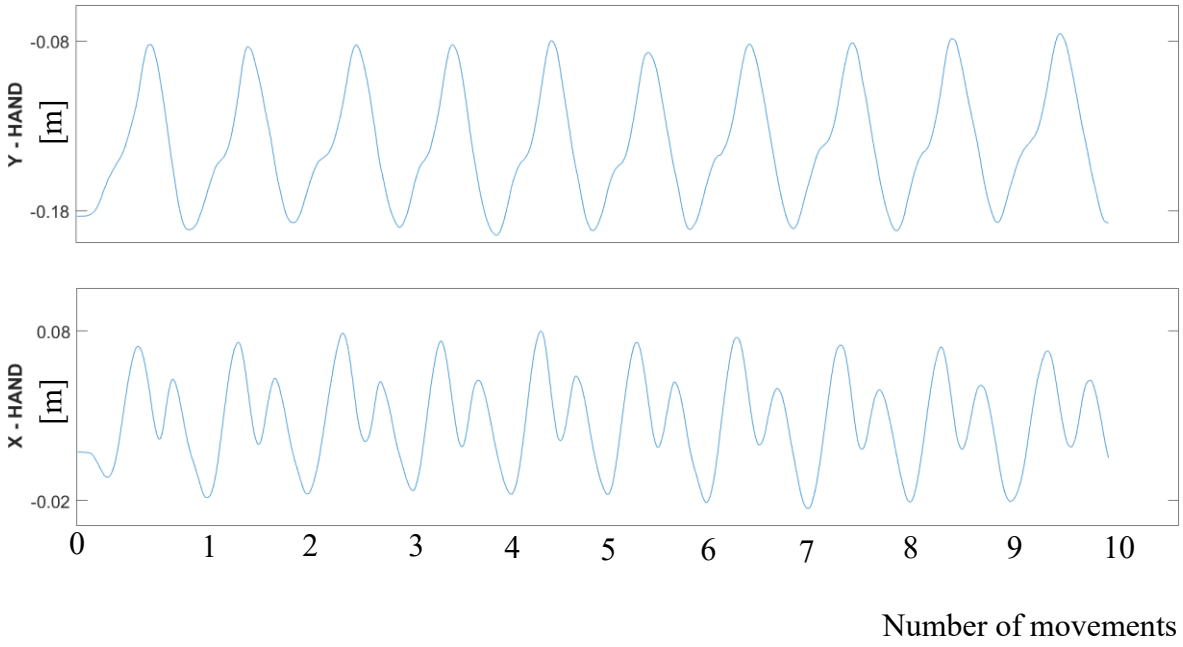

Figure 2.24: *Y and X trajectories of hand's marker during figure-8 movements.*

The sum of the spectral energy at f_x and f_y ($P_x + P_y$) is an indicator of the muscle activity correlated to the task, while the PSD components at the other frequencies are considered task-uncorrelated. The ratio between task-correlated components and the full spectrum energy is the TCI, calculated for each muscle:

$$TCI_m = \frac{P_x^m + P_y^m}{full\ spectrum\ energy}$$

We expect a greater magnitude of task-uncorrelated components, thus a lower *TCI*, for subjects with dystonia.

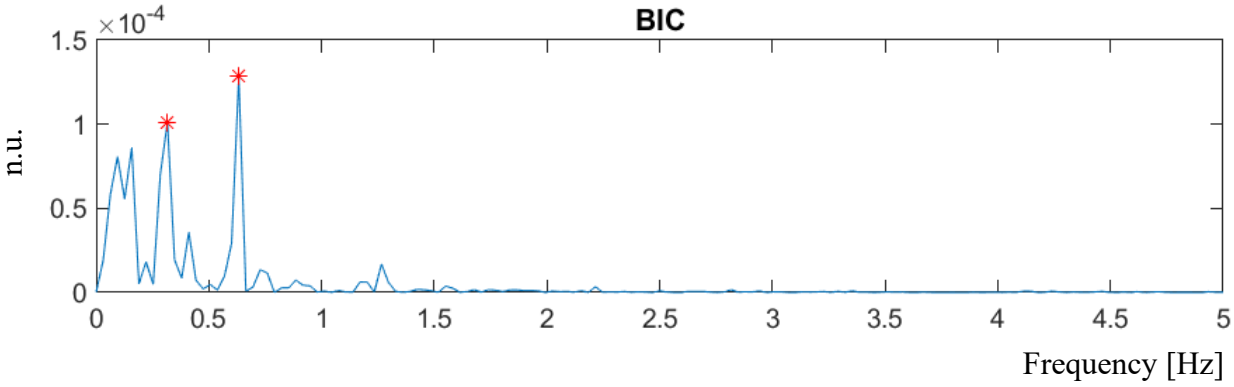

Figure 2.25: *Example of the PSD of the biceps of a control subject with clearly visible peaks at f_x and f_y .*

d. <u>Passive Stretching</u>

The passive stretching of the elbow embeds a series of indicators mainly related to the analysis of the EMG signal, in order to discover possible forms of spasticity. Anyway, the first step is the computation of the trend of the flexion-extension angle of the elbow, with the relative ROMs and average ROM, on the SMART Analyzer. After that, we set a threshold for 2 different reasons: i) detect possible activations of the triceps (the agonist), meaning that the movement is not completely passive, ii) detect possible catches of the biceps (the antagonist), meaning that the movement is corrupted by spastic components. To do that, the first step is selecting an appropriate threshold: we implemented two different options. The first choice is simply setting the threshold on the muscle envelope,

$$Threshold = \mu + J\sigma$$

where μ and σ are respectively the mean and the SD of the baseline of the EMG signal calculated on the period of inactivity of the muscle, while the constant J is set equal to 8 [57]. The second option uses the Teager-Kaiser (TK) Operator for the

identification of the onset times [63]. In this method, the operator transforms the signal as follows

$$y(n) = x^2(n) - x(n+1)x(n-1)$$

where $x(n)$ is the original EMG signal and n is the sample number. The threshold is detected on $y(n)$, using the same equation of the first method, with J set to 15 [57].
If the EMG signal of the agonist, in the time intervals referring to the extension, is above the threshold more than the 15% of the length of the time window, the movement is discarded. If the EMG signal of the antagonist, always in the same time intervals, eventually removing the not completely passive movements, is above the threshold for more than 20 frames, it will identify a muscular catch. Considering the angles and the angular velocities corresponding to the catches, it is possible to derive the angle-velocity relationship by linear regression and so the TSRT, the intercept at zero velocity, an indicator opportunely described in section 1.3.1 [30]. If the TSRT falls within the physiological range of motion of the joint, it means that the subject is not able to completely relax his/her muscle. The feature extraction was done on MATLAB, importing the filtered trajectories from SMART Analyzer, in particular filtering the angle with a low pass Butterworth filter at 1.5 Hz and the resulting angular velocity at 1 Hz.
Other meaningful parameters are the co-contraction ratios during voluntary flexion (*COFLEX*) and extension (*COEXT*), expressed as percentage, developed by Lebiedowska *et al.* [27]. For practicality, we used the MVC trial to assess these parameters, expected to be higher in subjects with dystonia.
Finally, it was calculated the so-called "*EMG-change*", namely the absolute change of the average EMG signal at fast and low velocity [34]; not all the movements were considered, but only the portions between the time interval 200 ms prior to peak velocity and the time corresponding to the 90% of the ROM of the elbow. The

average signal was the mean of the averages of each portion. Being spasticity velocity dependent, we expect a significant change for pathological children.

Exactly the same series of calculation and parameters' extraction was done for the passive flexion of the knee, considering that in this case the Rectus Femoris is the antagonist, the extensor, while Semitendinosus is the agonist, the flexor. The same considerations are valid also in these trials.

e. Gait Analysis

From the gait analysis, it is possible the extraction of 4 different categories of data: spatiotemporal parameters, kinematics, kinetics and EMG data [53]. The data are organized in reports containing numbers and plots.

The temporal parameters are calculated for each limb (right and left), and they express the duration of the *Gait Cycle* and the durations of *Stance*, *Swing* and *Double Support* phases [64]; the *Stance* phase is characterized by the foot in contact with the ground, in the *Swing* phase the foot is in oscillation, while during the *Double Support* phase both feet are in contact with the ground. These phases are also expressed as the percentage of the gait cycle, in particular, in physiological conditions, they are respectively near to 60% for *Stance* and 40% for *Swing*.

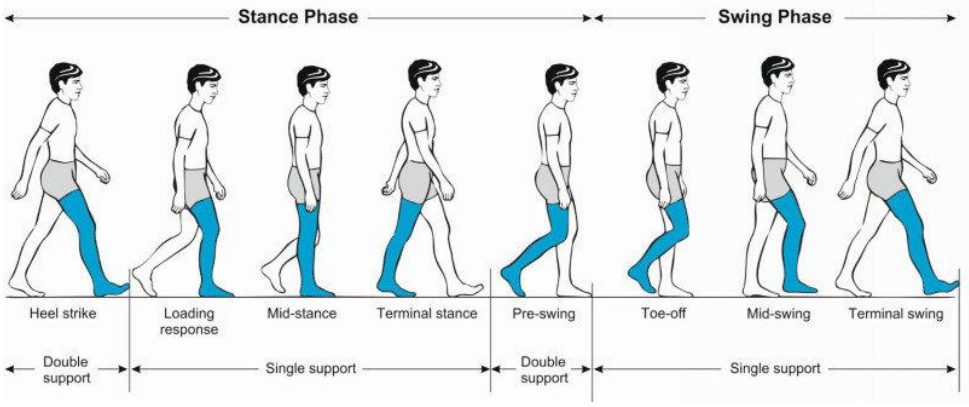

Figure 2.26: *Explanation of gait cycle from Pirker et al.* [64].

The spatial parameters refer to the *Stride Length* and the *Step Length* and *Step Width*. The *Stride Length* is defined as the distance from 2 subsequent contacts of the same, whereas the *Step Length* is the distance from 2 subsequent contacts of different feet; basically, the *Stride Length* is the sum of step right and step left. The ratio between *Step Length* and *Step Width* is the *Step Profile*, considered a meaningful parameter for the objective assessment of CP, together with the *Step Width* [65]. From the temporal and the spatial information, we can assess the *Walking Velocity*, usually lower in pathological conditions. Finally, in the last section of the first page of the report, there are contained the offset angles derived from the standing trial.

The second category of data is the kinematics, represented in the second page of the report, describing the trend of selected angles: *Pelvic* and *Trunk Obliquity*, *Tilt* and *Rotation*; *Hip Flexion-Extension*, *Rotation* and *Abdo-Adduction*; *Knee Flexion-Extension*; *Ankle Plantar-Dorsiflexion* and *Foot Progression*. It is also possible to compute the varus-valgus and the rotation of the knees, but these angles are very small and subjected to the errors mainly due to the movement of the patella, and so not considered for further analysis. In each graph, the X-axis reports the percentage of the cycle with in red the left foot, in green the right foot and in grey the normative band. Moreover, on each graph, there are plotted 2 vertical lines corresponding to the percentage of the stride phase of right and left foot.

The kinetics is reported in the 3rd page of the report, with the representation of moments and powers of hip, knee and ankle in the sagittal plane. Furthermore, the *Ground Reaction Forces* (*GRF*) in the *Antero-Posterior*, *Medio-Lateral* and *Vertical* directions are presented, normalized by the weight. In particular, the maximum of the medio-lateral component (*MaxGRF_ML*) is considered a significant parameter in CP children [65].

EMG data are particularly useful to check muscles' activities and their timing, comparing the signals with normative muscle activation patterns [66]. In this case,

we followed the signal processing procedure described in section 2.5.1, setting the last low-pass Butterworth filter at 5 Hz. Subsequently, we normalized each signal by the MVC of corresponding muscle and we divided the EMG signals according to the gait cycles; finally, we extracted the average signal.

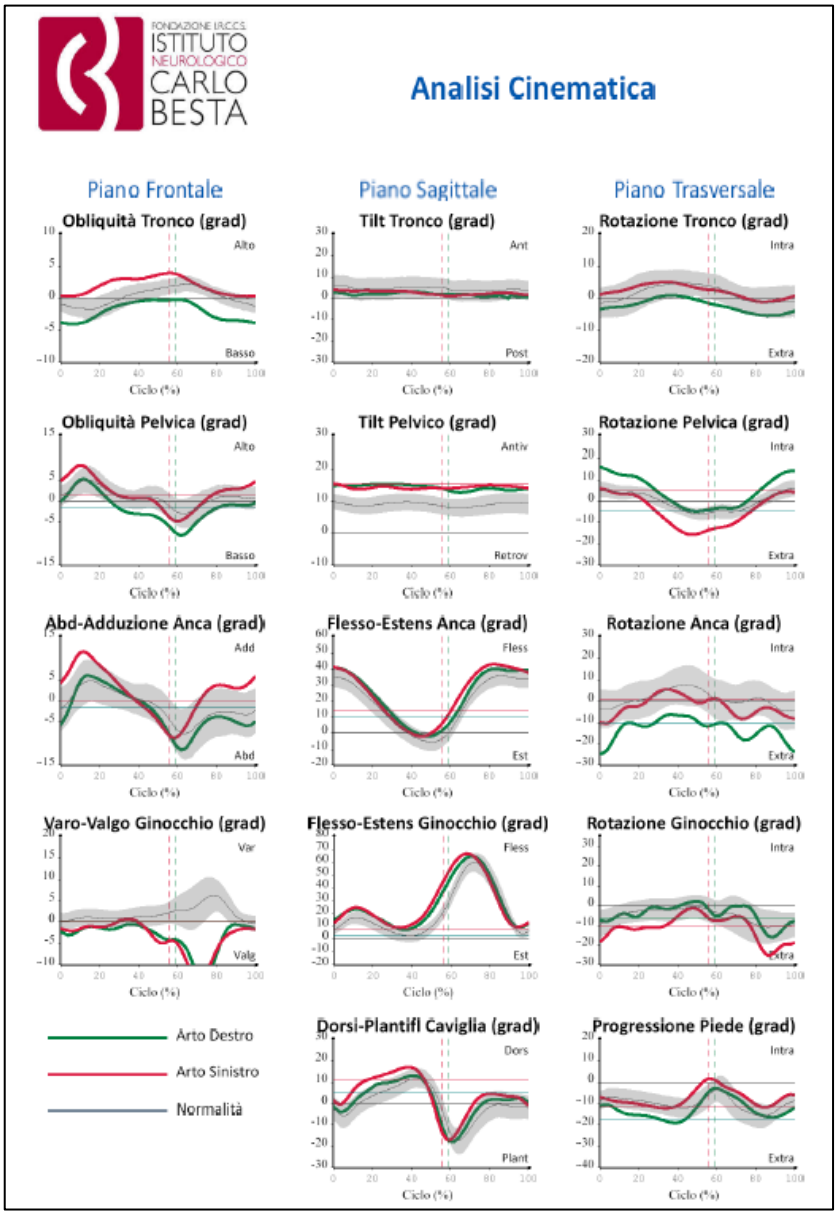

Figure 2.27: *Example of the 2nd page of the gait analysis report of a control.*

	REACHING	TAPPING	WRITING FIGURE-8	PASSIVE EXTENSION
Description	Reach a target with index finger	Join thumb and index finger of the same hand	Draw figures-8 following a template	Passive arm stretching from full flexion to full extension
Protocol	5 reps, 2 trials	Controlateral: 10 sec, 2 trials Ipsilateral: 10 sec, 2 trials	10 figures, 2 trials	Fast (60 BPM): 8 reps, 2 trials Medium (24 BPM): 8 reps, 2 trials Slow (12 BPM): 8 reps, 2 trials
Markers	**9**: RA, LA, STE, ME, LE, US, RS, 2MCP, IND	**8**: RA, LA, STE, ME, LE, US, RS, 2MCP	**8**: RA, LA, STE, ME, LE, US, RS, 2MCP	**6**: RA, LA, ME, LE, US, RS
Muscles	**8**: FCU, ECR, BIC, TRIC, AD, LD, PD, SS	**8**: FCU, ECR, BIC, TRIC, AD, LD, PD, SS	**8**: FCU, ECR, BIC, TRIC, AD, LD, PD, SS	**2**: BIC, TRIC
Rationale	Information about coordination and motor scheme	Dystonia alters the task	Information about coordination and frequency aspects related to musclar activation	Spasticity alters the task (possible catches)
Indicators	*SD, ROM and SD/ROM* for each angle; *SD* for each wrist velocity component; *3D Peak Velocity; Wrist Path Ratio; Accuracy; Jerk.* Cocontraction*: BIC-TRIC, ECR-FCU, AD-PD*	*Index of Dystonia* and *Modified Index of Dystonia; ROM* of the trunk	*Spatial Repeatability; SD, ROM and SD/ROM* of the trunk; *CRPV; Jerk; TCI* for each muscle	*TSRT; COFLEX* and *COEX: EMG-change: ROM* of the elbow

Table 2.1: *Description of upper limb tasks with the indication of marker set and EMG protocol used, and the indicators extracted.*

	GAIT ANALYSIS	PASSIVE FLEXION
Description	Walk in a straight line at a self-selected speed	Passive leg stretching from full extension to full flexion
Protocol	1 standing trial + at least 3 walking trials	Fast (72 BPM): 8 reps, 2 trials Medium (48 BPM): 8 reps, 2 trials Slow (24 BPM): 8 reps, 2 trials
Markers	**22**: C7, SAC, RA, LA, RASIS, LASIS, RGT, LGT, RMF, LMF, RHF, LHF, RFE, LFE, RMT, LMT, MAL, LMAL, RHELL, LHELL, RVM, LVM	**8**: RASIS, LASIS, GT, MF, HF, FE, MT, MAL
Muscles	**4**: TA, SO, RF, ST	**2**: RF, ST
Rationale	Quantitative evaluation of the gait	Spasticity alters the task (possible catches)
Indicators	*Gait Cycle, Stance, Swing, Double Support, Stride Length, Step Length, Step Width, Step Profile, Walking Velocity,* angles assessment, moments and powers assessment, *MaxGRF_ML,* EMG activity	*TSRT, COFLEX, COEXT, EMG-change, ROM* of the knee

Table 2.2: *Description of lower limb tasks with the indication of marker set and EMG protocol used, and the indicators extracted.*

3. Results

3.1 Participants

For the validation of the protocols, we recruited different subjects (patients and controls) performing the upper limb or the lower limb protocols.

The upper limb protocol was tested on a 14-year-old boy with dystonia pre- and post-Deep Brain Stimulation (DBS), after 3 months from the surgery; DBS is a technique consisting in the implantation of a pulse generator stimulating specific targets of the brain, stimulating parameters are adjustable in order to treat the movement disorder as good as possible [67]. We performed the protocol on 2 control children. In addition, we also tested it on 1 pathological adult, in order to investigate if the system can be suitable also for grown-up pathological populations.

The lower limb protocol was tested on 2 control children, 1 child with dystonia treated using a DBS implant, and 1 child with left hemiparesis due to a prenatal stroke of the middle cerebral artery. The letter subject underwent a surgery, 6 months before our evaluations, to treat a severe equino-varus deformity in the left foot. Participants' details, with the indications of the acquired trials, are presented in tables 3.1 and 3.2, divided for upper limb and lower limb.

SUBJECT	GROUP	SEX	AGE (YEARS)	DOMINANT ARM	ACQUIRED TRIALS
S001	Primary Dystonia	M	14	R	Pre DBS: 2 reaching, 4 tapping Post DBS: 2 reaching, 4 tapping, 2 figure-8, 6 passive extensions
S002	?	M	45	R	2 reaching, 4 tapping
C001	Control	F	7	R	2 reaching, 4 tapping, 2 figure-8, 6 passive extensions
C002	Control	M	14	L	2 reaching, 4 tapping, 2 figure-8, 6 passive extensions

Table 3.1: *Participants of the validation phase of the upper limb protocols.*

SUBJECT	GROUP	SEX	AGE (YEARS)	DOMINANT LEG	ACQUIRED TRIALS
S003	Primary Dystonia	F	12	R	Gait analysis (3 valid trials)
S004	Left Hemiparesis due to CP	M	15	L	Gait analysis (4 valid trials), 6 passive flexions
C003	Control	F	12	L	Gait analysis (3 valid trials), 6 passive flexions
C004	Control	F	15	R	Gait analysis (4 valid trials), 6 passive flexions

Table 3.2: *Participants of the validation phase of the lower limb protocols.*

3.2 Upper Limb Protocol Validation

From the validation trials executed by 2 control subjects (sequence of movements explained in section 2.3.1.1), we obtained the trends of the angles and so the corresponding conventions (positive/negative).

Shoulder

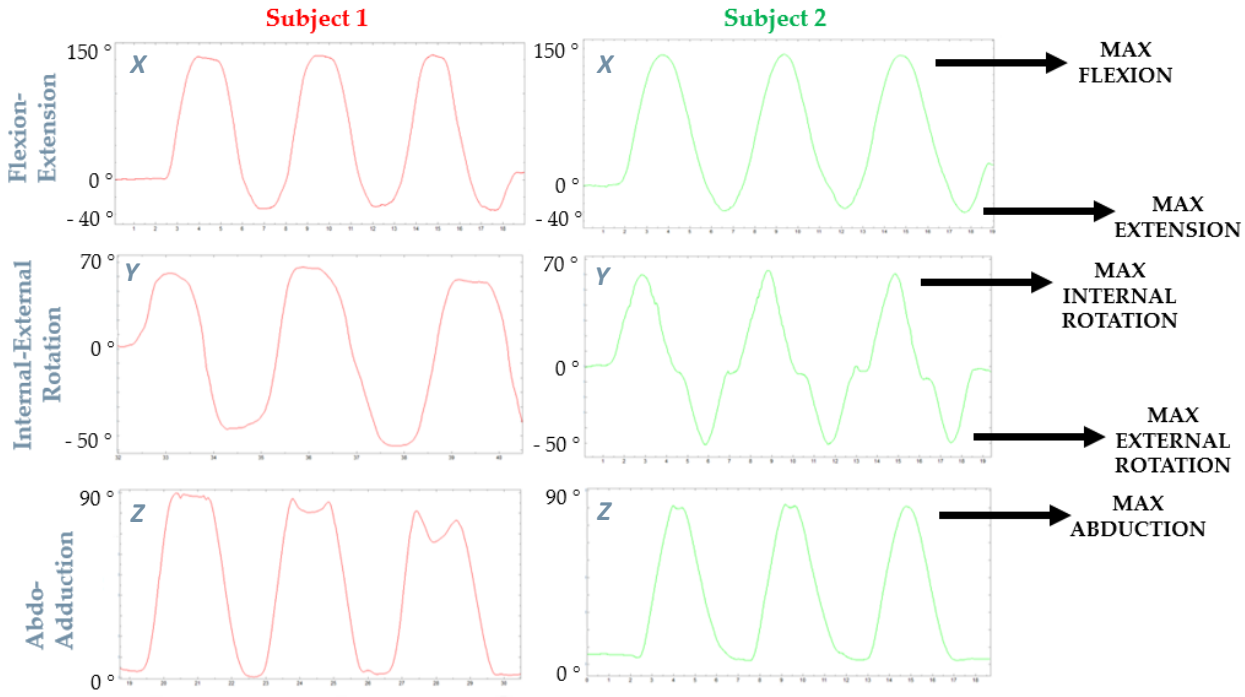

Figure 3.1: *Shoulder validation angles.*

Looking at the top plots in figure 3.1 (X-axis), we can see that shoulder flexion corresponds to positive values (from ≈ 0° to maximum flexion ≈ 145°), whereas values decrease while the shoulder goes in extension and reach negative values in hyperextension (≈ -35° at its maximum), for a ROM of about 180°. Similarly, we obtained positive values for internal rotation (maximum ≈ 60°) and negative values for external rotation (maximum ≈ -50°), so the ROM is about 110°; the different trend between the 2 subjects is due to the fact that subject 2 stopped a while between movements, while subject 1 performed the trials in a more fluid way. Finally, on the Z-axis, positive values mean abduction, reaching a maximum at about 90°, while values decrease when the arm returns near the medial line.

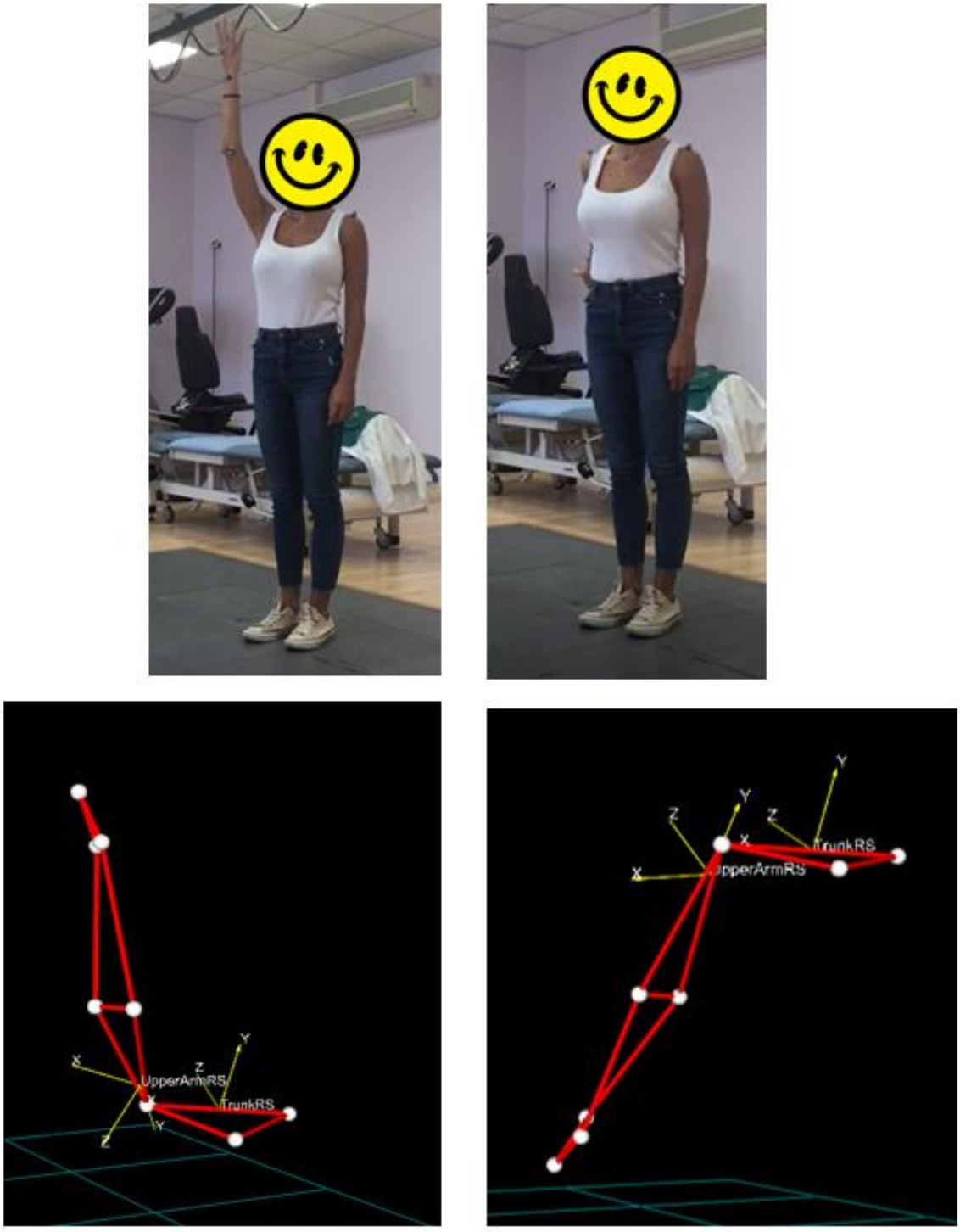

Figure 3.2: *Shoulder flexion (left) and shoulder hyperextension (right).*

Elbow

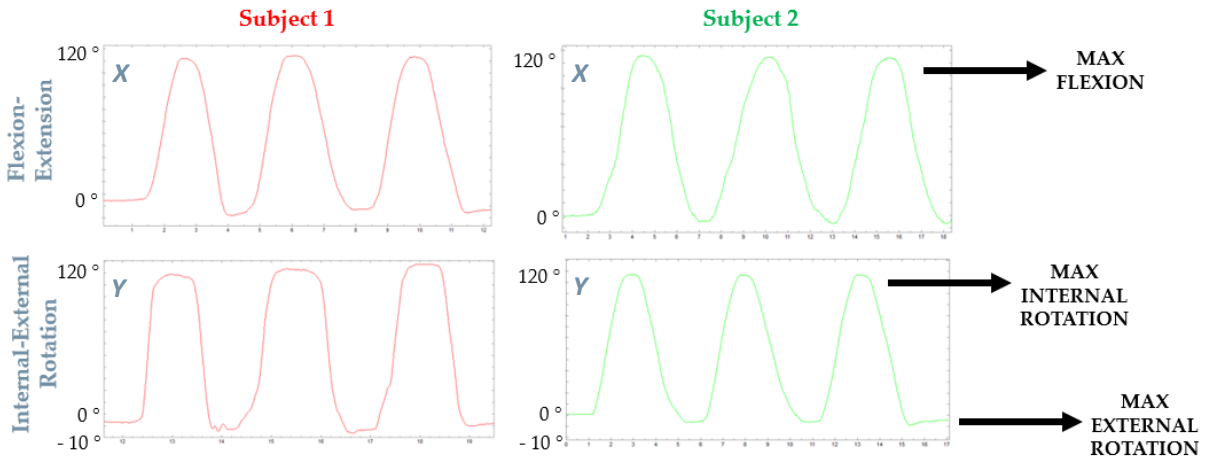

Figure 3.3: *Elbow validation angles.*

Also for the elbow (figure 3.3), on the X-axis positive values mean flexion (from ≈ 0° to maximum flexion ≈ 120°), and their amplitude decrease as the elbow extends. On the Y-axis it is plotted the rotation, with positive values for internal rotation (maximum ≈ 120°) and decreasing amplitudes for external rotation until few negative degrees (≈ -5°).

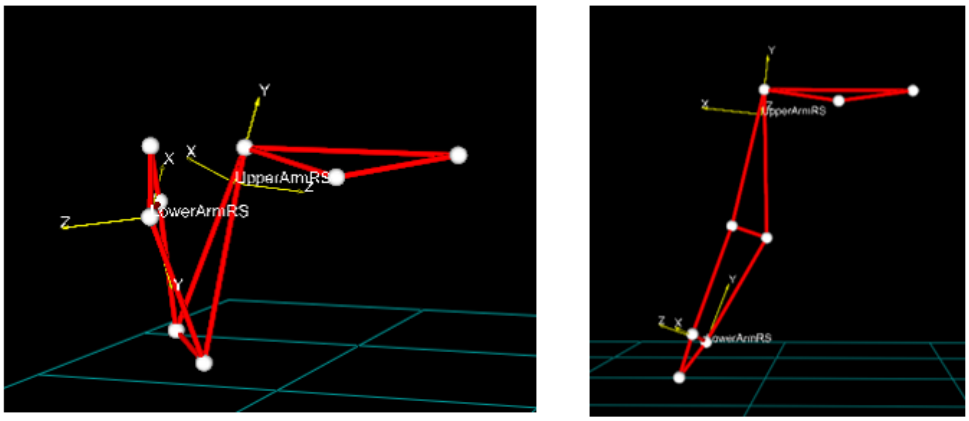

Figure 3.4: *Elbow flexion (left) and elbow extension (right).*

Wrist

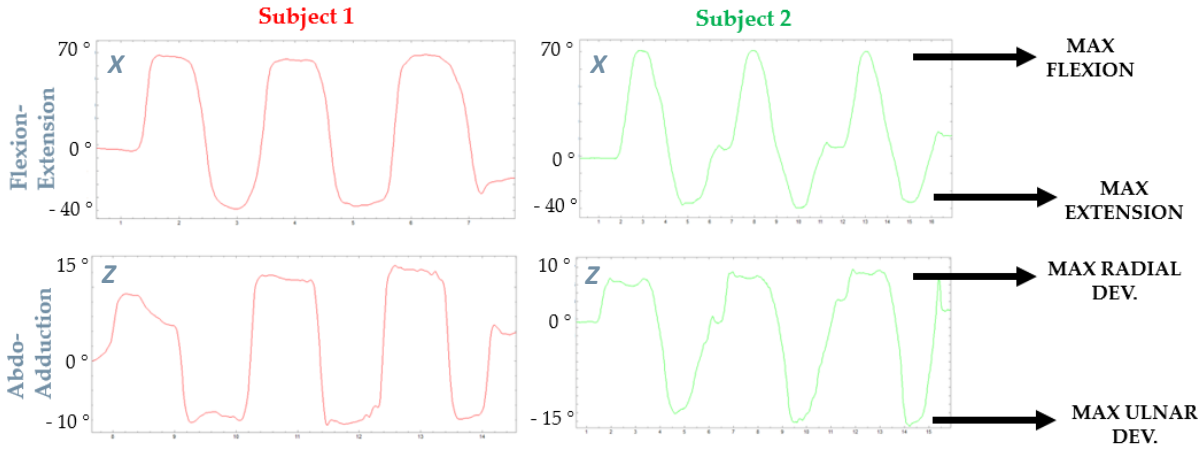

Figure 3.5: *Wrist validation angles.*

Again, looking at figure 3.5, in the X-axis positive values mean flexion and negative values mean extension, for a ROM of about 120° (≈ 65 ÷ -35°). On Z-axis, radial deviation is characterized by positive values, while ulnar deviation by negative

values, with maximum values strictly dependent on the wrist mobility of the subject.

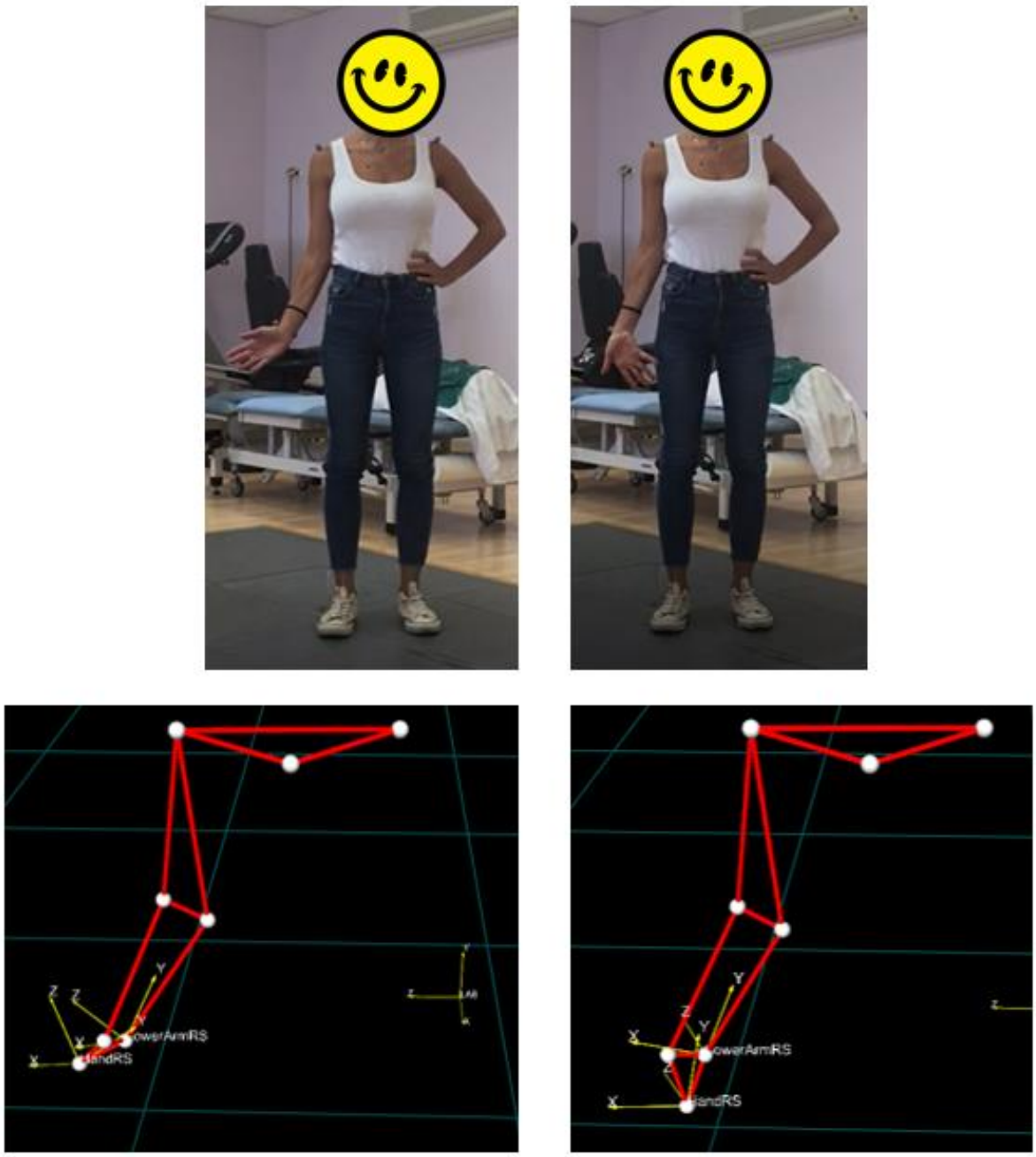

Figure 3.6: *Wrist radial deviation (left) and wrist ulnar deviation (right).*

Trunk

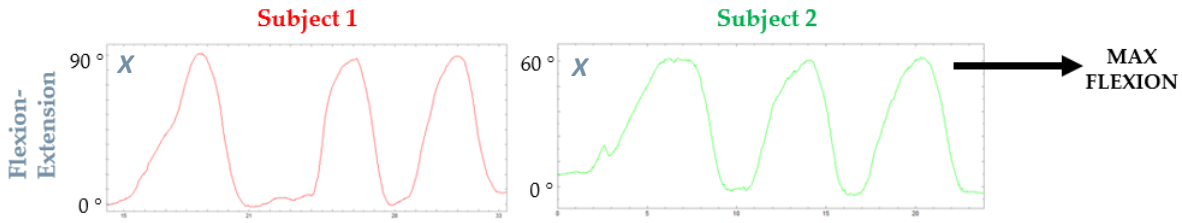

Figure 3.7: *Trunk validation angles.*

We can see from figure 3.7 that, for trunk, positive values mean flexion over a ROM depending on the flexibility of the subject.

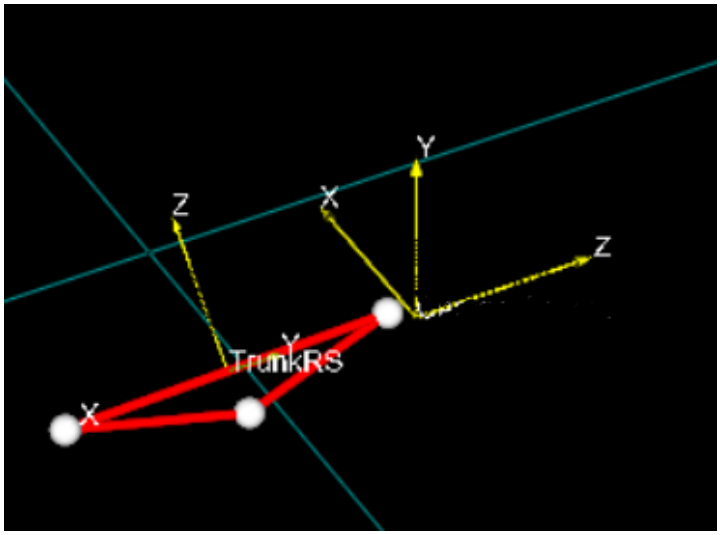

Figure 3.8: *Trunk flexion with respect to the laboratory triad.*

	FLEXION-EXTENSION (X)	INTERNAL-EXTERNAL ROTATION (Y)	ABDO-ADDUCTION (Z)
SHOULDER	Flexion + Extension –	Internal + External -	Abduction + Adduction –
ELBOW	Flexion + Extension –	Internal + External -	/
WRIST	Flexion + Extension –	/	Radial deviation + Ulnar deviation –
TRUNK	Flexion + Extension –	/	/

Table 3.3: *Summary of angle conventions.*

3.3 Functional Protocols

3.3.1 Upper Limb

a. **Dystonia vs Controls**

The first set of results are relative to the subject *S001* with dystonia, post-DBS, and the 2 controls (*C001* and *C002*), as described in table 3.1. We choose to use the data coming from the post-DBS trials because we had the opportunity to collect a complete dataset. For simplicity, in the tables are reported only the values of the *Mean Squared Jerk Normalized by Peak Velocity*, but all the jerk-based measures were computed (see section 2.5.2).

First of all, the computed indicators relative to the reaching tasks (1st trial, 2nd trial and the average between them) are presented; green rows represent indicators related to angle joints, blue rows represent the other computed indicators, while in yellow the EMG co-contraction indicators. It is also reported a table with only the averages of each subject for a better comparison.

Below, we expressed also all the joint angles extracted from one reaching task of each subject, normalized with respect to the gesture (from starting position to next starting position) and selecting only the 3 central movements.

	C001		AVERAGE
	Trial 1	Trial 2	
REACHING			
Shoulder Flex SD	5.05	12.38	**8.715**
Shoulder Flex ROM	58.22	96.6	**77.41**
Shoulder Flex SD/ROM	0.087	0.128	**0.107**
Shoulder Rotation SD [°]	5.54	5.15	**5.35**
Shoulder Rotation ROM [°]	12.64	26.02	**19.33**
Shoulder Rotation SD/ROM	0.438	0.198	**0.318**
Shoulder Abdo-adduction SD [°]	4.85	2.99	**3.92**
Shoulder Abdo-adduction ROM [°]	11.11	13.03	**12.07**
Shoulder Abdo-adduction SD/ROM	0.437	0.229	**0.333**
Elbow Flex SD [°]	2.76	6.60	**4.68**
Elbow Flex ROM [°]	19.4	44.68	**32.04**
Elbow Flex SD/ROM	0.142	0.148	**0.145**
Elbow Rotation SD [°]	3.5	2.16	**2.83**
Elbow Rotation ROM [°]	12.85	12.11	**12.48**
Elbow Rotation SD/ROM	0.272	0.178	**0.225**
Wrist Flex SD [°]	5.47	3.15	**4.31**
Wrist Flex ROM [°]	23	13.61	**18.31**
Wrist Flex SD/ROM	0.238	0.231	**0.235**
Wrist Abdo-adduction SD [°]	0.6	0.96	**0.78**
Wrist Abdo-adduction ROM [°]	3.87	5.23	**4.55**
Wrist Abdo-adduction SD/ROM	0.155	0.184	**0.169**
Trunk Flex SD [°]	3.45	4.8	**4.13**
Trunk Flex ROM [°]	13.63	25.27	**19.45**
Trunk Flex SD/ROM	0.253	0.190	**0.222**
Velocity medial wrist X SD [m/s]	0.049	0.095	**0.072**
Velocity medial wrist Y SD [m/s]	0.059	0.156	**0.1075**
Velocity medial wrist Z SD [m/s]	0.059	0.141	**0.1**
Wrist Path Ratio	1.045	1.075	**1.06**
Accuracy [m]	0.025	0.022	**0.0235**
3D Peak Velocity (medial wrist) [m/s]	1.212	1.126	**1.169**
Mean squared jerk normalized by peak velocity [m/s^5]	2002	2718	**2360**
ECR/FCU forth (%)	93.28	118.47	**105.88**
FCU/ECR back (%)	42.72	46.76	**44.74**
BIC/TRIC forth (%)	120.84	87.38	**104.11**
TRIC/BIC back (%)	99.55	86.82	**93.19**
PD/AD forth (%)	50.7	43.95	**47.33**
AD/PD back (%)	62.1	43.43	**52.77**

Table 3.4: *Indicators extracted from reaching tasks of control subject C001.*

	C002		AVERAGE
	Trial 1	Trial 2	
REACHING			
Shoulder Flex SD	4.67	3.24	**3.955**
Shoulder Flex ROM	70.44	70.39	**70.42**
Shoulder Flex SD/ROM	0.066	0.046	**0.056**
Shoulder Rotation SD [°]	1.43	2.42	**1.93**
Shoulder Rotation ROM [°]	9.95	10.81	**10.38**
Shoulder Rotation SD/ROM	0.144	0.224	**0.184**
Shoulder Abdo-adduction SD [°]	1.18	1.1	**1.14**
Shoulder Abdo-adduction ROM [°]	6.12	6.65	**6.39**
Shoulder Abdo-adduction SD/ROM	0.193	0.165	**0.179**
Elbow Flex SD [°]	2.66	3.33	**3.00**
Elbow Flex ROM [°]	39.08	35.34	**37.21**
Elbow Flex SD/ROM	0.068	0.094	**0.081**
Elbow Rotation SD [°]	2.62	8.43	**5.53**
Elbow Rotation ROM [°]	14.84	16.97	**15.91**
Elbow Rotation SD/ROM	0.177	0.497	**0.337**
Wrist Flex SD [°]	2.07	3.21	**2.64**
Wrist Flex ROM [°]	13.42	17.25	**15.34**
Wrist Flex SD/ROM	0.154	0.186	**0.170**
Wrist Abdo-adduction SD [°]	0.49	1.61	**1.05**
Wrist Abdo-adduction ROM [°]	5.27	6.36	**5.82**
Wrist Abdo-adduction SD/ROM	0.093	0.253	**0.173**
Trunk Flex SD [°]	4.4	3.06	**3.73**
Trunk Flex ROM [°]	31.45	31.64	**31.55**
Trunk Flex SD/ROM	0.140	0.097	**0.118**
Velocity medial wrist X SD [m/s]	0.024	0.019	**0.0215**
Velocity medial wrist Y SD [m/s]	0.027	0.049	**0.038**
Velocity medial wrist Z SD [m/s]	0.033	0.033	**0.033**
Wrist Path Ratio	1.061	1.05	**1.056**
Accuracy [m]	0.018	0.016	**0.017**
3D Peak Velocity (medial wrist) [m/s]	0.576	0.587	**0.5815**
Mean squared jerk normalized by peak velocity [m/s^5]	1932	1451	**1691.5**
ECR/FCU forth (%)	181.11	190.85	**185.98**
FCU/ECR back (%)	35.3	39.02	**37.16**
BIC/TRIC forth (%)	75.39	82.67	**79.03**
TRIC/BIC back (%)	117.55	116.86	**117.21**
PD/AD forth (%)	81.74	84.5	**83.12**
AD/PD back (%)	64.98	62.33	**63.66**

Table 3.5: *Indicators extracted from reaching tasks of control subject C002.*

	S001 - POST DBS		AVERAGE
	Trial 1	Trial 2	
REACHING			
Shoulder Flex SD	4.33	3.93	**4.13**
Shoulder Flex ROM	86.03	85.85	**85.94**
Shoulder Flex SD/ROM	0.050	0.046	**0.048**
Shoulder Rotation SD [°]	5.12	5.62	**5.37**
Shoulder Rotation ROM [°]	92.98	86.68	**89.83**
Shoulder Rotation SD/ROM	0.055	0.065	**0.060**
Shoulder Abdo-adduction SD [°]	2.76	2.59	**2.68**
Shoulder Abdo-adduction ROM [°]	42.89	48.25	**45.57**
Shoulder Abdo-adduction SD/ROM	0.064	0.054	**0.059**
Elbow Flex SD [°]	3.36	3.37	**3.37**
Elbow Flex ROM [°]	47.09	54.83	**50.96**
Elbow Flex SD/ROM	0.071	0.061	**0.066**
Elbow Rotation SD [°]	3.79	8.61	**6.2**
Elbow Rotation ROM [°]	54.23	85.24	**69.74**
Elbow Rotation SD/ROM	0.070	0.101	**0.085**
Wrist Flex SD [°]	3.43	2.65	**3.04**
Wrist Flex ROM [°]	17.53	19.58	**18.56**
Wrist Flex SD/ROM	0.196	0.135	**0.166**
Wrist Abdo-adduction SD [°]	0.62	1.26	**0.94**
Wrist Abdo-adduction ROM [°]	8.36	11.44	**9.9**
Wrist Abdo-adduction SD/ROM	0.074	0.110	**0.092**
Trunk Flex SD [°]	1.55	1.43	**1.49**
Trunk Flex ROM [°]	13.35	11.490	**12.42**
Trunk Flex SD/ROM	0.116	0.124	**0.120**
Velocity medial wrist X SD [m/s]	0.174	0.122	**0.148**
Velocity medial wrist Y SD [m/s]	0.106	0.077	**0.0915**
Velocity medial wrist Z SD [m/s]	0.104	0.107	**0.1055**
Wrist Path Ratio	1.467	1.58	**1.5235**
Accuracy [m]	0.017	0.018	**0.0175**
3D Peak Velocity (medial wrist) [m/s]	1.48	1.71	**1.595**
Mean squared jerk normalized by peak velocity [m/s^5]	20138	15775	**17956.5**
ECR/FCU forth (%)	63.54	64.68	**64.11**
FCU/ECR back (%)	92.68	163.51	**128.10**
BIC/TRIC forth (%)	87.09	101.07	**94.08**
TRIC/BIC back (%)	67.04	82.97	**75.01**
PD/AD forth (%)	58.65	63.11	**60.88**
AD/PD back (%)	129.55	119.86	**124.71**

Table 3.6: *Indicators extracted from reaching tasks of subject S001 (post-DBS).*

	AVERAGE		
	C001	*C002*	*S001* - POST DBS
REACHING			
Shoulder Flex SD	8.72	3.96	4.13
Shoulder Flex ROM	77.41	70.42	85.94
Shoulder Flex SD/ROM	0.107	0.056	0.048
Shoulder Rotation SD [°]	5.35	1.93	5.37
Shoulder Rotation ROM [°]	19.33	10.38	89.83
Shoulder Rotation SD/ROM	0.318	0.184	0.060
Shoulder Abdo-adduction SD [°]	3.92	1.14	2.675
Shoulder Abdo-adduction ROM [°]	12.07	6.39	45.57
Shoulder Abdo-adduction SD/ROM	0.333	0.179	0.059
Elbow Flex SD [°]	4.68	3.00	3.36
Elbow Flex ROM [°]	32.04	37.21	50.96
Elbow Flex SD/ROM	0.145	0.081	0.066
Elbow Rotation SD [°]	2.83	5.53	6.2
Elbow Rotation ROM [°]	12.48	15.91	69.74
Elbow Rotation SD/ROM	0.225	0.337	0.085
Wrist Flex SD [°]	4.31	2.64	3.04
Wrist Flex ROM [°]	18.31	15.34	18.56
Wrist Flex SD/ROM	0.235	0.170	0.166
Wrist Abdo-adduction SD [°]	0.78	1.05	0.94
Wrist Abdo-adduction ROM [°]	4.55	5.82	9.9
Wrist Abdo-adduction SD/ROM	0.169	0.173	0.092
Trunk Flex SD [°]	4.13	3.73	1.49
Trunk Flex ROM [°]	19.45	31.55	12.42
Trunk Flex SD/ROM	0.222	0.118	0.120
Velocity medial wrist X SD [m/s]	0.072	0.0215	0.148
Velocity medial wrist Y SD [m/s]	0.1075	0.038	0.0915
Velocity medial wrist Z SD [m/s]	0.1	0.033	0.1055
Wrist Path Ratio	1.06	1.056	1.5235
Accuracy [m]	0.0235	0.017	0.0175
3D Peak Velocity (medial wrist) [m/s]	1.169	0.5815	1.595
Mean squared jerk normalized by peak velocity [m/s^5]	2360	1691.5	17956.5
ECR/FCU forth (%)	105.88	185.98	64.11
FCU/ECR back (%)	44.74	37.16	128.10
BIC/TRIC forth (%)	104.11	79.03	94.08
TRIC/BIC back (%)	93.19	117.21	75.01
PD/AD forth (%)	47.33	83.12	60.88
AD/PD back (%)	52.77	63.66	124.71

Table 3.7: *Averages of the indicators extracted from reaching tasks of control subjects C001, C002 and the subject with dystonia S001 (post-DBS).*

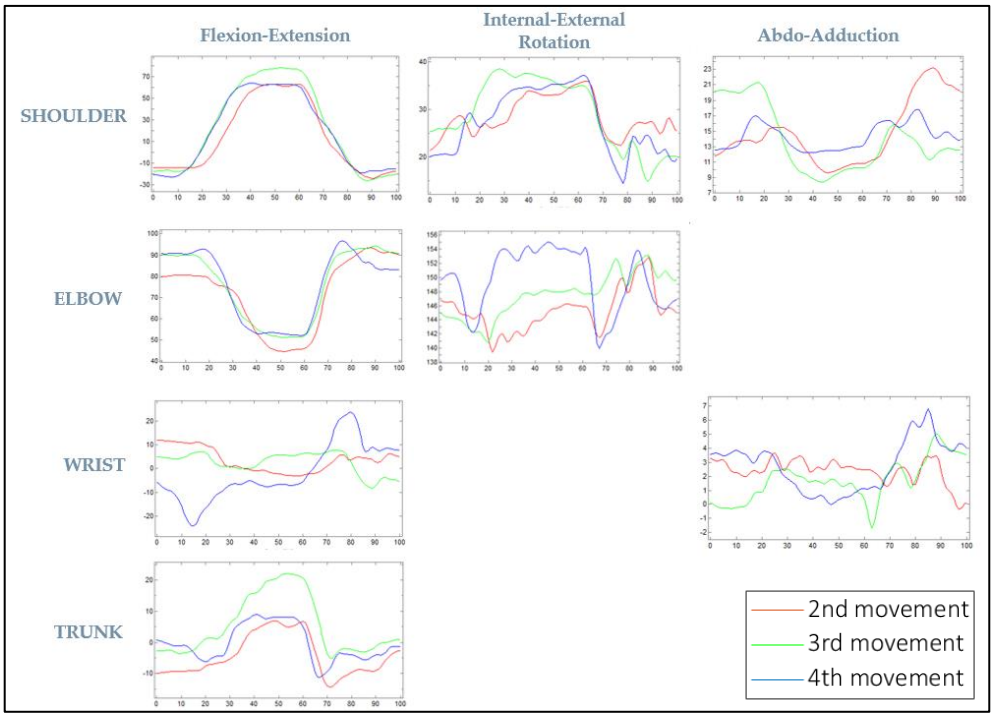

Figure 3.9: *Angles [°] of control subject C001 during reaching task (2nd trial).*

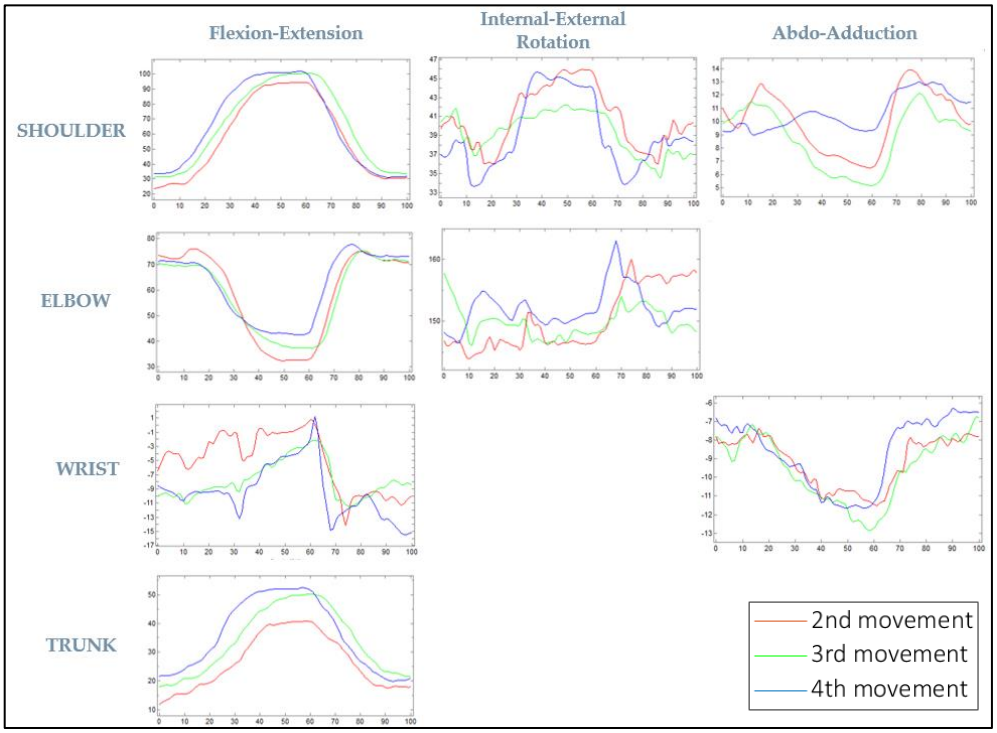

Figure 3.10: *Angles [°] of control subject C002 during reaching task (1st trial).*

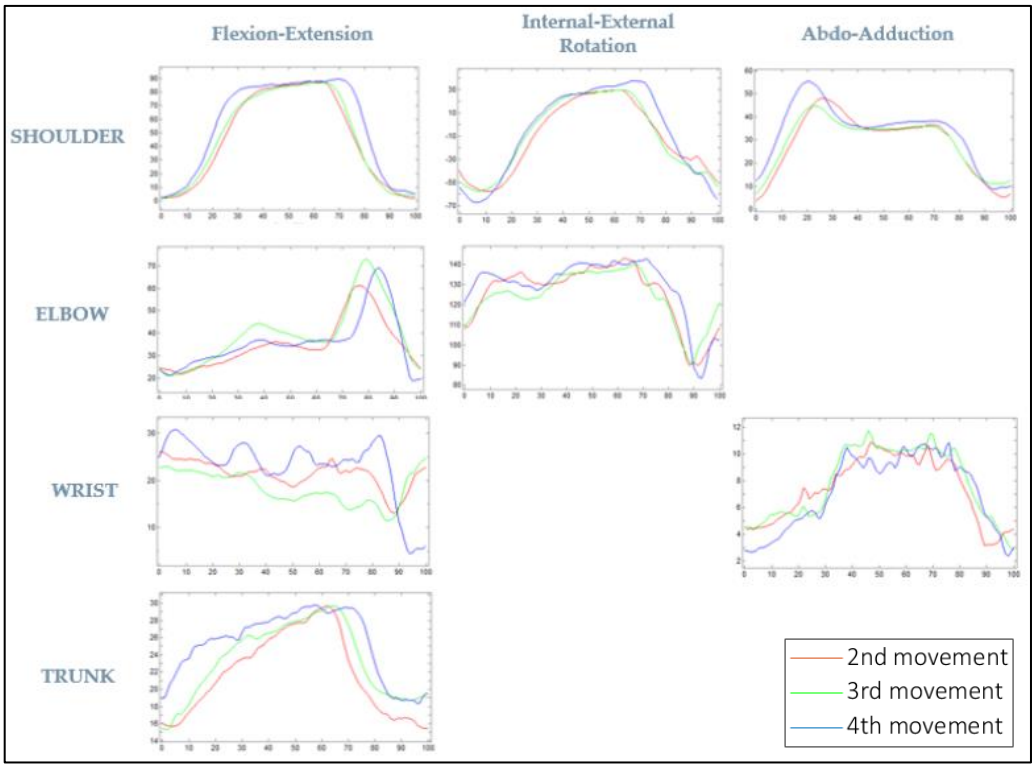

Figure 3.11: *Angles [°] of subject S001 (post-DBS) during reaching task (1st trial).*

Since the statistical sample is too small, we cannot perform statistical tests in order to underline significant differences between groups, however we can still draw some simple considerations on the data obtained.

The first thing we want to highlight is the low repeatability between trial 1 and trial 2 in subject *C001*, this is particularly notable looking at the *Shoulder Flexion-Extension ROM* (from 58.22° to 96.6°) or the *Elbow Flexion-Extension ROM* (from 19.4° to 44.68°). This is due to the very young age of the subject (7 years old), which could be felt uncomfortable with all the markers set and the EMG probes placed on her, and so she was likely to change her motor scheme between trials. It is known from literature that motor performance changes according to age [68], and so it is correct to compare the patient's performance with an age matched control. This is why we

are going to compare the pathological subject with only *C002*, who is perfectly age-matched with *S001* (both 14 years old).

Comparing the results in table 3.7 and the angles' trends, we can notice that some angles are comparable, while others have a similar pattern but significant different ROM, or they can be very different, as a result of different motor strategies.

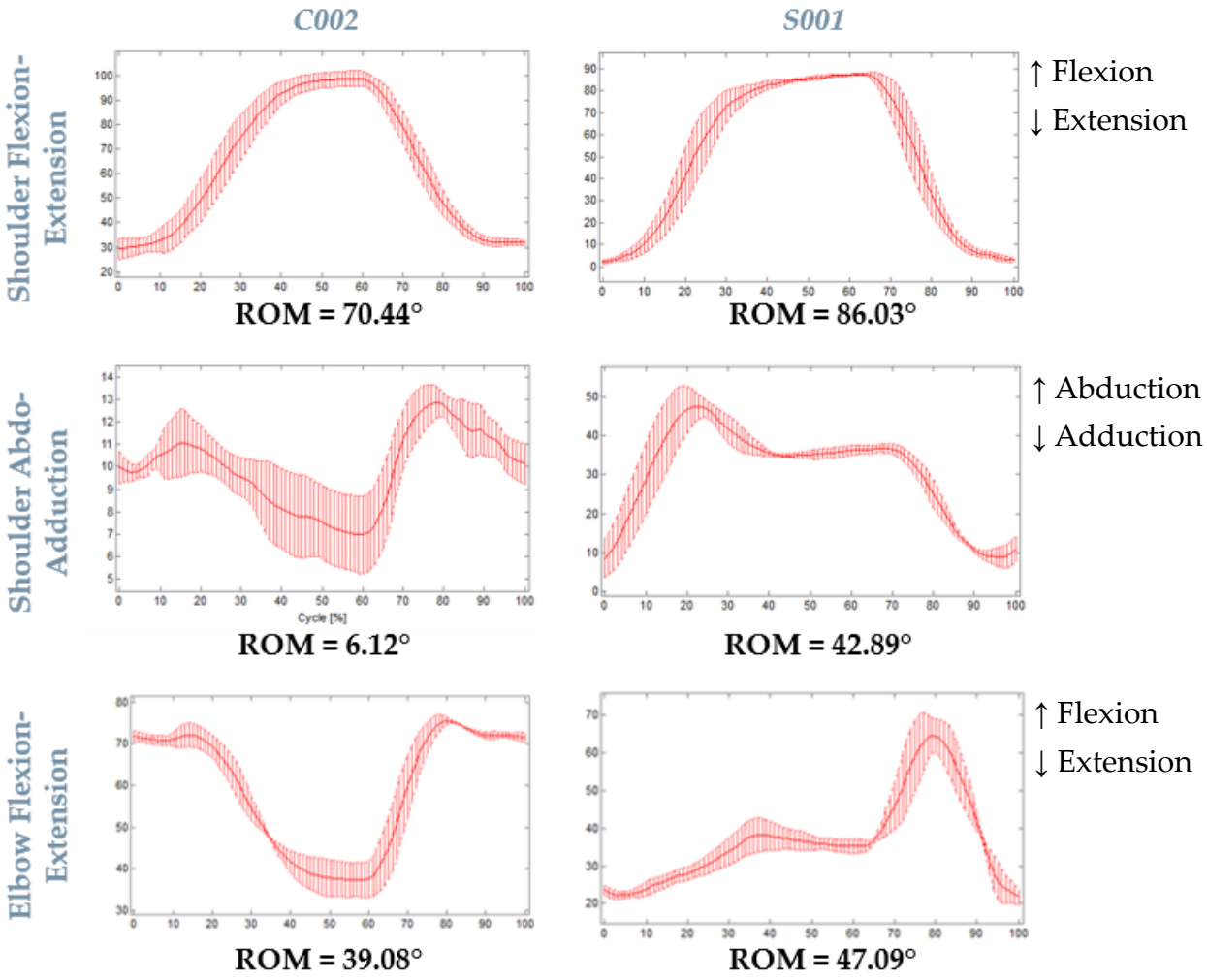

Figure 3.12: *Average tracks (mean ± SD) of Shoulder Flexion-Extension, Shoulder Abdo-Adduction and Elbow Flexion-Extension of subjects C002 and S001 (post-DBS) during reaching task; below each graph is reported the corresponding ROM.*

Indeed, referring to figure 3.12 (in which are reported some angles' examples), we can observe that the trends of *Shoulder Flexion-Extension* are comparable between the two subjects (flexion followed by an extension), although the ROM in the pathological subject is slightly greater. In *Shoulder Abdo-Adduction*, for subject *S001*, the abduction is clearly more accentuated, reaching almost 50°, leading to a significant different ROM with respect to *C002.* In the last graphs, referred to *Elbow Flexion-Extension*, the ROMs are comparable but the strategy to approach the target is totally different: the control subject firstly goes in extension to reach the target and then draws back the elbow flexing it, while the subject with dystonia mainly uses the shoulder abduction to reach the target, flexing the elbow to reach the target and then extending it to get back to rest position.

Other meaningful considerations regard the *Wrist Path Ratio*, with a value closer to 1 for the control subject, as expected from literature. This is confirmed also when comparing *S001* to *C001*, even if not perfectly age matched. For this reason, the *Wrist Path Ratio* seems to be a sensitive measure of dystonia, independently from the subject's age. As for *Peak Velocity*, results show that it is subject-dependent since the protocol is performed at a self-selected speed. On the other hand, we can notice that the SDs of the velocity tracks, obtained from the medial wrist marker, in all the directions, are smaller for the control subject. The *Accuracy* seems good in both the cases (17 mm between finger and target on average).

Finally, we can observe that co-contractions indexes are very different, depending on the subject and the specific muscular activation pattern. Values near 100% mean that the muscular activity is comparable between the selected muscular pair, thus showing higher co-contraction, while values far from 100% underline a specific prevalence of one muscle on the other.

Regarding the finger tapping tasks, we present the extracted indicators divided for subject both during ipsilateral and contralateral tasks. We also report the comparison between the averages, as for the reaching task. Blue rows describe the *Indexes of Dystonia*, while in green indication about the trunk ROM.

	C001		AVERAGE
	Trial 1	Trial 2	
TAPPING IPSILATERAL			
Index of Dystonia [°]	61.54	77.47	**69.505**
Modified Index of Dystonia [°]	66.22	82.92	**74.57**
Trunk Flex ROM [°]	6.21	6.2	**6.205**
TAPPING CONTRALATERAL			
Index of Dystonia [°]	35.15	24.7	**29.925**
Modified Index of Dystonia [°]	37.55	26.53	**32.04**
Trunk Flex ROM [°]	13.62	6.41	**10.015**

Table 3.8: *Indicators extracted from finger tapping tasks of control subject C001.*

	C002		AVERAGE
	Trial 1	Trial 2	
TAPPING IPSILATERAL			
Index of Dystonia [°]	48.68	35.55	**42.115**
Modified Index of Dystonia [°]	54.77	40.03	**47.4**
Trunk Flex ROM [°]	1.19	4.3	**2.745**
TAPPING CONTRALATERAL			
Index of Dystonia [°]	10.72	12.59	**11.655**
Modified Index of Dystonia [°]	11.08	13.2	**12.14**
Trunk Flex ROM [°]	3.47	5.28	**4.375**

Table 3.9: *Indicators extracted from finger tapping tasks of control subject C002.*

	S001 - POST DBS		AVERAGE
	Trial 1	Trial 2	
TAPPING IPSILATERAL			
Index of Dystonia [°]	124.9	134.35	**129.63**
Modified Index of Dystonia [°]	135.38	145.67	**140.53**
Trunk Flex ROM [°]	5.61	7.74	**6.68**
TAPPING CONTRALATERAL			
Index of Dystonia [°]	25.2	53.07	**39.14**
Modified Index of Dystonia [°]	26.98	55.74	**41.36**
Trunk Flex ROM [°]	2.79	4.7	**3.75**

Table 3.10: *Indicators extracted from finger tapping tasks of subject S001 (post-DBS).*

	AVERAGE		
	C001	C002	S001 - POST DBS
TAPPING IPSILATERAL			
Index of Dystonia [°]	**69.505**	**42.115**	**129.63**
Modified Index of Dystonia [°]	**74.57**	**47.4**	**140.53**
Trunk Flex ROM [°]	**6.205**	**2.745**	**6.68**
TAPPING CONTRALATERAL			
Index of Dystonia [°]	**29.925**	**12.59**	**39.14**
Modified Index of Dystonia [°]	**32.04**	**13.2**	**41.36**
Trunk Flex ROM [°]	**10.015**	**5.28**	**3.75**

Table 3.11: *Averages of the indicators extracted from tapping tasks of subjects C001, C002 and S001 (post-DBS).*

The *Index of Dystonia* results greater for the pathological subject, with respect to both the control subjects, in both finger tapping tasks (ipsilateral and contralateral), in line with the literature [19].

Finally, we reported the indicators related to the figure-8 writing task. In yellow, the indicators related to EMG activation (*Task Correlation Index*), in green, the indicators about angles and coordination, while the blue row refers to the *Jerk*.

	C001		AVERAGE
	Trial 1	Trial 2	
FIGURE 8			
TCI FCU	0.39	0.44	**0.415**
TCI ECR	0.75	0.53	**0.64**
TCI BIC	0.49	0.68	**0.585**
TCI TRIC	0.59	0.61	**0.6**
TCI AD	0.63	0.76	**0.695**
TCI LD	0.38	0.43	**0.405**
TCI PD	0.78	0.68	**0.73**
TCI SS	0.32	0.33	**0.325**
Spatial variability [m]	0.008	0.01	**0.009**
Time variability [s]	2.01	1.1	**1.555**
Trunk Flex SD [°]	3.81	3.78	**3.795**
Trunk Flex ROM [°]	11.35	10.84	**11.095**
Trunk Flex SD/ROM	0.336	0.349	**0.342**
Mean squared jerk normalized by peak velocity [m/s^5]	3141	9199	**6170**
CRPV arm-forearm [°]	34	43.03	**38.515**
CRPV forearm-hand [°]	56.26	39.02	**47.64**

Table 3.12: *Indicators extracted from figure-8 writing tasks of control subject C001.*

	C002		AVERAGE
	Trial 1	Trial 2	
FIGURE 8			
TCI FCU	0.72	0.61	**0.665**
TCI ECR	0.46	0.49	**0.475**
TCI BIC	0.34	0.4	**0.37**
TCI TRIC	0.32	0.56	**0.44**
TCI AD	0.45	0.32	**0.385**
TCI LD	0.65	0.69	**0.67**
TCI PD	0.73	0.71	**0.72**
TCI SS	0.36	0.39	**0.375**
Spatial variability [m]	0.005	0.006	**0.0055**
Time variability [s]	0.21	0.186	**0.198**
Trunk Flex SD [°]	1.87	1.46	**1.665**
Trunk Flex ROM [°]	4.07	4.3	**4.185**
Trunk Flex SD/ROM	0.459	0.340	**0.399**
Mean squared jerk normalized by peak velocity [m/s^5]	3969	5073	**4521**
CRPV arm-forearm [°]	20.33	17.21	**18.77**
CRPV forearm-hand [°]	21.51	16.98	**19.245**

Table 3.13: *Indicators extracted from figure-8 writing tasks of control subject C002.*

	S001 - POST DBS		AVERAGE
	Trial 1	Trial 2	
FIGURE 8			
TCI FCU	0.63	0.7	**0.665**
TCI ECR	0.55	0.69	**0.62**
TCI BIC	0.28	0.29	**0.285**
TCI TRIC	0.67	0.7	**0.685**
TCI AD	0.66	/	**0.66**
TCI LD	0.87	/	**0.87**
TCI PD	0.85	/	**0.85**
TCI SS	0.4	/	**0.4**
Spatial variability [m]	0.017	0.01	**0.014**
Time variability [s]	0.81	0.72	**0.77**
Trunk Flex SD [°]	2.17	2.04	**2.11**
Trunk Flex ROM [°]	5.88	5.77	**5.83**
Trunk Flex SD/ROM	0.369	0.354	**0.361**
Mean squared jerk normalized by peak velocity [m/s^5]	8866	9803	**9334.5**
CRPV arm-forearm [°]	43.11	51.23	**47.17**
CRPV forearm-hand [°]	56.97	44.83	**50.9**

Table 3.14: *Indicators extracted from figure-8 writing tasks of subject S001 (post-DBS). Some TCIs are missing due to problems with EMG probes.*

	AVERAGE		
	C001	*C002*	*S001* - POST DBS
FIGURE 8			
TCI FCU	0.415	0.665	0.665
TCI ECR	0.64	0.475	0.62
TCI BIC	0.585	0.37	0.285
TCI TRIC	0.6	0.44	0.685
TCI AD	0.695	0.385	0.66
TCI LD	0.405	0.67	0.87
TCI PD	0.73	0.72	0.85
TCI SS	0.325	0.375	0.4
Spatial variability [m]	0.009	0.0055	0.014
Time variability [s]	1.555	0.198	0.77
Trunk Flex SD [°]	3.795	1.665	2.11
Trunk Flex ROM [°]	11.095	4.185	5.83
Trunk Flex SD/ROM	0.342	0.399	0.361
Mean squared jerk normalized by peak velocity [m/s^5]	6170	4521	9334.5
CRPV arm-forearm [°]	38.515	18.77	47.17
CRPV forearm-hand [°]	47.64	19.245	50.9

Table 3.15: *Averages of the indicators extracted from figure-8 writing tasks of subjects C001, C002 and S001 (post-DBS).*

We can observe that *CRP* variability (*CRPV*) values are higher in *S001* with respect to controls, both for arm-forearm and forearm-hand. This reduced coordination can be seen also graphically, plotting the CRP (figure 3.13).

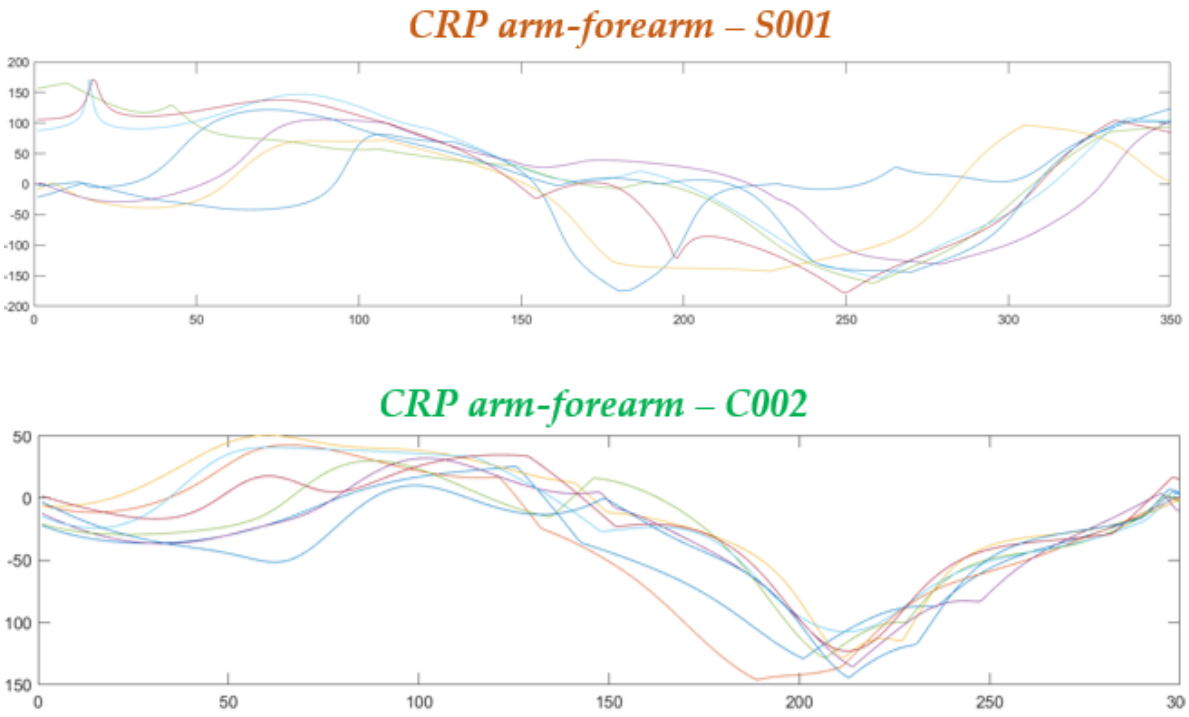

Figure 3.13: *CRP arm-forearm from 1st trial of S001 (post-DBS) and 2nd trial of C002 during figure-8 writing task; each line represents a figure-8 movement.*

The *Spatial Variability* assumes slightly higher values for the patient (14 mm vs 5 mm), and so the *Time Variability* (0.77 s vs 0.2 s). The movements of the trunk consist in a few degrees for both the subjects.

b. **Comparison pre- and post-DBS**

The second set of results is relative to the subject *S001* pre- and post-DBS. In this section, we will present the extracted indicators and the comparison between the trials before and after surgery. The first two tables refer to reaching task indicators, while the following figure shows the trends of the angles.

	S001 - PRE DBS		AVERAGE
	Trial 1	Trial 2	
REACHING			
Shoulder Flex SD	2.36	2.53	**2.45**
Shoulder Flex ROM	72.7	77.17	**74.94**
Shoulder Flex SD/ROM	0.032	0.033	**0.033**
Shoulder Rotation SD [°]	3.09	2.51	**2.80**
Shoulder Rotation ROM [°]	39.87	39.22	**39.55**
Shoulder Rotation SD/ROM	0.078	0.064	**0.071**
Shoulder Abdo-adduction SD [°]	1.7	1.69	**1.70**
Shoulder Abdo-adduction ROM [°]	25.8	25.99	**25.90**
Shoulder Abdo-adduction SD/ROM	0.066	0.065	**0.065**
Elbow Flex SD [°]	1.91	1.86	**1.89**
Elbow Flex ROM [°]	15.29	26.28	**20.79**
Elbow Flex SD/ROM	0.125	0.071	**0.098**
Elbow Rotation SD [°]	4.93	5.89	**5.41**
Elbow Rotation ROM [°]	30.89	28.22	**29.56**
Elbow Rotation SD/ROM	0.160	0.209	**0.184**
Wrist Flex SD [°]	2.26	2.34	**2.30**
Wrist Flex ROM [°]	16.66	17.56	**17.11**
Wrist Flex SD/ROM	0.136	0.133	**0.134**
Wrist Abdo-adduction SD [°]	0.8	1.03	**0.92**
Wrist Abdo-adduction ROM [°]	7.89	7.45	**7.67**
Wrist Abdo-adduction SD/ROM	0.101	0.138	**0.120**
Trunk Flex SD [°]	0.81	0.93	**0.87**
Trunk Flex ROM [°]	10.57	10.28	**10.43**
Trunk Flex SD/ROM	0.077	0.090	**0.084**
Velocity medial wrist X SD [m/s]	0.048	0.086	**0.067**
Velocity medial wrist Y SD [m/s]	0.063	0.047	**0.055**
Velocity medial wrist Z SD [m/s]	0.036	0.087	**0.062**
Wrist Path Ratio	1.413	1.306	**1.360**
Accuracy [m]	0.026	/	**0.026**
3D Peak Velocity (medial wrist) [m/s]	1.401	1.541	**1.471**
Mean squared jerk normalized by peak velocity [m/s^5]	7738	7666	**7702.0**

Table 3.16: *Indicators extracted from reaching tasks of subject S001 (pre-DBS).*

	AVERAGE	
	S001 - PRE DBS	*S001* - POST DBS
REACHING		
Shoulder Flex SD	2.45	4.13
Shoulder Flex ROM	74.94	85.94
Shoulder Flex SD/ROM	0.033	0.048
Shoulder Rotation SD [°]	2.80	5.37
Shoulder Rotation ROM [°]	39.55	89.83
Shoulder Rotation SD/ROM	0.071	0.060
Shoulder Abdo-adduction SD [°]	1.70	2.675
Shoulder Abdo-adduction ROM [°]	25.90	45.57
Shoulder Abdo-adduction SD/ROM	0.065	0.059
Elbow Flex SD [°]	1.89	3.365
Elbow Flex ROM [°]	20.79	50.96
Elbow Flex SD/ROM	0.098	0.066
Elbow Rotation SD [°]	5.41	6.2
Elbow Rotation ROM [°]	29.56	69.74
Elbow Rotation SD/ROM	0.184	0.085
Wrist Flex SD [°]	2.30	3.04
Wrist Flex ROM [°]	17.11	18.56
Wrist Flex SD/ROM	0.134	0.166
Wrist Abdo-adduction SD [°]	0.92	0.94
Wrist Abdo-adduction ROM [°]	7.67	9.9
Wrist Abdo-adduction SD/ROM	0.120	0.092
Trunk Flex SD [°]	0.87	1.49
Trunk Flex ROM [°]	10.43	12.42
Trunk Flex SD/ROM	0.084	0.120
Velocity medial wrist X SD [m/s]	0.067	0.148
Velocity medial wrist Y SD [m/s]	0.055	0.0915
Velocity medial wrist Z SD [m/s]	0.062	0.1055
Wrist Path Ratio	1.360	1.5235
Accuracy [m]	0.026	0.0175
3D Peak Velocity (medial wrist) [m/s]	1.471	1.595
Mean squared jerk normalized by peak velocity [m/s^5]	7702.0	17956.5

Table 3.17: *Averages of the indicators extracted from reaching tasks of subject S001, pre- and post-DBS.*

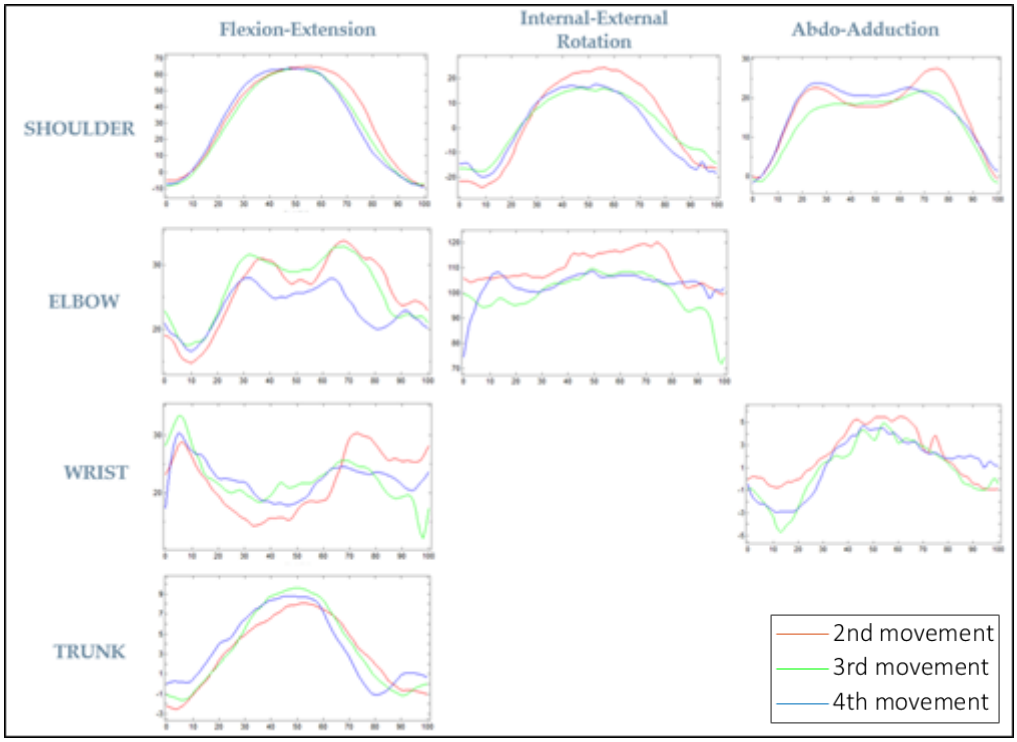

Figure 3.14: *Angles [°] of subject S001 (pre-DBS) during reaching task (1st trial).*

From the comparison table 3.16, we can notice that the greatest differences are related to the ROMs of the gesture, wider after 3 months from DBS: for instance, shoulder rotation goes from 39.55° to 89.83° or elbow flexion from 20.79° to 50.96°. Anyway, we can observe that the motor strategy is not significantly altered.

As previously, below are reported the *Indexes of Dystonia* and the indications about the trunk ROM of the finger tapping tasks.

	S001 - PRE DBS		AVERAGE
	Trial 1	Trial 2	
TAPPING IPSILATERAL			
Index of Dystonia [°]	116.52	100.43	**108.48**
Modified Index of Dystonia [°]	121.77	105.07	**113.42**
Trunk Flex ROM [°]	3.06	2.19	**2.63**
TAPPING CONTRALATERAL			
Index of Dystonia [°]	63.09	54.48	**58.79**
Modified Index of Dystonia [°]	65.72	56.93	**61.33**
Trunk Flex ROM [°]	4.66	6	**5.33**

Table 3.18: *Indicators extracted from finger tapping tasks of subject S001 (pre-DBS).*

	AVERAGE	
	S001 - PRE DBS	*S001* - POST DBS
TAPPING IPSILATERAL		
Index of Dystonia [°]	**108.48**	**129.63**
Modified Index of Dystonia [°]	**113.42**	**140.53**
Trunk Flex ROM [°]	**2.63**	**6.68**
TAPPING CONTRALATERAL		
Index of Dystonia [°]	**58.79**	**39.14**
Modified Index of Dystonia [°]	**61.33**	**41.36**
Trunk Flex ROM [°]	**5.33**	**3.75**

Table 3.19: *Averages of the indicators extracted from tapping tasks of subject S001, pre- and post-DBS.*

It seems that the *Index of Dystonia* on the contralateral arm is reduced (39.14° vs 58.79°), but the ipsilateral *Index of Dystonia* movement is increased (129.63° vs 108.48°). These results are in line with the literature [19], in which it is reported only the contralateral task, suggesting higher values for subjects with dystonia.

c. Adult pathological subject

The third and last section of the upper limb protocol results regards the indicators extracted from an adult pathological subject (*S002*). In this case, the diagnosis was unknown, but the patient showed a visible tremor on the right arm.

Below are presented all the values extracted from the reaching tasks, with the description of the trends of the angles, and the tapping tasks.

	S002		AVERAGE
	Trial 1	Trial 2	
REACHING			
Shoulder Flex SD	4.28	8.07	**6.175**
Shoulder Flex ROM	60.74	56.72	**58.73**
Shoulder Flex SD/ROM	0.070	0.142	**0.106**
Shoulder Rotation SD [°]	2.57	4.49	**3.53**
Shoulder Rotation ROM [°]	22.27	28.44	**25.36**
Shoulder Rotation SD/ROM	0.115	0.158	**0.137**
Shoulder Abdo-adduction SD [°]	1.03	2	**1.515**
Shoulder Abdo-adduction ROM [°]	5.91	11.36	**8.635**
Shoulder Abdo-adduction SD/ROM	0.174	0.176	**0.175**
Elbow Flex SD [°]	3.59	3.53	**3.56**
Elbow Flex ROM [°]	19.31	20.25	**19.78**
Elbow Flex SD/ROM	0.186	0.174	**0.180**
Elbow Rotation SD [°]	1.66	3.02	**2.34**
Elbow Rotation ROM [°]	14.3	22.52	**18.41**
Elbow Rotation SD/ROM	0.116	0.134	**0.125**
Wrist Flex SD [°]	4.05	3.38	**3.715**
Wrist Flex ROM [°]	21.65	32.59	**27.12**
Wrist Flex SD/ROM	0.187	0.104	**0.145**
Wrist Abdo-adduction SD [°]	0.49	0.81	**0.65**
Wrist Abdo-adduction ROM [°]	3.84	4.75	**4.30**
Wrist Abdo-adduction SD/ROM	0.128	0.171	**0.149**
Trunk Flex SD [°]	1.35	1.83	**1.59**
Trunk Flex ROM [°]	12.39	13.71	**13.05**
Trunk Flex SD/ROM	0.109	0.133	**0.121**
Velocity medial wrist X SD [m/s]	0.043	0.056	**0.0495**
Velocity medial wrist Y SD [m/s]	0.082	0.082	**0.082**
Velocity medial wrist Z SD [m/s]	0.064	0.061	**0.0625**
Wrist Path Ratio	1.348	1.392	**1.370**
Accuracy [m]	0.067	0.055	**0.061**
3D Peak Velocity (medial wrist) [m/s]	0.68	0.752	**0.716**
Mean squared jerk normalized by peak velocity [m/s^5]	3848	1912	**2880**
ECR/FCU forth (%)	128.03	113.17	**120.6**
FCU/ECR back (%)	80.32	90.12	**85.22**
BIC/TRIC forth (%)	143.35	88.28	**115.82**
TRIC/BIC back (%)	70.65	106.44	**88.55**
PD/AD forth (%)	103.64	125.98	**114.81**
AD/PD back (%)	59.15	48.2	**53.68**

Table 3.20: *Indicators extracted from reaching tasks of subject S002.*

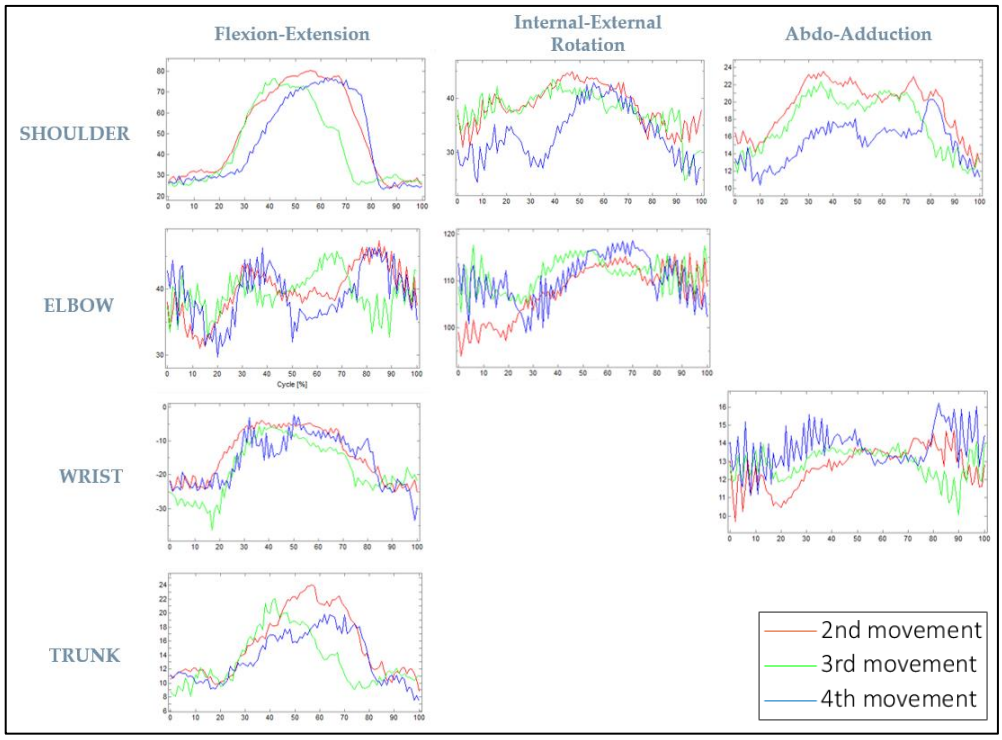

Figure 3.15: *Angles [°] of subject S002 during reaching task (2nd trial).*

The sign of tremor is clearly visible in the graphs of figure 3.15, which alters in a significant way the quality of the execution of the task: the *Wrist Path Ratio* is higher with respect to the previous control subjects and the *Accuracy* is worse.

	S002		AVERAGE
	Trial 1	Trial 2	
TAPPING IPSILATERAL			
Index of Dystonia [°]	107	63.51	**85.255**
Modified Index of Dystonia [°]	113.58	66.78	**90.18**
Trunk Flex ROM [°]	8.55	7.97	**8.26**
TAPPING CONTRALATERAL			
Index of Dystonia [°]	91.92	105.72	**98.82**
Modified Index of Dystonia [°]	98.57	113.47	**106.02**
Trunk Flex ROM [°]	10.79	16.76	**13.775**

Table 3.21: *Indicators extracted from finger tapping tasks of subject S002.*

Also this case, with a grown-up subject, all the set of indicators were successfully extracted. As we can expected, the contralateral *Index of Dystonia* is the highest among all the subjects evaluated (98.82°), and also the ipsilateral index is higher compared to the controls.

3.3.2 Lower Limb

In this section are reported the indicators from the gait analysis of 2 control subjects (*C003* and *C004*) and 2 patients (*S003* and *S004*), as described in table 3.2. Subject *S003* presents a more severe impairment to the right side of the body, whereas *S004* has a left hemiparesis. We are going to present all the spatiotemporal parameters and selected meaningful plots from kinematics and kinetics in order to make possible comparisons.

Looking at the spatiotemporal parameters (table 3.22), we can observe that for *S003* the gait pattern is compromised, and this is visible from the altered ratio, referred to the right limb, between *Swing* and *Stance* phase that characterizes her walking. Besides, the *Double Support* phase, in percentage, is below the normative band and quite different from the left limb. Moreover, the *Normalized Walking Velocity* by the height, for the pathological subject, is slower and so is the *Cadence*. The last indicator we want to highlight is the *Step Length*, for which there are no significant differences between right and left foot in control subjects, but becomes quite different for the subject with dystonia *S003* (64 cm vs 50 cm). For the latter subject, the resulting *Step Profile* is in fact quite different from left to right foot.

Analysing the indicators of subject *S004*, it is evident that the gait is slower compared to the normative pattern (in terms of *Walking Velocity*, *Normalized Walking Velocity*, and *Cadence*), and the *Stride Length* and *Step Length* are shorter. Moreover,

the *Step Width* is increased and the *Step Profile* results smaller with respect to the controls.

	C003		*C004*		Normative Bands
	R	L	R	L	
Temporal Parameters					
Gait Cycle [s]	1.06 ± 0	1.07 ± 0.01	1.01 ± 0.02	0.99 ± 0.02	**0.93 ± 0.04**
Stance [s]	0.64 ± 0.01	0.64 ± 0.02	0.59 ± 0.01	0.58 ± 0.01	**0.54 ± 0.05**
Swing [s]	0.42 ± 0.02	0.43 ± 0.02	0.41 ± 0.01	0.41 ± 0.02	**0.39 ± 0.03**
Stance [%]	60.22 ± 1.15	59.92 ± 1.52	58.83 ± 0.56	58.64 ± 0.3	**57.97 ± 1.93**
Swing [%]	39.84 ± 1.73	40.05 ± 1.83	40.95 ± 0.14	41.92 ± 0.85	**42.03 ± 1.93**
Double Support [%]	9.99 ± 1.74	9.79 ± 1.19	9.3 ± 0.58	7.39 ± 0.09	**12.4 ± 2.21**
Walking Velocity [m/s]	1.2 ± 0		1.6 ± 0.1		**1.2 ± 0.2**
Normalized Walking Velocity [%height/s]	74.07 ± 1.26		97.7 ± 6.24		**80 ± 5**
Cadence [steps/min]	112.95 ± 0.5		120.2 ± 2.26		**129.6 ± 8.4**
Spatial Parameters					
Stride Length [m]	1.27 ± 0.02	1.28 ± 0.01	1.42 ± 0.01	1.42 ± 0.02	**1.13 ± 0.1**
Stride Length [%height]	78.68 ± 1.37	79.05 ± 0.69	87.18 ± 0.87	87.09 ± 1.09	**80 ± 10**
Step Length [m]	0.65 ± 0.01	0.63 ± 0.01	0.7 ± 0.01	0.72 ± 0.01	**0.58 ± 0.06**
Step Width [m]	0.12 ±0.01		0.1 ± 0.01		**0.11 ± 0.02**
Step Profile	5.42	5.25	7.00	7.20	
	S003		*S004*		Normative Bands
	R	L	R	L	
Temporal Parameters					
Gait Cycle [s]	1.04 ± 0.02	1.05 ± 0.02	1.25 ± 0.02	1.25 ± 0.02	**0.93 ± 0.04**
Stance [s]	0.55 ± 0.01	0.64 ± 0.01	0.78 ± 0.02	0.74 ± 0.02	**0.54 ± 0.05**
Swing [s]	0.5 ± 0.01	0.41 ± 0.02	0.47 ± 0.01	0.52 ± 0.03	**0.39 ± 0.03**
Stance [%]	52.83 ± 1.35	61.17 ± 0.98	62.25 ± 0.55	59.18 ± 1.8	**57.97 ± 1.93**
Swing [%]	47.68 ± 0.83	39.45 ± 1.34	37.68 ± 0.64	41.5 ± 2.17	**42.03 ± 1.93**
Double Support [%]	5.67 ± 0.72	9.45 ± 0.4	12.24 ± 2.1	8.86 ± 0.86	**12.4 ± 2.21**
Walking Velocity [m/s]	1.1 ± 0		0.8 ± 0		**1.2 ± 0.2**
Normalized Walking Velocity [%height/s]	67.06 ± 1.3		46.3 ± 2.09		**80 ± 5**
Cadence [steps/min]	115 ± 2.04		96.3 ± 1.375		**129.6 ± 8.4**
Spatial Parameters					
Stride Length [m]	1.14 ± 0.01	1.15 ± 0.03	0.95 ± 0.03	0.95 ± 0.03	**1.13 ± 0.1**
Stride Length [%height]	69.74 ± 0.8	70. 22 ± 1.9	57.59 ± 1.75	57.79 ± 2.12	**80 ± 10**
Step Length [m]	0.64 ± 0.01	0.5 ± 0.02	0.44 ± 0.03	0.51 ± 0.01	**0.58 ± 0.06**
Step Width [m]	0.08 ± 0.01		0.17 ± 0.01		**0.11 ± 0.02**
Step Profile	8.00	6.25	2.59	3.00	

Table 3.22: *Spatiotemporal parameters from control subjects C003 and C004, and subjects S003 and S004. The last column reports the normative bands for children population.*

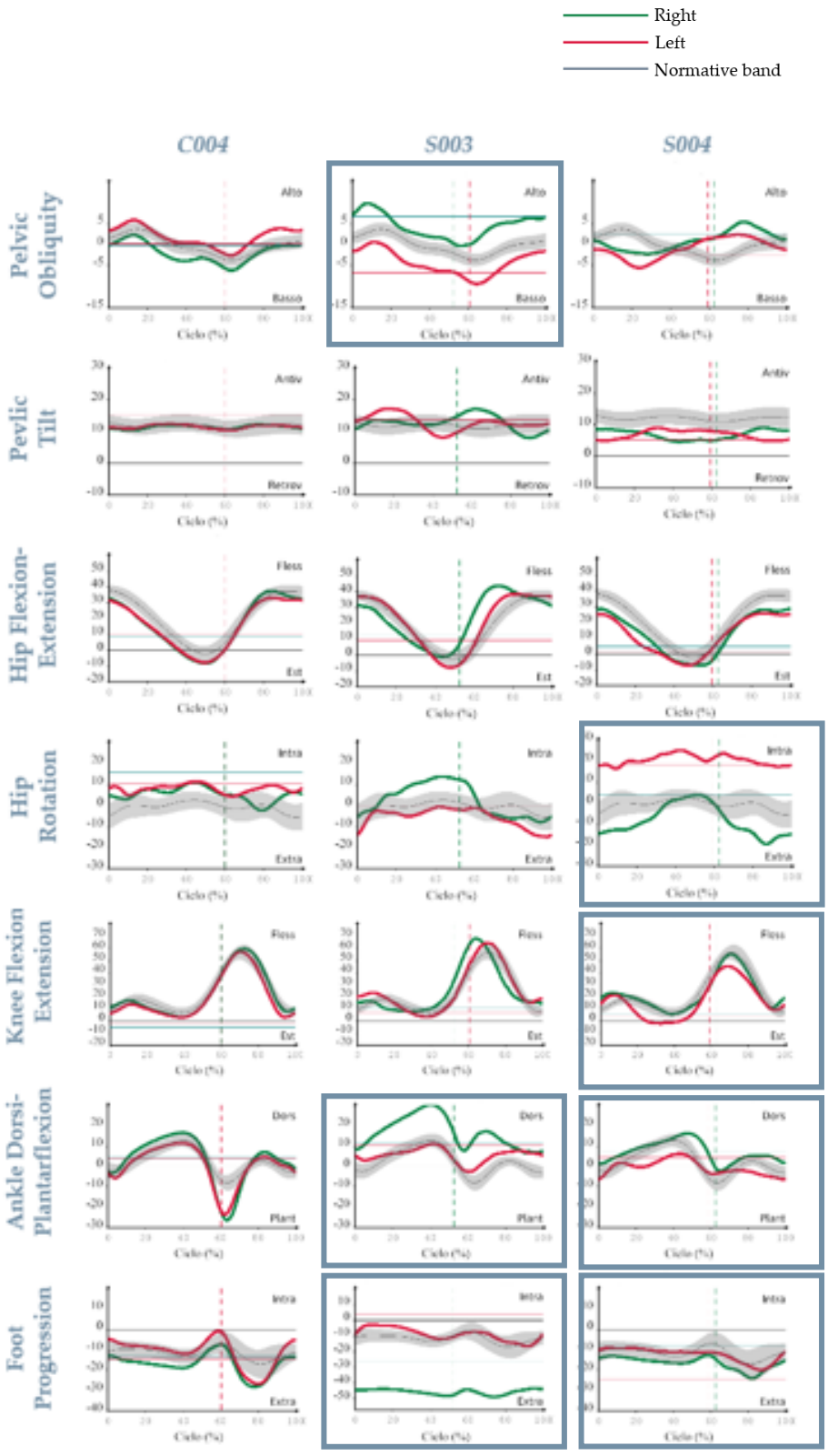

Figure 3.16: *Selected kinematics graphs of control subject C004, and subjects S003 and S004.*

In figure 3.16 are reported the most significant kinematics graphs in order to highlight the differences between the control subject *C004* and the pediatric patients *S003* (more severe right impairment) and *S004* (more severe left impairment). From the analysis, it is evident that the pattern is more altered for the most impaired limb. From *S003*'s results, we can observe that for pelvic obliquity the right side is more oriented upwards, while the left side downwards, highlighting a leg discrepancy. The right ankle has a very increased dorsiflexion, whereas the right foot is greatly in extrarotation. Conversely, these two angles follow the normative trends for the left limb. Passing to *S004*, the first thing to highlight is the increased internal left hip rotation. The left foot presents an almost flat trend, always in extrarotation, while the right foot is always extrarotated as well, but the trend has a shape similar to the normative band. The left knee flexion-extension is altered: during mid-stance the knee goes in hyperextension, and, during swing, the flexion peak is reduced with respect to the controls. Finally, the dorsiflexion of the left foot is very limited, and so the total ROM, showing a prevalent plantarflexion during the entire the gait cycle.

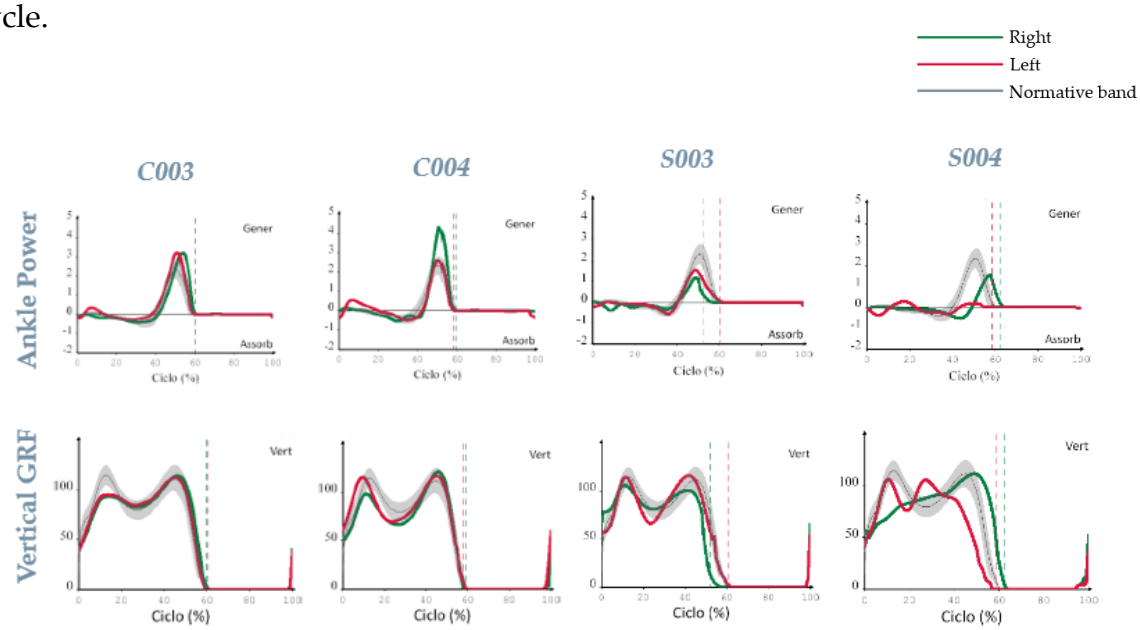

Figure 3.17: *Ankle power and vertical Ground Reaction Force of control subjects C003, C004, and subjects S003 and S004.*

The most significant results from the kinetics regard the push-off ability, with the peak (*MaxPushOff*) strongly reduced in the pathological subjects, especially for the most impaired limb (figure 3.17 and table 3.23). The lowest value appears for the left foot of subject *S004* (0.4 W/Kg). The vertical component of the GRF (figure 3.17) reflects an altered pattern for *S003* in the right (impaired) limb, whereas the patterns are altered in both limbs for *S004*, showing that an altered strategy is adopted also for the least compromised limb, probably to compensate for the most compromised one. In addition, the maximum values from the medio-lateral component of GRF (*MaxGRF_ML*) result, on average, to be higher for the pathological subjects (table 3.22), as suggested in literature [65].

	C003		*C004*	
	R	L	R	L
Kinematic Parameters				
MaxGRF_ML [%weight]	5.25	11.57	7.99	9.75
MaxPushOff [W/Kg]	4.4	2.7	3.4	3.4
	S003		*S004*	
	R	L	R	L
Kinematic Parameters				
MaxGRF_ML [%weight]	10.07	10.78	8.44	10.89
MaxPushOff [W/Kg]	1.2	1.6	1.6	0.4

Table 3.23: *Maximum GRF in the medio-lateral plane and maximum ankle power of control subjects C003 and C004, and subjects S003 and S004.*

The last category of data to assess is the EMG signals, comparing the activation timings with an adult normative reference [66], described in figure 3.18.

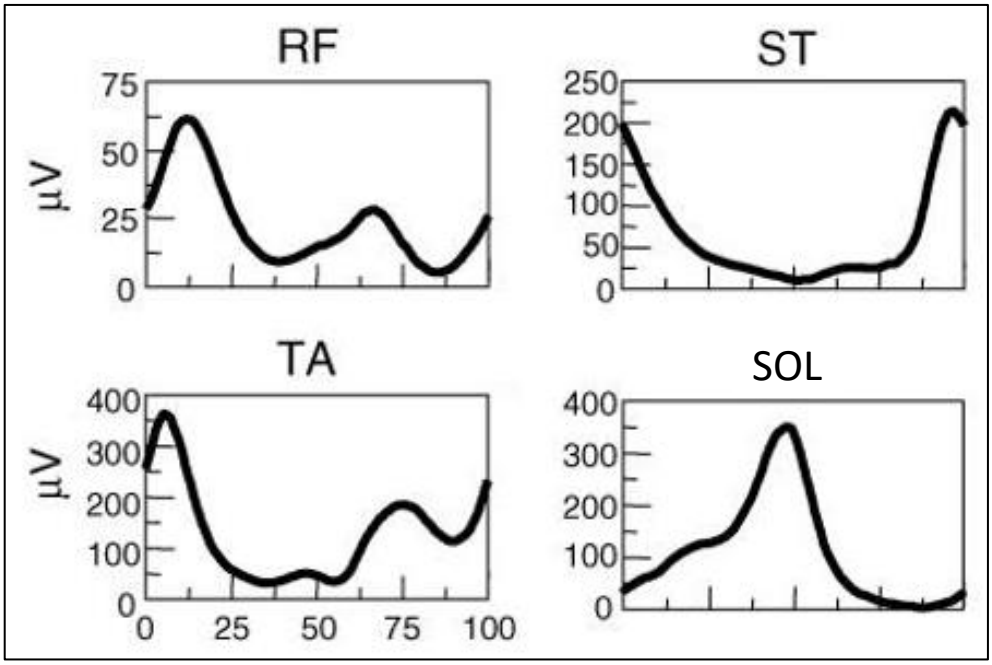

Figure 3.18: *Normative EMG muscle activation during gait of RF, ST, TA and SOL by Ivanenko et al.* [66].

Firstly, we present the EMG envelopes coming from the gait trials of control subject *C004*, with the trends of the four selected muscles, normalized by the MVCs, and described along the percentage of the gait cycle, with also the indication of the average toe-offs. The black curve is the average of all the grey trials. Below, instead, the same graphs are presented for the pathological subjects.

The EMG data recorded from the left ST are not reliable due to problem with the EMG probe, and so they are not reported.

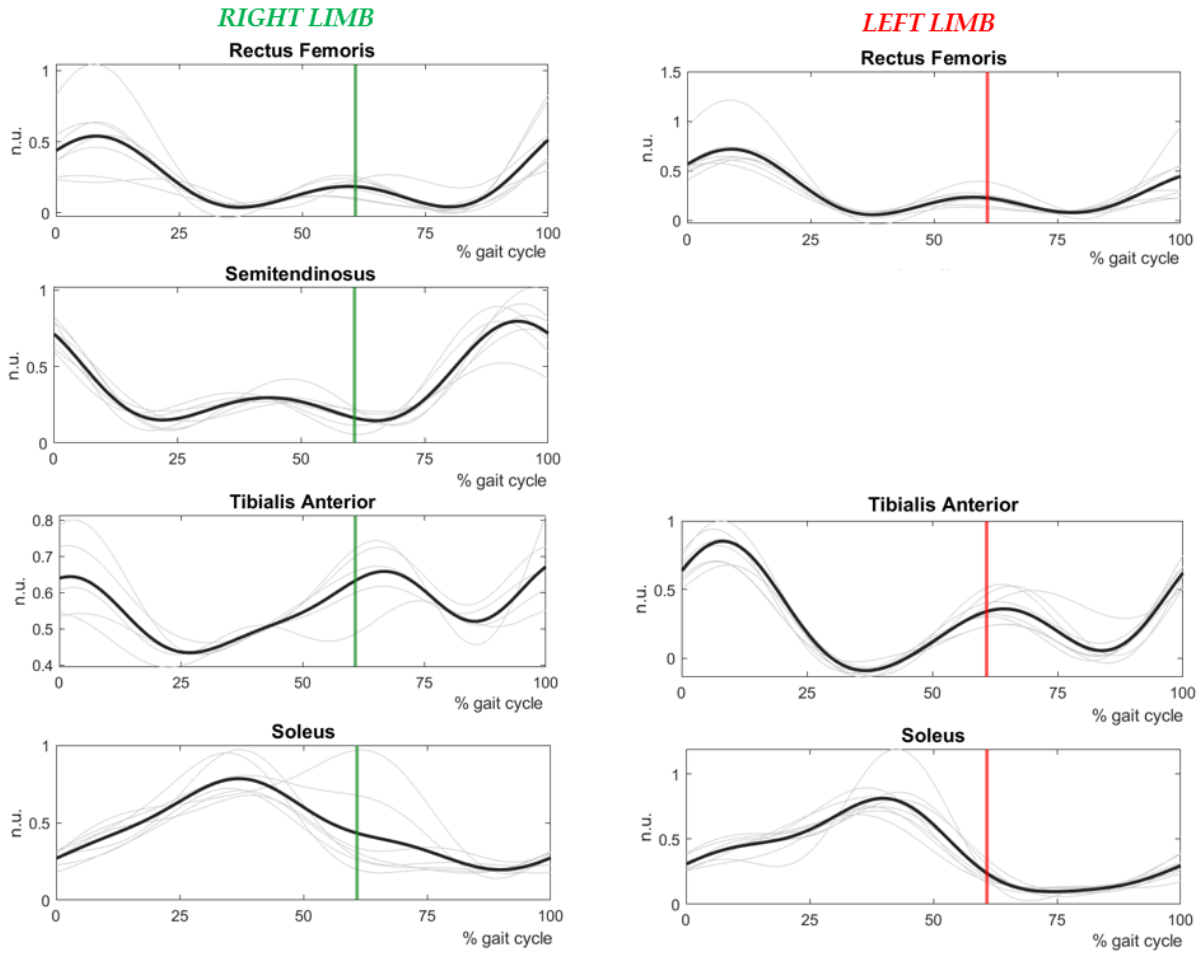

Figure 3.19: EMG muscle activation during gait of subject *C004*.

Comparing figure 3.19 with the normative patterns of figure 3.19, we can observe that all the signals are in line with the literature:

- for the RF envelope, we can clearly see the two activation peaks, for both left and right limb, one at the beginning of the gait cycle, right after the heel strike, and the other in correspondence of the toe-off;
- in the ST envelope we can again detect two bursts of activation, at the beginning and at the end of the gait cycle;

- as for TA, there is one activation at the beginning of the gait cycle and the second one in correspondence of the toe-off, for both the limbs, similarly to the RF;
- looking at the SOL envelopes, there is only one evident activation right before the swing phases.

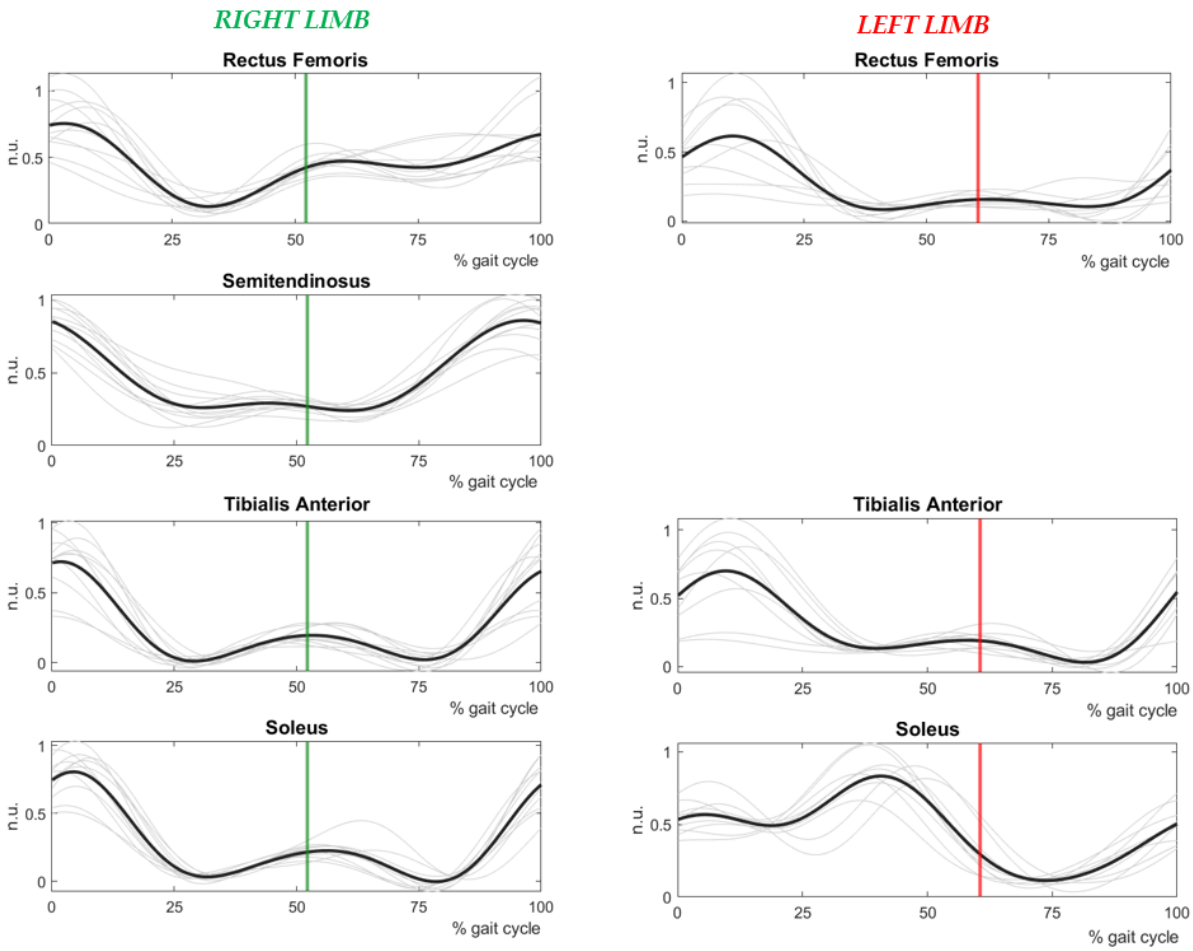

Figure 3.20: EMG muscle activation during gait of subject *S003*.

The situation is different for the subject with dystonia *S003* (figure 3.20), where we can also observe the increased alteration for the right limb. The signals that mostly differ from the normative patterns are the TA, for which the activation in correspondence of the toe-off is not clearly visible, and the right SOL, which does

not show the normative prominent peak, conversely visible in the left limb. The right ST behaves as expected, whereas the RFs are quite different from the normative patterns: the second activation peak is not so evident in the left leg.

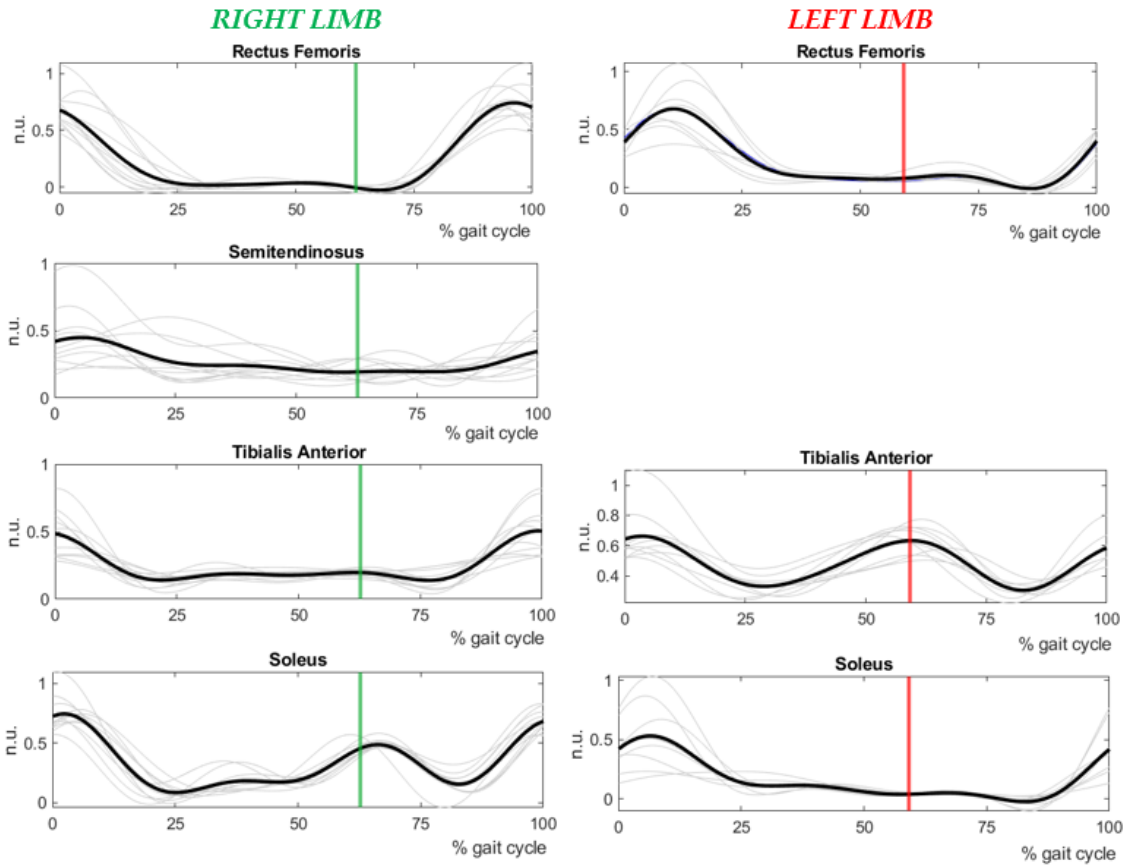

Figure 3.21: EMG muscle activation during gait of subject *S004*.

Finally, some differences can be observed also in the EMG signals of pathological subject *S004* (figure 3.21). The impairment on the left side is visible in the SOL, which lacks the peak in correspondence of the toe-off. Also the RFs do not show the expected 2nd bursts of activation, whereas the signals coming from right TA and ST are characterized by just very small activations in correspondence of the heel strikes.

3.4 Passive Stretching

For passive arm extensions, we evaluated the data coming from control subjects *C001*, *C002* and the subject *S001* with Primary Dystonia (post -DBS), conversely, for passive leg flexions, the analysed data came from controls *C003* and *C004*, and the pathological subject *S004*.
In all the cases, we set an activation threshold on the EMG signals of agonist and antagonist muscles using the two methods explained in section 2.5.2, in order to find any possible catches; in addition, we extracted other related indicators (*COFLEX*, *COEXT* and *EMG-change*).

Considering both the upper limb and the lower limb, below are reported examples of EMG signals from the antagonist and the agonist muscles. In each figure, the first two graphs are the energy signals, with in red the activation thresholds set using the TK method, while the last two graphs report the envelopes of the signal, with the threshold set based on the baseline of the envelope. In each pair, the top plot describes the antagonist, while the bottom plot describes the agonist.

As an example, we consider one fast trial of the control subject *C002* (figure 3.22). We can observe that the agonist signal (Triceps) never exceeds the threshold between start and stop, so it means that the movement is completely passive. Moreover, also the antagonist signal (Biceps) never exceeds the threshold, so no catches have been detected, as expected. These considerations are valid for both the threshold methods, even if the TK method identifies a higher and more appropriate activation threshold.
For *C002*, these trends can be found in all the trials for all the velocities.

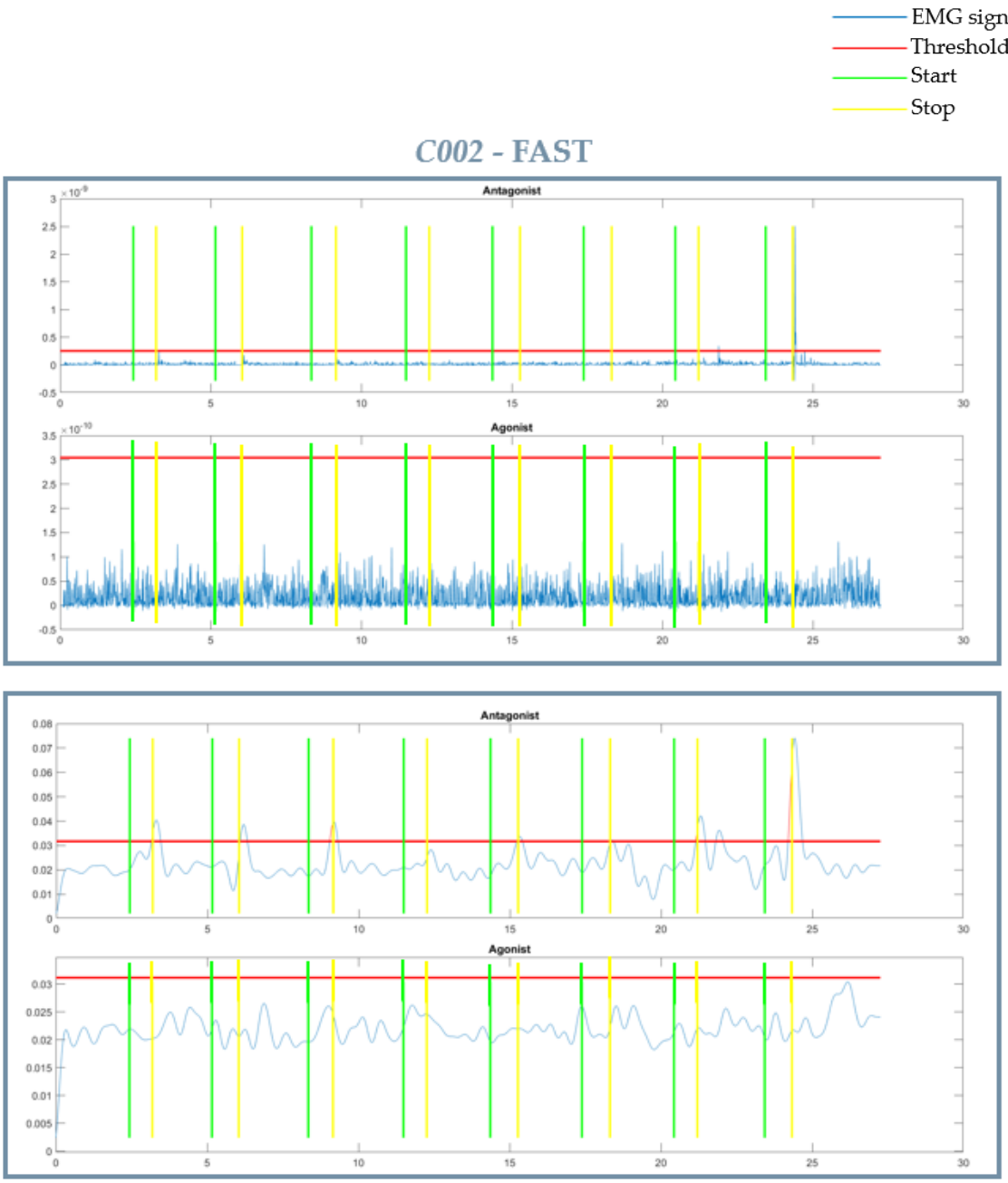

Figure 3.22: *EMG signals from C002 fast arm extension (1st trial).*

The situation is different considering the trials of control subject *C001*. Taking as example the 1st slow trial (figure 3.23), we can notice that the agonist EMG signal often exceeds the threshold during the stretching, in both the methods, meaning that the movement is not completely passive and so those windows will be

eventually discarded. Also in this case, the envelope activation threshold is lower with respect to the TK one, which instead seems more reliable. Anyway, no catches were detected considering all the trials.

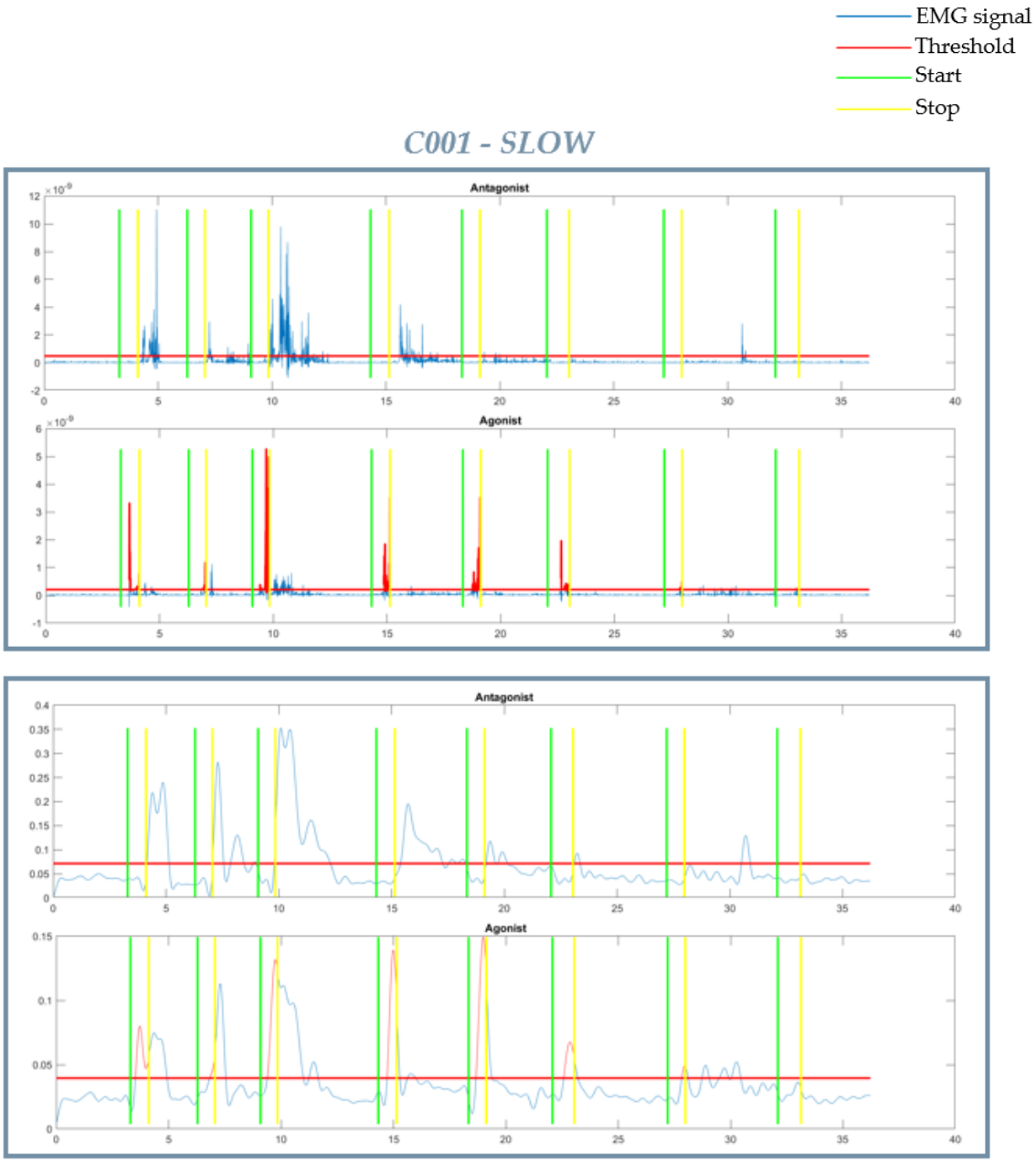

Figure 3.23: *EMG signals from C001 slow arm extension (1st trial).*

Considering the last example in figure 3.24, referring to *S001*, the two methods behave in a different way. The energy signals never exceed the threshold, while the

envelopes of both antagonist and agonist muscles exceed the threshold in the same time windows: this means that the movement is not completely passive. However, during this trial, the operator did not detect any sign of spasticity, so we are led to think that the energy signals and their relative activation threshold identified with the TK method are the most reliable ones, whereas the thresholds set on the envelopes are too low and so the reported activations are not significant.

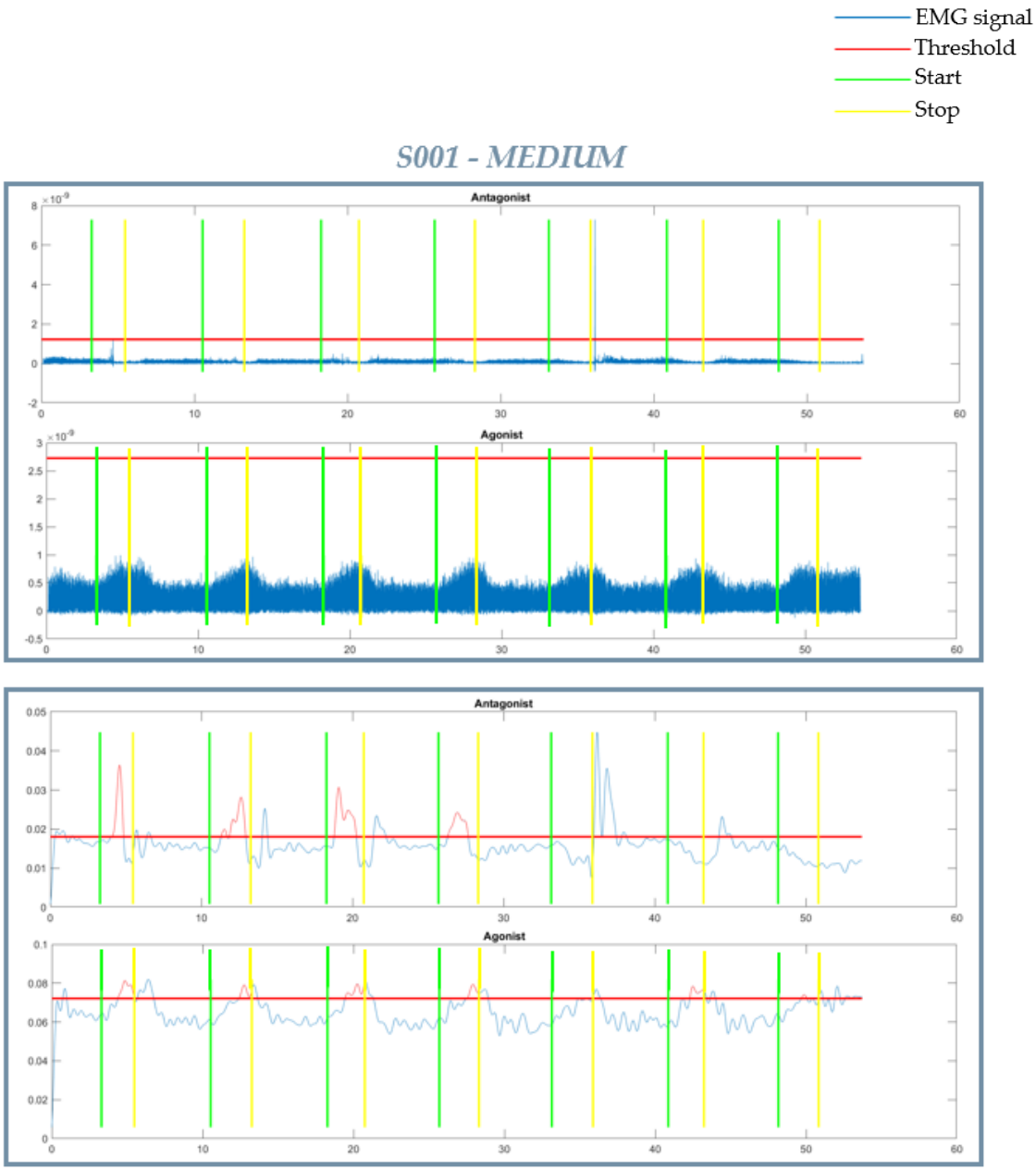

Figure 3.24: *EMG signals from S001 medium arm extension (2nd trial).*

Considering also the other trials of *S001*, we can observe the same trend: the envelope signals sometimes exceed the threshold, but the energy signals do not record any activation.

Passing to the last indicators (table 3.24), the indexes of co-contraction result very subject-dependent: *COFLEX* ranges from 8% to 34%, while *COEXT* ranges from 6% to 32%. The *EMG-change*, both for the agonist and the antagonist, is always below the 1%, so do not evidence any significant change between fast and slow trials.

	C001	*C002*	*S001* - POST DBS
ARM EXTENSION			
COFLEX (%)	34.58	8.73	18.74
COEXT (%)	17.42	32.85	6.58
EMG-change antagonist (%)	0.333	0.183	0.00002
EMG-change agonist (%)	0.028	0.046	0.35

Table 3.24: *Co-contraction ratios and EMG-change indicators from control subjects C001, C002, and subject S001.*

Considering the lower limb passive extensions, the agonist signal refers to the Semitendinosus (ST), while the antagonist is the Rectus Femoris (RF). With respect to our trials, in some cases the envelope slightly exceeds the threshold (figure 3.25), while the energy signal do not. In line with the previous considerations, we think that the most reliable method is the TK.

Figure 3.25: *EMG signals from S003 slow leg flexion (2nd trial).*

As for the subject *S004* with left hemiparesis, the EMG analysis reveals that during almost the totality of the stretches the movement was not passive, but there was an active contribution of the agonist muscle, reported by both the methods (example

in figure 3.26). Considering the wrong execution of the trials, no catches were detected.

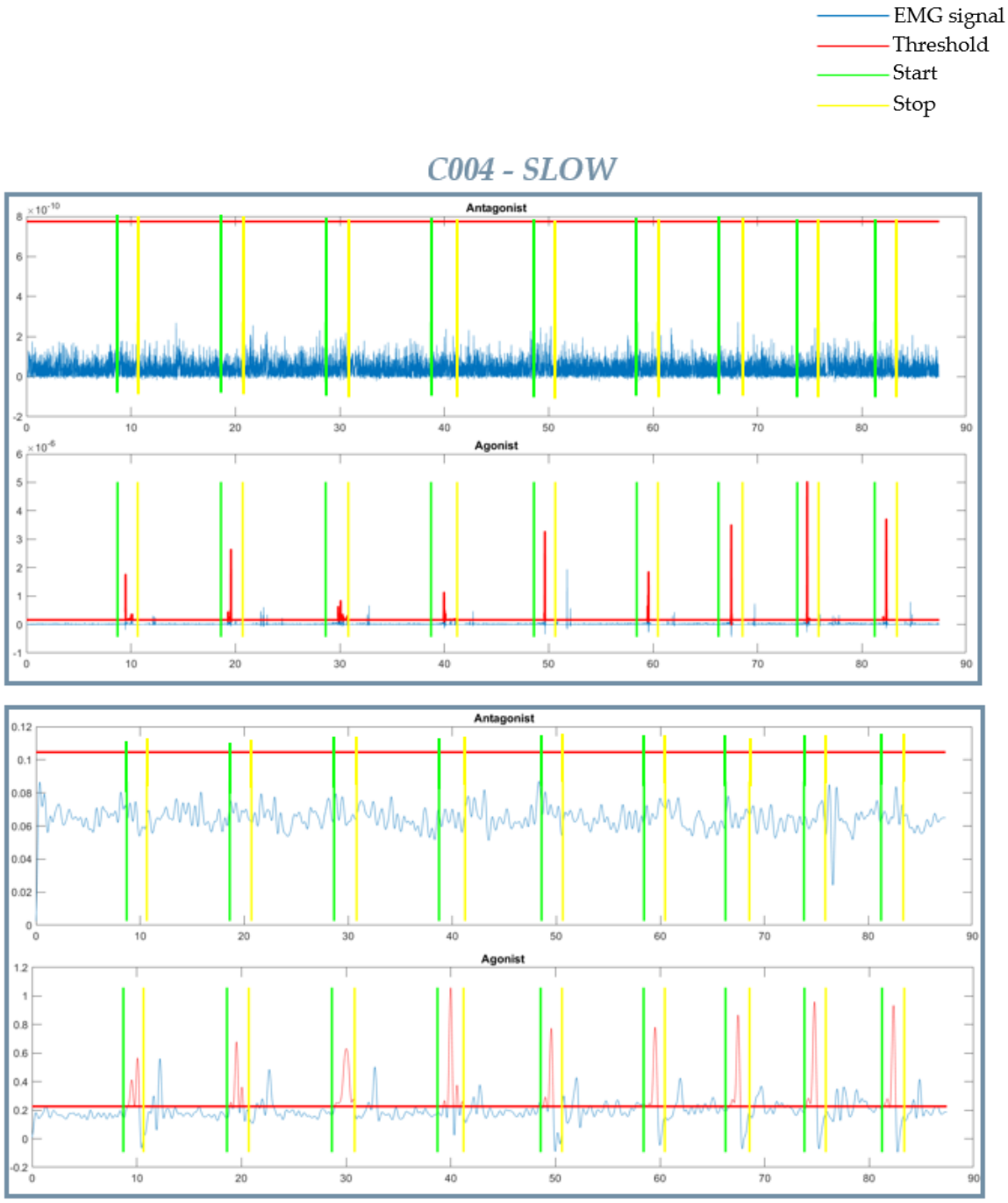

Figure 3.26: *EMG signals from S004 slow leg flexion (2nd trial).*

Analyzing the last indicators (table 3.25), for leg flexion, the *COFLEX* index is stable at 14% for control subjects, whereas is quite increased for *S004* (55.59%). The *COEXT* index, instead, is variable, passing from 6.89% to 36.47% between controls, while is again increased in the pathological case (53.91%). As previously, the *EMG-change* indicators are below or slightly above the 1%, with the only exception considering the agonist muscle of subject *S004*, which is higher than 1%. We think it is due to the fact that the stretching were never passive, and so the indicator reflects a distorted situation.

	C003	*C004*	*S004*
LEG FLEXION			
COFLEX (%)	14.5	14.32	55.59
COEXT (%)	36.47	6.89	53.91
EMG-change antagonist (%)	0.898	0.732	0.316
EMG-change agonist (%)	1.132	0.805	18.86

Table 3.25: *Co-contraction ratios and EMG-change indicators from control subjects C003 and C004, and subject S004.*

4. Discussion

This thesis work presents a novel neuro-motor assessment to quantify dystonia and spasticity in children, developing and extracting a series of indicators both from upper limb and lower limb, overcoming the limits related to the classical clinical scales. The work was carried out at the Movement Analysis Laboratory of Fondazione I.R.C.C.S. Istituto Neurologico Carlo Besta in Milan within the framework of the research project "The DYSPA System", using an optoelectronic system synchronized with force platforms, to extract parameters related to kinematics and kinetics, and EMG probes for the analysis of the muscular activity. This first part of the project deals with the definition and the validation of the protocols, regarding both the placement of the markers and the EMG probes, and the data analysis that follows for the extraction of clinically-relevant indicators. The protocols are designed to be easy to perform - since we are dealing with paediatric patients - and comprehend functional tasks and passive stretching for both upper and lower limbs. In this context, we recruited children with movement disorders and healthy age matched subjects to test the feasibility of the protocols. Moreover, an adult subject was tested to evaluate whether the designed protocols could be feasible and used also for the adult population in case of future developments. The statistical sample envisaged for the protocol validation is too small to perform any statistical test, anyway some meaningful considerations can still be drawn. Based

on them, improvements to the protocols and data analysis algorithms can be introduced for the actual acquisition campaign.

The very first aim of the project was to develop a marker placement protocol for both the upper limb and the lower limb. For the latter, the supporting literature is wide and so we could select the most widely known gait protocol, the Davis marker set [52], composed of 22 passive markers placed on the patient, which is suitable also for the paediatric population [69]. The preparation phase is quite time consuming, comprising a series of anthropometric measures that have to be taken, but it allows to easily detect the lower limb joint centres (hip, knee and ankle) and so to compute all the gait related parameters. The marker set used during the leg passive stretches is a subset of the Davis protocol, leaving only the markers strictly necessary to derive the joint centres on the selected leg. Conversely, the literature referring to upper limb marker protocols is dispersive and surely not as developed and precise as the lower limb. Anyway, following the ISB recommendations [41], and other very useful related works dealing with upper limb biomechanical models [51], [70], we were able to develop a monolateral 9-marker protocol. The choice was guided by the necessity to develop a protocol with as few as possible markers in order to extract the relevant joint angles, highlighted in literature, to study children with movement disorders. In this case, the preparation phase is very fast: we do not need any anthropometric measure because all the joint centres (glenohumeral, elbow and wrist) are approximated from the markers' position. The validation trials confirmed the solidity of this protocol, showing meaningful results for all the selected joints in all the tested directions. Moreover, the limited number of the markers is important to allow as much freedom of movement as possible, which is particularly important for paediatric patients and children in general.

Below, we are going to discuss the extracted indicators, both from upper limb and lower limb. From the analysis of the data coming from the reaching tasks, a significant variability between trials for the youngest control subject (7-year-old) emerged. When observing the child performing the task, we realized that this was probably due to the initial discomfort caused by the equipment mounted on her, which could lead her to change her motor strategy in the initial trials. This observation led us to the conclusion that future acquisitions should include some acquaintance trials, before the real ones, in order to put children at ease with all the equipment mounted on them.

As for the comparison between pathological and control subjects, rather than comparing the two groups as a whole, the results suggest that it is better to compare the performance of a patient with dystonia with an age-matched control subject to get more reliable information. Indeed, motor control literature shows how there is an evident change in motor performance between childhood and adolescence [68]. Moreover, a study from Leversen *et al.* asserts that the motor performance increases from childhood to young adulthood, so approximately from 7-9 to 19-25 years old, and then a slow descent begins [71].

This is why our comparison related to the upper limb protocols focused mostly between *S001* and *C002*, both 14-year-old boys. First of all, looking at the different joint angles' plots, we can observe that the two subjects followed a completely different strategy to reach the target: the control subject mainly used flexion-extension of the shoulder and elbow joints, following a more linear path to reach the target placed in front of him. On the other hand, the subject with dystonia mainly used the shoulder abduction/adduction to reach the target, while the elbow joint presented an almost constant extension, which resulted in a more curvilinear path to reach the target. The different motor strategies adopted by the two subjects can be studied through the analysis of the extracted indicators and of the joint angle

profiles over time. It is important to underline that a single parameter is not enough to describe a whole situation, but we need a complete analysis covering different aspects of the motor performance, related also to the clinical and psychological status of the subject. The same applies to the analysis of the gait report, where we do not stress just a single indicator, but the overall evaluation.

However, investing all the parameters, we can observe that the *Wrist Path Ratio* presents better values for both controls, suggesting that is a robust indicator of dystonia independently from the subject's age. This result is perfectly in line with the literature [19], [43], [45].

As for *Peak Velocity*, we realized that the analysis of this indicator in a task for which no indications were provided about the execution speed, may not be strictly related to the presence of dystonia. A solution in this direction may be to instruct the subject to choose a specific execution speed (e.g., "perform the task at the maximum possible speed") in order to allow the comparison between populations. However, from the confrontation with the clinical experts, we decided to let the subject execute the gesture as naturally as possible, so without adding any additional time constraints. Also in other studies, the execution speed of the studied task is self-imposed by the subject [19], [43], [45].

Analysing the finger tapping tasks, another relevant result emerged: the *Index of Dystonia*, the principal quantitative indicator to assess dystonia in literature [19], is always worse in the pathological subject, even compared to the younger control subject; this finding further proves that this is a reliable indicator for this kind of task. Also the modified version that we introduced, with the addition of wrist abdo-adduction, shows the same trend.

Passing to the figure-8 writing task, another important achievement of the devised protocol can be seen in the use of the *CRP*, not only applied to the lower limb as seen in literature [62], but also extendible to the upper limb. In order to compute the

CRP, we successfully extracted the phase of shoulder, elbow and wrist joints, and it is clearly possible to observe the phase coordination between segments during the figure-8 writing task: in a not compromised movement, shoulder and elbow result to be in anti-phase, while elbow and wrist in phase (figure 4.1).

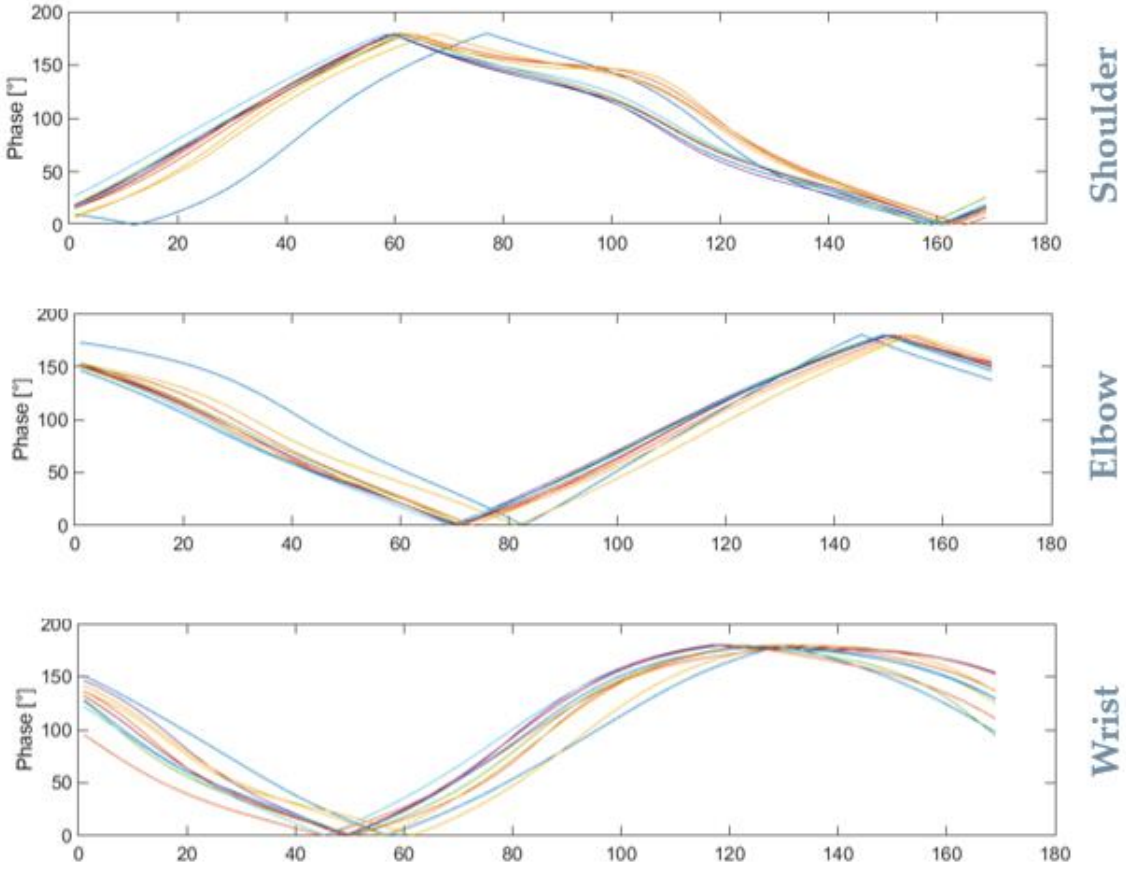

Figure 4.1: *Phase angles during figure-8 writing of a control subject; each line represent a figure-8 movement.*

For *Time Variability*, we can make a similar consideration we made above for *Peak Velocity*: the use of a metronome will probably smooth out the differences due to execution, but this could influence the gesture. The results show that the pathological subject had a variability of 0.77 seconds, whereas the control subject of

only 0.2 seconds; this is in line with literature, suggesting that the performance of children with dystonia is characterized by increased variability, both in space and time [46].

We had also the possibility to test the developed upper limb protocol assessing a subject with dystonia pre- and post-DBS, 3 months after surgery. In fact, one aim of the project is also the possibility to compare the differences due to a specific treatment, in the most quantitative way. In this case, probably due to the fact that the assessment was quite close in time to the surgery, no relevant improvements were detected. Indeed, a study from Loher *at al.* on a population of 14 dystonia patients showed that it took up to 6 months until full benefits from DBS upon adjustment of the voltage [72]. Nowadays, the most established stimulation technique for dystonia is targeting the globus pallidus pars interna (GPi); usually the patients respond well to this surgery. However, the predictors of outcome within this population are not well known [67]. Despite the uncertainty of the treatment, especially in the early stages, we can see that the *Index of Dystonia* decreased, as a possible sign of the post-surgery improvement.

The upper limb protocol was successfully performed also on a grown-up pathological subject, characterized by a consistent tremor on the right arm. We mounted the right compromised limb, coinciding with the dominant arm, and we were able to extract all the indicators from reaching and tapping tasks. The trends of the angles during reaching are evidently compromised by the significant tremor and so the *Wrist Path Ratio* was worse with respect to the controls. The *Wrist Path Ratio* is an index not only studied on children, but also on the adult population; for example, there are studies recruiting Parkinson's Disease (PD) subject to perform reaching tasks and assess the grade of curvature of the gesture [73], [74]. In these

specific studies, no significant differences emerged between PD and control populations regarding the *Wrist Path Ratio*. Passing to the finger tapping tasks, also in this case the *Index of Dystonia* was high, underlying a motor dysfunction. In this case, there are no studies in literature computing the latter index on adult population because they usually referred to CP children. However, we think that it can be computed also on grown-up people without any complication.

The gait analysis trials highlight different tendencies between pathological and control subjects, as expected. The indicators of the subject with dystonia (*S003*) reflect her damage, especially to the right side of the body, characterized by a gait with the right foot greatly dorsiflexed and externally rotated. The increased ankle dorsiflexion is usually caused by a weak Soleus [53]; a confirmation of this hypothesis can be found by examining the EMG data referred to the right Soleus, which completely lacks the distinguished peak right before the toe-off. The reduced strength can be observed also from the ankle power graph, which presents a peak well below the normative band. The difference in the hip abduction between legs is a further confirmation of the more severe damage of just one leg, the right one, which is reflected also on the pelvic obliquity. In fact, the right side is over the normative band, while the left side is below, confirming the leg discrepancy. All these alterations resulted in abnormal spatio-temporal parameters, indeed the ratio referred to the right limb between *Stance* and *Swing* phase was altered (52.83% - 47.17%), and the Step Profile was quite different from right to left (8 – 6.5).
Differently from dystonia, for which gait analysis is still not deeply investigated, the literature for hemiplegia, and CP in general, is instead wide [53], [75]. Winters *et al.* identified four homogenous groups of gait patterns in CP based on the kinematics on the sagittal plane [76]. According to this classification and its description, our tested subject *S004* is closer Type II category, characterized by

equinus foot, recurvatum knee, and extended hip. However, a study from Galli *et al.* aimed to achieve a quantitative evaluation of the gait through a series of selected spatio-temporal and kinematic parameters, with the final aim to distinguish right and left hemiplegia gait patterns in the four gait categories [75]. All the evaluated subjects were classified according to Winters classification. In this context, this study can be useful for us to check if the selected parameters extracted on our subject are closer to the average values of the categories by Winters. Among the aforementioned indicators, we can find the flexion-extension angles corresponding to the initial contact of hip (*HIC*), knee (*KIC*), and ankle (*AIC*). Moreover, maximum and minimum values are selected on the same graphs: minimum hip flexion during stance (*HmSt*); minimum knee flexion during stance (*KmSt*) and maximum during swing (*KMSw*); minimum ankle dorsiflexion during stance (*AmSt*) and maximum during swing (*AMSw*). *KmSt* represents knee extension ability, while *KMSt* represents knee flexion ability. Similarly, *AmSt* and *AMSw* represent ankle dorsiflexion ability, respectively, during stance and swing. Comparing our results with the average data reported in the article, we can observe that *HIC*, *HmSt*, and *AMSw* are more similar to Type I left hemiplegia, whereas *KmSt* and *AIC* are closer Type II. This comparison led us to the conclusion that the subject can be classified in a sort of category between Type I and Type II, without a strictly assignment to one or the other category. This could be in line with the fact that the subject underwent a surgery to the left foot; indeed, Type I is quite infrequent "in nature", and it is proper of an after-surgery situation [77]. Moreover, from the GA of subject *S004*, we highlighted that his left knee had a reduced flexion during swing; this can be coherent to the fact that the indexes of co-contractions during stretching resulted to be higher with respect to the controls, as reported in literature [53]. Other characterizing signs of pathology can be observed in the pelvic obliquity, which results to be outside the normative band, pattern recognised in literature to be as

typical of hemiparesis [53]. Finally, the ankle dorsi-plantarflexion of *S004* reflects the outcome of the surgery after 6 months to reduce the equinus foot: the left foot is now slightly in plantarflexion; however, the ROM is still quite limited and so is the dorsiflexion. The EMG signal recorded from the left Soleus is in line with these considerations, lacking the activation in correspondence of the toe-off, and so the push-off ability is extremely reduced on the left side. It is worth to mention that also the right push-off ability is reduced, highlighting the fact that hemiparesis does affect more severely one side of the body, but in turn also the other side is inevitably affected to compensate for the hemiplegic one.

The overall EMG data analysis reveals the different activation patterns between controls and patients, and the discrepancy between the least and the most compromised sides. In this case, we used a normative table based on adult subjects because nowadays there are only few studies trying to quantify the normative EMG patterns during gait in children [78], [79]. Currently, the most used normative reference in clinical settings is still the work of Perry of 1992 [80].

As for gait analysis, it is important to point out that the most delicate and time-consuming part of the protocol is the subjects' preparation, which needs to be done as precisely as possible, but without causing discomfort in subjects, and especially in paediatric patients.

Finally, considering the passive stretching, our considerations concern the two methods implemented for the detection of the activation threshold. We observed that, in some cases, the threshold set on the envelopes was exceeded even when no real bursts were present. This was never the case for the TK method. This is because the threshold set on the envelope resulted always lower compared to the other method, very near to the signal baseline, and in some cases reported a muscular activation which was not real. Apart from the subject with hemiparesis, none of the

other tested subjects had signs of spasticity, and no spastic catches were detected by the operator. The subject with Primary Dystonia did not present any catch; in fact, Primary Dystonia is not usually characterized by spasticity. The subject with hemiparesis did not show catches during our evaluations probably because he actively assisted the movements.

We can conclude that the energy method is more reliable to detect muscle activation threshold.

Since spasticity is defined as a velocity-dependent resistance of a muscle to stretch [1], we expect the *EMG-change*, namely the absolute change between fast and slow trials, to present significant values only in presence of spastic signs. In line with these considerations, and so with the literature [34], the computed values for the antagonist in our cases were always very close or below 1%, so a further proof that spasticity was not present.

4.1 Conclusions & Future Developments

In conclusion, we successfully developed protocols – for upper and lower limb - able to be performed both by children and grown-up patients, in order to extract meaningful parameters to assess the presence of spasticity and dystonia. In particular, our work focused more on the creation of the upper limb protocol: the marker set is composed of a limited number of markers located in easily accessible body landmarks and allowing a fast preparation; moreover, the tasks executed are easy and fast to be performed, two fundamental points when dealing with children. After this first phase of protocol validation, we can draw some considerations for the further development of the project, based on the data analysis and the confrontation with child neurologist. Hereafter, to further refine the upper limb protocol, we could maintain the index finger marker for the tapping tasks in order

to analyse the velocity of the finger and the trend of the velocity along the execution of the movement. Indeed, a decreasing trend in speed along the movement execution may be an important parameter, as already studied in literature for PD [81].

Moreover, a static trial could be added at the beginning of the protocol to derive the offset angles also for the upper limb, as we did in the validation trials.

Regarding the passive stretching, a further set of voluntary movements to be executed by the subjects could be added. These additional movements are derived from the Brain Motor Control Assessment (BMCA) protocol, which was developed originally for the lower limb [82], [83], but can be also extended to the upper limb [84]. The BMCA protocol consists in a series of manoeuvres, among which we can highlight 10 specific voluntary movements: hip flexion-extension (bilateral and unilateral), knee flexion-extension (bilateral and unilateral), and unilateral dorsi-plantarflexion. During these trials, sEMG electrodes are placed on Quadriceps, Adductors, Hamstrings, Tibilias Anterior and Triceps Surae of each leg in order to investigate the muscle activity. The interpretation of these data provides clinicians with detailed information about the motor control and possible forms of spasticity. The upper limb version is, conversely, composed of shoulder abdo-adduction (bilateral and unilateral), and unilateral elbow flexion-extension and wrist flexion-extension (palm up and palm down). The aim is the same of the lower limb version, but the selected muscles are 12, 6 from each side: Pectoralis Major, Deltoid, Biceps, Triceps, and wrist flexor and extensor muscle groups. A subset of manoeuvres and muscles - that fit our experimental setup - can be selected from the BMCA protocol to further investigate spasticity.

As for spasticity trials, the main limit was the fact that we managed to recruit and test only one paediatric subject with spasticity, but he did not show any catches during the acquisition, probably due to the wrong execution (active support to

operator during stretching). Dealing with patients, we were bound to the clinical practice of the Institute, for which patient recruitment is not as predictable as for control subjects. The next trials will foresee the testing of more subjects with spasticity, so that it will be possible to optimize the data analysis referred to the extraction of the spasticity-related indicators. Future development for passive stretching protocols could be the use of earplugs by the operator, so that the subject cannot ear the metronome tone, trying to limit his/her active cooperation.

Another limit of the validation trials, again linked to the clinical practice, was the absence of mixed-hypertonia subjects, the most difficult clinical phenotype to assess.

Bibliography

[1] T. D. Sanger, M. R. Delgado, D. Gaebler-Spira, M. Hallett, and J. W. Mink, "Classification and Definition of Disorders Causing Hypertonia in Childhood," 2003. [Online]. Available: www.aappublications.org/news

[2] "Surveillance of cerebral palsy in Europe: a collaboration of cerebral palsy surveys and registers Surveillance of Cerebral Palsy in Europe (SCPE)."

[3] D. S. Reddihough and K. J. Collins, "The epidemiology and causes of cerebral palsy," *Australian Journal of Physiotherapy*, vol. 49, no. 1. Australian Physiotherapy Association, pp. 7–12, Jan. 01, 2003. doi: 10.1016/S0004-9514(14)60183-5.

[4] M. Bax, C. Tydeman, and O. Flodmark, "Clinical and MRI correlates of cerebral palsy: The European cerebral palsy study," *Journal of the American Medical Association*, vol. 296, no. 13, pp. 1602–1608, Oct. 2006, doi: 10.1001/jama.296.13.1602.

[5] L. A. Koman, B. P. Smith, and R. Balkrishnan, "Spasticity associated with cerebral palsy in children: Guidelines for the use of botulinum A toxin," *Pediatric Drugs*, vol. 5, no. 1. Adis International Ltd, pp. 11–23, Dec. 18, 2003. doi: 10.2165/00128072-200305010-00002.

[6] N. A. Murphy, M. C. N. Irwin, and C. Hoff, "Intrathecal baclofen therapy in children with cerebral palsy: Efficacy and complications," *Archives of Physical Medicine and Rehabilitation*, vol. 83, no. 12, pp. 1721–1725, Dec. 2002, doi: 10.1053/apmr.2002.36068.

[7] K. W. Krigger, "Cerebral Palsy: An Overview," *American Family Physician*, vol. 73, no. 1, pp. 91–100, 2006.

[8] T. D. Sanger *et al.*, "Definition and classification of hyperkinetic movements in childhood," *Movement Disorders*, vol. 25, no. 11, pp. 1538–1549, Aug. 2010, doi: 10.1002/mds.23088.

[9] I. Novak *et al.*, "Early, accurate diagnosis and early intervention in cerebral palsy: Advances in diagnosis and treatment," *JAMA Pediatrics*, vol. 171, no. 9. American Medical Association, pp. 897–907, Sep. 01, 2017. doi: 10.1001/jamapediatrics.2017.1689.

[10] J. K. Fink, "Hereditary spastic paraplegia," *Current Neurology and Neuroscience Reports*, vol. 6, no. 1. Springer, pp. 65–76, Jan. 2006. doi: 10.1007/s11910-996-0011-1.

[11] J. M. Polo, J. Calleja, O. Combarros, and J. Berciano, "Hereditary ataxias and paraplegias in cantabria, Spain: An epidemiological and clinical study," *Brain*, vol. 114, no. 2, pp. 855–866, Apr. 1991, doi: 10.1093/brain/114.2.855.

[12] R. Battini *et al.*, “Clinical and genetic findings in a series of Italian children with pure hereditary spastic paraplegia,” *European Journal of Neurology*, vol. 18, no. 1, pp. 150–157, Jan. 2011, doi: 10.1111/j.1468-1331.2010.03102.x.

[13] S. T. de Bot, B. P. C. van de Warrenburg, H. P. H. Kremer, and M. A. A. P. Willemsen, “Child Neurology: Hereditary spastic paraplegia in children,” *Neurology*, vol. 75, no. 19, pp. e75–e79, Nov. 2010, doi: 10.1212/WNL.0b013e3181fc2776.

[14] A. Berardelli, J. C. Rothwell, M. Hallett, P. D. Thompson, M. Manfredi, and C. D. Marsden, “The pathophysiology of primary dystonia,” *Brain*, vol. 121, no. 7. Oxford University Press, pp. 1195–1212, Jul. 01, 1998. doi: 10.1093/brain/121.7.1195.

[15] T. D. Steeves, L. Day, J. Dykeman, N. Jette, and T. Pringsheim, “The prevalence of primary dystonia: A systematic review and meta-analysis,” *Movement Disorders*, vol. 27, no. 14, pp. 1789–1796, Dec. 2012, doi: 10.1002/mds.25244.

[16] C. P. Charalambous, “Interrater reliability of a modified ashworth scale of muscle spasticity,” in *Classic Papers in Orthopaedics*, Springer-Verlag London Ltd, 2014, pp. 415–417. doi: 10.1007/978-1-4471-5451-8_105.

[17] M. J. Barry, J. M. VanSwearingen, and A. L. Albright, “Reliability and responsiveness of the Barry-Albright Dystonia Scale,” *Developmental Medicine & Child Neurology*, vol. 41, no. 6, pp. 404–411, Feb. 2007, doi: 10.1111/j.1469-8749.1999.tb00626.x.

[18] A. Jethwa, J. Mink, C. Macarthur, S. Knights, T. Fehlings, and D. Fehlings, “Development of the Hypertonia Assessment Tool (HAT): A discriminative tool for hypertonia in children,” *Developmental Medicine and Child Neurology*, vol. 52, no. 5, pp. 83–87, 2010, doi: 10.1111/j.1469-8749.2009.03483.x.

[19] L. M. Gordon, J. L. Keller, E. E. Stashinko, A. H. Hoon, and A. J. Bastian, “Can Spasticity and Dystonia Be Independently Measured in Cerebral Palsy?,” *Pediatric Neurology*, vol. 35, no. 6, pp. 375–381, 2006, doi: 10.1016/j.pediatrneurol.2006.06.015.

[20] D. L. Sackett, W. M. C. Rosenberg, J. A. M. Gray, R. B. Haynes, and W. S. Richardson, “Evidence based medicine,” BMJ Publishing Group, 1996. Accessed: Jun. 27, 2021. [Online]. Available: https://www.ncbi.nlm.nih.gov/pmc/articles/PMC2351566/

[21] K.-C. Lee, L. Carson, E. Kinnin, and V. Patterson, “The Ashworth Scale: A Reliable and Reproducible Method of Measuring Spasticity,” *Neurorehabilitation and Neural Repair*, vol. 3, no. 4, pp. 205–209, Jan. 1989, doi: 10.1177/136140968900300406.

[22] R. E. Burke, S. Fahn, C. D. Marsden, S. B. Bressman, C. Moskowitz, and J. Friedman, “Validity and reliability of a rating scale for the primary torsion dystonias,” *Neurology*, vol. 35, no. 1, pp. 73–77, Jan. 1985, doi: 10.1212/wnl.35.1.73.

[23] L. Pavone, J. Burton, and D. Gaebler-Spira, “Dystonia in childhood: Clinical and objective measures and functional implications,” *Journal of Child Neurology*, vol. 28, no. 3, pp. 340–350, Mar. 2013, doi: 10.1177/0883073812444312.

[24] D. Fehlings, “Hypertonia Assessment Tool (HAT) Hypertonia Assessment Tool (HAT): User Manual,” no. June, pp. 1–10, 2010.

[25] S. Knights, N. Datoo, A. Kawamura, L. Switzer, and D. Fehlings, “Further evaluation of the scoring, reliability, and validity of the hypertonia assessment tool (HAT),” *Journal of Child Neurology*, vol. 29, no. 4, pp. 500–504, Apr. 2014, doi: 10.1177/0883073813483903.

[26] R. J. Palisano, D. Cameron, P. L. Rosenbaum, S. D. Walter, and D. Russell, “Stability of the Gross Motor Function Classification System,” *Developmental Medicine & Child Neurology*, vol. 48, no. 6, pp. 424–428, Feb. 2007, doi: 10.1111/j.1469-8749.2006.tb01290.x.

[27] M. K. Lebiedowska, D. Gaebler-Spira, R. S. Burns, and J. R. Fisk, “Biomechanic characteristics of patients with spastic and dystonic hypertonia in cerebral palsy,” *Archives of Physical Medicine and Rehabilitation*, vol. 85, no. 6, pp. 875–880, Jun. 2004, doi: 10.1016/j.apmr.2003.06.032.

[28] J. R. Engsberg, K. S. Olree, S. A. Ross, and T. S. Park, “Quantitative clinical measure of spasticity in children with cerebral palsy,” *Archives of Physical Medicine and Rehabilitation*, vol. 77, no. 6, pp. 594–599, Jun. 1996, doi: 10.1016/S0003-9993(96)90301-9.

[29] D. L. Damiano, J. M. Quinlivan, B. F. Owen, P. Payne, K. C. Nelson, and M. F. Abel, “What does the Ashworth scale really measure and are instrumented measures more valid and precise?,” *Developmental Medicine & Child Neurology*, vol. 44, no. 2, pp. 112–118, Feb. 2007, doi: 10.1111/j.1469-8749.2002.tb00296.x.

[30] A. Jobin and M. F. Levin, “Regulation of stretch reflex threshold in elbow flexors in children with cerebral palsy: a new measure of spasticity,” *Developmental Medicine & Child Neurology*, vol. 42, no. 8, pp. 531–540, Feb. 2007, doi: 10.1111/j.1469-8749.2000.tb00709.x.

[31] A. Calota, A. G. Feldman, and M. F. Levin, “Spasticity measurement based on tonic stretch reflex threshold in stroke using a portable device,” *Clinical Neurophysiology*, vol. 119, no. 10, pp. 2329–2337, Oct. 2008, doi: 10.1016/j.clinph.2008.07.215.

[32] L. Marinelli *et al.*, “Spasticity and spastic dystonia: the two faces of velocity-dependent hypertonia,” *Journal of Electromyography and Kinesiology*, vol. 37, no. September, pp. 84–89, 2017, doi: 10.1016/j.jelekin.2017.09.005.

[33] A. G. Feldman, “Once more on the equilibrium-point hypothesis (λ model) for motor control,” *Journal of Motor Behavior*, vol. 18, no. 1, pp. 17–54, 1986, doi: 10.1080/00222895.1986.10735369.

[34] L. Bar-On *et al.*, “A clinical measurement to quantify spasticity in children with cerebral palsy by integration of multidimensional signals,” *Gait and Posture*, vol. 38, no. 1, pp. 141–147, 2013, doi: 10.1016/j.gaitpost.2012.11.003.

[35] S. Choi, Y. B. Shin, S. Y. Kim, and J. Kim, “A novel sensor-based assessment of lower limb spasticity in children with cerebral palsy,” *Journal of NeuroEngineering and Rehabilitation*, vol. 15, no. 1, pp. 1–16, 2018, doi: 10.1186/s12984-018-0388-5.

[36] A. Haugh, A. Pandyan, and G. Johnson, “A systematic review of the Tardieu Scale for the measurement of spasticity,” *Disability and Rehabilitation*, vol. 28, no. 15. Taylor & Francis, pp. 899–907, Aug. 2006. doi: 10.1080/09638280500404305.

[37] Y. N. Wu, Y. Ren, A. Goldsmith, D. Gaebler, S. Q. Liu, and L. Q. Zhang, “Characterization of spasticity in cerebral palsy: Dependence of catch angle on velocity,” *Developmental Medicine*

and Child Neurology, vol. 52, no. 6, pp. 563–569, Jun. 2010, doi: 10.1111/j.1469-8749.2009.03602.x.

[38] G. Rabita, L. Dupont, A. Thevenon, G. Lensel-Corbeil, C. Pérot, and J. Vanvelcenaher, "Differences in kinematic parameters and plantarflexor reflex responses between manual (Ashworth) and isokinetic mobilisations in spasticity assessment," *Clinical Neurophysiology*, vol. 116, no. 1, pp. 93–100, Jan. 2005, doi: 10.1016/j.clinph.2004.07.029.

[39] E. Jaspers *et al.*, "The reliability of upper limb kinematics in children with hemiplegic cerebral palsy," *Gait and Posture*, vol. 33, no. 4, pp. 568–575, Apr. 2011, doi: 10.1016/j.gaitpost.2011.01.011.

[40] E. Jaspers, H. Feys, H. Bruyninckx, J. Harlaar, G. Molenaers, and K. Desloovere, "Upper limb kinematics: Development and reliability of a clinical protocol for children," *Gait and Posture*, vol. 33, no. 2, pp. 279–285, Feb. 2011, doi: 10.1016/j.gaitpost.2010.11.021.

[41] G. Wu *et al.*, "ISB recommendation on definitions of joint coordinate systems of various joints for the reporting of human joint motion - Part II: Shoulder, elbow, wrist and hand," *Journal of Biomechanics*, vol. 38, no. 5, pp. 981–992, May 2005, doi: 10.1016/j.jbiomech.2004.05.042.

[42] A. Kawamura, S. Klejman, and D. Fehlings, "Reliability and validity of the kinematic dystonia measure for children with upper extremity dystonia," *Journal of Child Neurology*, vol. 27, no. 7, pp. 907–913, 2012, doi: 10.1177/0883073812443086.

[43] R. Pons *et al.*, "Upper Limb Function, Kinematic Analysis, and Dystonia Assessment in Children with Spastic Diplegic Cerebral Palsy and Periventricular Leukomalacia," *Journal of Child Neurology*, vol. 32, no. 11, pp. 936–941, 2017, doi: 10.1177/0883073817722451.

[44] A. Vanezis, M. A. Robinson, and N. Darras, "The reliability of the ELEPAP clinical protocol for the 3D kinematic evaluation of upper limb function," *Gait and Posture*, vol. 41, no. 2, pp. 431–439, Feb. 2015, doi: 10.1016/j.gaitpost.2014.11.007.

[45] C. Casellato, G. Zorzi, A. Pedrocchi, G. Ferrigno, and N. Nardocci, "Reaching and writing movements: Sensitive and reliable tools to measure genetic dystonia in children," *Journal of Child Neurology*, vol. 26, no. 7, pp. 822–829, Jul. 2011, doi: 10.1177/0883073810392997.

[46] F. Lunardini, S. Maggioni, C. Casellato, M. Bertucco, A. L. G. Pedrocchi, and T. D. Sanger, "Increased task-uncorrelated muscle activity in childhood dystonia," *Journal of NeuroEngineering and Rehabilitation*, vol. 12, no. 1, Jun. 2015, doi: 10.1186/s12984-015-0045-1.

[47] "www.btsbioengineering.com".

[48] H. J. Hermens *et al.*, "European Recommendations for Surface ElectroMyoGraphy Results of the SENIAM project".

[49] A. Leardini, Z. Sawacha, G. Paolini, S. Ingrosso, R. Nativo, and M. G. Benedetti, "A new anatomically based protocol for gait analysis in children," *Gait and Posture*, vol. 26, no. 4, pp. 560–571, Oct. 2007, doi: 10.1016/j.gaitpost.2006.12.018.

[50] H. B, M. JR, W. M, and H. GF, “An upper extremity kinematic model for evaluation of hemiparetic stroke,” *Journal of biomechanics*, vol. 39, no. 4, pp. 681–688, 2006, doi: 10.1016/J.JBIOMECH.2005.01.008.

[51] G. Rab, K. Petuskey, and A. Bagley, “A method for determination of upper extremity kinematics,” in *Gait and Posture*, Apr. 2002, vol. 15, no. 2, pp. 113–119. doi: 10.1016/S0966-6362(01)00155-2.

[52] R. B. Davis, S. Õunpuu, D. Tyburski, and J. R. Gage, “A gait analysis data collection and reduction technique,” *Human Movement Science*, vol. 10, no. 5, pp. 575–587, Oct. 1991, doi: 10.1016/0167-9457(91)90046-Z.

[53] A. S, D. G, and B.-M. A, “Gait analysis in children with cerebral palsy,” *EFORT open reviews*, vol. 1, no. 12, pp. 448–460, Dec. 2016, doi: 10.1302/2058-5241.1.000052.

[54] R. Baker, “Gait analysis methods in rehabilitation,” *Journal of NeuroEngineering and Rehabilitation 2006 3:1*, vol. 3, no. 1, pp. 1–10, Mar. 2006, doi: 10.1186/1743-0003-3-4.

[55] J. R. Gage, “Gait Analysis in Cerebral Palsy (Clinics in Developmental Medicine (Mac Keith Press)),” p. 206, 1991, Accessed: Oct. 04, 2021. [Online]. Available: https://books.google.com/books/about/Gait_Analysis_in_Cerebral_Palsy.html?hl=it&id=bof4MQEACAAJ

[56] D. PA, D. RB, O. S, R. S, and S. R, “Alterations in surgical decision making in patients with cerebral palsy based on three-dimensional gait analysis,” *Journal of pediatric orthopedics*, vol. 17, no. 5, pp. 608–614, Sep. 1997, doi: 10.1097/00004694-199709000-00007.

[57] W. Rose, “KAAP686 Mathematics and Signal Processing for Biomechanics Electromyogram analysis,” 2011.

[58] P. C. Raffalt, S. Vallabhajosula, J. J. Renz, M. Mukherjee, and N. Stergiou, “Lower limb joint angle variability and dimensionality are different in stairmill climbing and treadmill walking,” *Royal Society Open Science*, vol. 5, no. 12, Dec. 2018, doi: 10.1098/RSOS.180996.

[59] N. Hogan, “An organizing principle for a class of voluntary movements,” *Journal of Neuroscience*, vol. 4, no. 11, pp. 2745–2754, Nov. 1984, doi: 10.1523/JNEUROSCI.04-11-02745.1984.

[60] N. Hogan and D. Sternad, “Sensitivity of Smoothness Measures to Movement Duration, Amplitude and Arrests,” *Journal of motor behavior*, vol. 41, no. 6, p. 529, 2009, doi: 10.3200/35-09-004-RC.

[61] H. J, van E. RE, H. BC, and L. L, “A dynamical systems approach to lower extremity running injuries,” *Clinical biomechanics (Bristol, Avon)*, vol. 14, no. 5, pp. 297–308, 1999, doi: 10.1016/S0268-0033(98)90092-4.

[62] R. Mehri, A. Abbasi, S. Abbasi, M. K. Tazji, and K. Nazarpour, “Intra-Segment Coordination Variability in Road Cyclists during Pedaling at Different Intensities,” *Applied Sciences 2020, Vol. 10, Page 8964*, vol. 10, no. 24, p. 8964, Dec. 2020, doi: 10.3390/APP10248964.

[63] S. Solnik, P. Rider, K. Steinweg, P. Devita, and T. Hortobágyi, “Teager-Kaiser energy operator signal conditioning improves EMG onset detection,” *European Journal of Applied Physiology*, vol. 110, no. 3, pp. 489–498, Oct. 2010, doi: 10.1007/S00421-010-1521-8.

[64] W. Pirker and R. Katzenschlager, “Gait disorders in adults and the elderly: A clinical guide,” *Wiener Klinische Wochenschrift*, vol. 129, no. 3–4, pp. 81–95, Feb. 2017, doi: 10.1007/S00508-016-1096-4.

[65] J. R. Davids, T. Foti, J. Dabelstein, D. W. Blackhurst, and A. Bagley, “Objective assessment of dyskinesia in children with cerebral palsy,” *Gait and Posture*, vol. 6, no. 3, p. 269, 1997, doi: 10.1016/S0966-6362(97)90067-9.

[66] Y. P. Ivanenko, R. E. Poppele, and F. Lacquaniti, “Five basic muscle activation patterns account for muscle activity during human locomotion,” *The Journal of Physiology*, vol. 556, no. Pt 1, p. 267, Apr. 2004, doi: 10.1113/JPHYSIOL.2003.057174.

[67] J. L. Ostrem and P. A. Starr, “Treatment of Dystonia with Deep Brain Stimulation,” *Neurotherapeutics*, vol. 5, no. 2, pp. 320–330, Apr. 2008, doi: 10.1016/J.NURT.2008.01.002.

[68] C. Branta, J. Haubenstricker, and V. Seefeldt, “Age changes in motor skills during childhood and adolescence.,” *Exercise and Sport Sciences Reviews*, vol. 12, no. 1, pp. 467–520, Jan. 1984, doi: 10.1249/00003677-198401000-00015.

[69] A. Massaad, A. Assi, W. Skalli, and I. Ghanem, “Repeatability and validation of Gait Deviation Index in children: Typically developing and cerebral palsy,” *Gait & Posture*, vol. 39, no. 1, pp. 354–358, Jan. 2014, doi: 10.1016/J.GAITPOST.2013.08.001.

[70] B. Hingtgen, J. R. McGuire, M. Wang, and G. F. Harris, “An upper extremity kinematic model for evaluation of hemiparetic stroke,” *Journal of Biomechanics*, vol. 39, no. 4, pp. 681–688, Jan. 2006, doi: 10.1016/J.JBIOMECH.2005.01.008.

[71] J. S. R. Leversen, M. Haga, and H. Sigmundsson, “From Children to Adults: Motor Performance across the Life-Span,” *PLOS ONE*, vol. 7, no. 6, p. e38830, Jun. 2012, doi: 10.1371/JOURNAL.PONE.0038830.

[72] T. J. Loher *et al.*, “Deep brain stimulation for dystonia: outcome at long-term follow-up,” *Journal of Neurology 2008 255:6*, vol. 255, no. 6, pp. 881–884, Mar. 2008, doi: 10.1007/S00415-008-0798-6.

[73] A. J. Bastian, V. E. Kelly, F. J. Revilla, J. S. Perlmutter, and J. W. Mink, “Different effects of unilateral versus bilateral subthalamic nucleus stimulation on walking and reaching in Parkinson’s disease,” *Movement Disorders*, vol. 18, no. 9, pp. 1000–1007, Sep. 2003, doi: 10.1002/MDS.10493.

[74] V. E. Kelly, A. S. Hyngstrom, M. M. Rundle, and A. J. Bastian, “Interaction of levodopa and cues on voluntary reaching in Parkinson’s disease,” *Movement Disorders*, vol. 17, no. 1, pp. 38–44, Jan. 2002, doi: 10.1002/MDS.10000.

[75] M. Galli, V. Cimolin, C. Rigoldi, N. Tenore, and G. Albertini, “Gait patterns in hemiplegic children with Cerebral Palsy: Comparison of right and left hemiplegia,” *Research in Developmental Disabilities*, vol. 31, no. 6, pp. 1340–1345, Nov. 2010, doi: 10.1016/J.RIDD.2010.07.007.

[76] Winters TF Jr., Gage JR, and Hicks R, “Gait patterns in spastic hemiplegia in children and young adults,” *J Bone Joint Surg Am. Mar;69(3)*, 1987.

[77] Physiopedia, “Classification of Gait Patterns in Cerebral Palsy.”

[78] D. M. Bojanic, B. D. Petrovacki-Balj, N. D. Jorgovanovic, and V. R. Ilic, “Quantification of dynamic EMG patterns during gait in children with cerebral palsy,” *Journal of Neuroscience Methods*, vol. 198, no. 2, pp. 325–331, Jun. 2011, doi: 10.1016/J.JNEUMETH.2011.04.030.

[79] V. Agostini, A. Nascimbeni, A. Gaffuri, P. Imazio, M. G. Benedetti, and M. Knaflitz, “Normative EMG activation patterns of school-age children during gait,” *Gait & Posture*, vol. 32, no. 3, pp. 285–289, Jul. 2010, doi: 10.1016/J.GAITPOST.2010.06.024.

[80] J. E. ; Perry and J. M. Burnfield, “Gait Analysis: Normal and Pathological Function-2nd”.

[81] R. Okuno, M. Yokoe, K. Akazawa, K. Abe, and S. Sakoda, “Finger taps movement acceleration measurement system for quantitative diagnosis of Parkinson’s disease,” *Annual International Conference of the IEEE Engineering in Medicine and Biology - Proceedings*, pp. 6623–6626, 2006, doi: 10.1109/IEMBS.2006.260904.

[82] D. C. Lee, H. K. Lim, W. B. McKay, M. M. Priebe, S. A. Holmes, and A. M. Sherwood, “Toward an objective interpretation of surface EMG patterns: a voluntary response index (VRI),” *Journal of Electromyography and Kinesiology*, vol. 14, no. 3, pp. 379–388, Jun. 2004, doi: 10.1016/J.JELEKIN.2003.10.006.

[83] M. J. Hong *et al.*, “Quantitative Evaluation of Post-stroke Spasticity Using Neurophysiological and Radiological Tools: A Pilot Study,” *Annals of Rehabilitation Medicine*, vol. 42, no. 3, p. 384, Jun. 2018, doi: 10.5535/ARM.2018.42.3.384.

[84] M. Zoghi, M. Galea, and D. Morgan, “A Brain Motor Control Assessment (BMCA) Protocol for Upper Limb Function,” *PLOS ONE*, vol. 8, no. 11, p. e79483, Nov. 2013, doi: 10.1371/JOURNAL.PONE.0079483.

List of Figures

List of Tables